

CRWR Online Report 98-9

Assessing the Impact of Climate Change on Water Resources
for the Edwards Aquifer

by

Kris Lawrence Martinez, M.S.E.

Graduate Research Assistant

and

David R. Maidment, PhD.

Principal Investigator

May 1998

CENTER FOR RESEARCH IN WATER RESOURCES

Bureau of Engineering Research • The University of Texas at Austin
J.J. Pickle Research Campus • Austin, TX 78712-4497

This document is available online via World Wide Web at
<http://www.ce.utexas.edu/centers/crwr/reports/online.html>

Copyright
by
Kris Lawrence Martinez
1998

**Assessing the Impact of Climate Change on Water Resources
for the Edwards Aquifer**

by

Kris Lawrence Martinez, B.S.E.

Thesis

Presented to the Faculty of the Graduate School of

The University of Texas at Austin

in Partial Fulfillment

of the Requirements

for the Degree of

Master of Science in Engineering

The University of Texas at Austin

May 1998

**Assessing the Impact of Climate Change on Water Resources
for the Edwards Aquifer**

**Approved by
Supervising Committee:**

David R. Maidment

Daene C. McKinney

Acknowledgements

I would like to thank my advisors, Dr. David Maidment and Dr. Daene McKinney for opening up their doors to me. Their insights and expertise regarding water resources and hydrology were indispensable to this research.

I sincerely appreciate the help of fellow graduate students Seann Reed and David Watkins, Jr., because they designed the blueprints for me to follow throughout the course of my work. Seann and David were always quick to respond to my questions. They even provided me with information that I did not ask for, but knew I would need in the future.

My family laid the foundation for what I was to become as an adult.

I thank them for their love and guidance.

Finally, I am very grateful to my best friend, Tom, who furnished the bricks and mortar needed to accomplish this task. He has been an unlimited source of support and encouragement. It has been a long road, and I would not have been able to make it without him.

May 1998

Abstract

Assessing the Impact of Climate Change on Water Resources for the Edwards Aquifer

Kris Lawrence Martinez, M.S.E.

The University of Texas at Austin, 1998

Supervisor: David R. Maidment

This study examines how climate change will affect water availability in the Edwards Aquifer region of Central Texas. A rainfall-runoff model and a groundwater model are run under altered climate scenarios which simulate precipitation and temperature changes resulting from doubled atmospheric concentrations of carbon dioxide. Results from six global climate models indicate that gradually rising carbon dioxide levels will bring about a warmer climate in the study area. Because precipitation is not expected to increase, greater evaporation losses will lead to decreased streamflows, spring flows, and aquifer water levels. Climate change will magnify the effects of San Antonio's increasing water needs. The predictions have a considerable range of uncertainty, but the weight of the evidence is that the Edwards Aquifer will be increasingly stressed by the impacts of future climate change.

Table of Contents

List of Tables	ix
List of Figures.....	x
Chapter 1: Introduction.....	1
1.1 Background.....	2
1.1.1 The Edwards Aquifer–A Natural Resource.....	3
1.1.2 Climate Change	6
1.2 Methodology.....	7
1.3 Literature Review	11
Chapter 2: Base Map Development.....	15
2.1 Application of GIS.....	15
2.2 Map Projection	16
2.3 Watershed Delineation	18
2.3.1 Digital Elevation Models.....	18
2.3.2 Burning In the Streams	23
2.3.3 Boundary Determination	25
2.3.4 Accuracy Considerations.....	34
Chapter 3: Historical Climate	36
3.1 VEMAP Climate Data	36
3.1.1 Historical Precipitation	38
3.1.2 Historical Temperature	39
3.2 Climate Mapping	41
3.2.1 Processing Climate Data in ARC/INFO.....	41
3.2.2 Climate Variability	43
3.3 Climate Interpolation.....	45

Chapter 4: Climate and Surface Water	51
4.1 Soil-water Balance Model	52
4.1.1 Assumptions	52
4.1.2 Methodology	54
4.2 Soil-Water Holding Capacity	56
4.2.1 STATSGO Soils Data	56
4.2.2 Average Available Water Capacity	57
4.3 Evaporation	59
4.4 Runoff	62
4.4.1 Constant Runoff Coefficient Method	63
4.4.2 Soil Saturation Curve Method	65
4.5 Model Calibration and Validation	66
4.5.1 Calibration Procedure	67
4.5.2 Validation Results	68
Chapter 5: Surface Water and Groundwater	74
5.1 Tank Model Overview	74
5.2 Water Movement	77
5.3 Recharge Functions	80
5.4 Methodology	82
5.5 Results	86
Chapter 6: Climate Change	93
6.1 Methodology	93
6.2 Results	98
Chapter 7: Conclusions	115
7.1 Summary of Results	115
7.2 Study Limitations	118
7.3 Contributions	119

Appendix A: Data Dictionary.....	121
Appendix B: Programs and Scripts	125
Glossary	180
Bibliography	182
Vita	186

List of Tables

Table 2.1	Modified Texas Statewide Mapping System.....	17
Table 2.2	Station Coordinate File	28
Table 2.3	Watershed Area Comparison.....	34
Table 3.1	Linking Table from Excel.....	42
Table 3.2	Average Monthly Precipitation Interpolated for each Watershed	50
Table 4.1	Calibration Factors and Associated Accuracy Measures for Simulated Streamflows (1975-1990).....	69
Table 5.1	Watersheds and Associated Gauges and Wells	76
Table 6.1	Annual Scaling Factors for Temperature (°C)	97
Table 6.2	Annual Scaling Factors for Precipitation.....	97
Table 6.3	Annual Scaling Factors for Streamflow in the Nueces River Basin	100
Table 6.4	Average Change in Water Levels (ft.) from 1975 to 1990.....	103
Table 6.5	Annual Scaling Factors for Spring Flows from Comal Springs.....	110
Table 6.6	Annual Scaling Factors for Spring Flows from San Marcos Springs	110
Table 7.1	Effects of Climate Change in the Edwards Aquifer Region.....	115

List of Figures

Figure 1.1	Edwards Aquifer Study Area.....	3
Figure 2.1	USGS 1:250,000 Quadrangles Covering the Study Region.....	19
Figure 2.3	Topography of the Edwards Region.....	22
Figure 2.4	Rivers and Streams of the Edwards Region	25
Figure 2.5	Creating a Point Coverage.....	30
Figure 2.6	Field Definition.....	30
Figure 2.7	Modifying Gauge Locations.....	31
Figure 2.8	Editing the Attribute Table.....	32
Figure 2.9	Setting the Grid Analysis Environment.....	32
Figure 2.10	Watersheds in the Edwards Aquifer Region.....	33
Figure 3.1	VEMAP Coverage of the 0.5° Cells in the Study Region.....	37
Figure 3.2	Historical 12-Month Moving Average Precipitation.....	38
Figure 3.4	A Map of Historical Average Climate Data from 1895 to 1993	44
Figure 3.5	Zonal Mean Calculation	46
Figure 3.6	Specifying a Zone and Value Theme	47
Figure 3.7	Boundary Approximation from Different Cell Sizes.....	49
Figure 4.1	Water Holding Capacity in the Nueces River Basin	59
Figure 4.2	Nueces River Basin: Rainfall versus Combined Streamflows from Gauges 8190500 and 8190000 (1975-1990).....	64
Figure 4.3	12-Month Moving Average Streamflows for the Nueces River: Observed and Predicted by the Soil-Water Balance Model	70

Figure 4.4	12-Month Moving Average Streamflows for the Nueces River: Observed and Predicted by the Constant Coefficient Method.....	70
Figure 4.5	12-Month Moving Average Streamflows for the Blanco River	71
Figure 4.6	12-Month Moving Average Streamflows for Helotes-Salado Creek	72
Figure 5.1	Watersheds and Associated Gauges	76
Figure 5.2	Movement of Water Within the Edwards Aquifer	78
Figure 5.3	Tank Configuration.....	79
Figure 5.4	Groundwater Transport Simulated with a Tank Model.....	82
Figure 5.5	Relationship Between Precipitation, Streamflows and Water Levels for the Nueces River Basin	88
Figure 5.6	Nueces River Basin: Observed and Predicted Water Levels.....	89
Figure 5.7	Helotes-Salado Creek Basin: Observed and Predicted Water Levels	90
Figure 5.8	Comal Springs: Observed and Predicted Spring Flows.....	91
Figure 5.9	Relationship Between Pumping Rates and Water Levels for the Helotes-Salado Creek Basin	92
Figure 6.1	Annual Scaling Factors for Temperature from GCMs	96
Figure 6.2	Annual Scaling Factors for Precipitation from GCMs	96
Figure 6.3	Average Streamflow Scaling Factors for the Nueces River Basin from 1975-1990 Predicted from GCM Climate Scenarios	99
Figure 6.4	Average Water Levels for the Nueces River Basin from 1975-1990 Predicted from GCM Scaling Factors	102

Figure 6.5	Average Water Levels for the Helotes-Salado Creek Basin from 1975-1990 Predicted from GCM Scaling Factors	102
Figure 6.6	Water Level Variability for the Nueces River Basin from 1975-1990 Predicted from GCM Scaling Factors (Legend Ordered by Decreasing Average Water Level)	104
Figure 6.7	Water Level Variability for the Helotes-Salado Creek Basin from 1975-1990 Predicted from GCM Scaling Factors (Legend Ordered by Decreasing Average Water Level)	105
Figure 6.8	Range of Water Level Predictions for the Nueces River Basin	106
Figure 6.9	Range of Water Level Predictions for the Helotes-Salado Creek Basin	107
Figure 6.10	Range of Water Level Predictions for the Blanco River Basin	107
Figure 6.11	Average Scaling Factors for Spring Flows from Comal Springs Predicted from GCM Climate Scenarios (1975-1990)	109
Figure 6.12	Average Scaling Factors for Spring Flows from San Marcos Springs Predicted from GCM Climate Scenarios (1975-1990)	109
Figure 6.13	Range of Spring Flow Predictions for Comal Springs	111
Figure 6.14	Range of Spring Flow Predictions for San Marcos Springs	112
Figure 6.15	Index Well J-17 Water Levels Predicted Under Increased Pumping	113
Figure 6.16	Spring Flows for Comal Springs Predicted Under Increased Pumping	114

Chapter 1: Introduction

If global warming continues unabated, the rate of climate change over the next century will probably be greater than any seen in the last 10,000 years (Clark and Jäger, 1997). A statistically significant rise in global mean temperatures during the last century is now detectable (Houghton et al., 1996). Moreover, increased temperatures are not the only consequence of climate change. Other effects include rising sea levels, altered precipitation patterns, shifting ecological zones, and alterations in areas that are suitable for farming. Coastal areas may become increasingly plagued by flooding during storm surges. Erratic weather, such as tropical storms and extended heat waves, could cause a higher incidence of death and injury. Finally, agriculture in regions that are currently only marginally productive will probably become even more difficult. It is for these reasons that climate change has become a major topic of interest to the scientific community.

This study examines the effects of climate change on a regional scale. The objective of this research is to evaluate how climate change would influence the availability of water resources for the Edwards Aquifer in central Texas. The Edwards Aquifer has been designated as a “sole source” drinking water supply for the 1.5-million people who live in and around San Antonio, Texas, the eighth largest city in the United States (Wanakule and Anaya, 1993). Besides providing drinking water, the aquifer also supports the agricultural and light industrial economy of the region. This research does not attempt to determine the impact

that climate change would have on socioeconomic conditions. Rather, it analyzes the complex interactions between climate and hydrology that affect the flow and piezometric elevation of the Edwards Aquifer. The mechanisms driving the movement of water must be understood before predictions can be made regarding the effects of climate change. Thus, the first five chapters of this thesis discuss relationships between historical climate, surface water, and groundwater. The effects of modified climate forcing on the aquifer are addressed in Chapter 6.

1.1 BACKGROUND

The Edwards Aquifer serves the domestic, agricultural, industrial, and other water needs of a continuously growing population in central Texas (Eckhardt, 1995). According to the historical pumping data provided by Wanakule and Anaya (1993), pumping of the aquifer reached a record high 542,400 acre-feet (AF) in 1989. The USGS estimates that the average annual recharge is 651,700 AF (Eckhardt, 1995). Programs that simulate climate change, known as General Circulation Models (GCMs), consistently predict rising temperatures in this region during the next century (Valdés, 1997). Drier conditions could potentially lead to decreased recharge of the aquifer. This, in turn, would lower the amount of pumping that could be sustained without overdrafting the aquifer. This research explores the hydrologic system that comprises the Edwards Aquifer region. It also considers how the system could be impacted by climate changes that are expected to occur over the coming decades.

1.1.1 The Edwards Aquifer—A Natural Resource

The Edwards Aquifer extends along the narrow belt of the Balcones Fault Zone (BFZ) and underlies the cities of Austin and San Antonio, as shown in Figure 1.1. The aquifer is approximately 160 miles in length and flow moves east and then northeast towards the main discharge springs. The western edge of the aquifer is near the town of Bracketville. The formation curves around to its northeastern end, which is near the town of Kyle. Several major river basins cross over the aquifer's recharge zone, including the Nueces, San Antonio, and Guadalupe River Basins. There are many natural springs in the region, including the highly productive Comal and San Marcos Springs. The geographic features of the study area are shown in Figure 1.1.

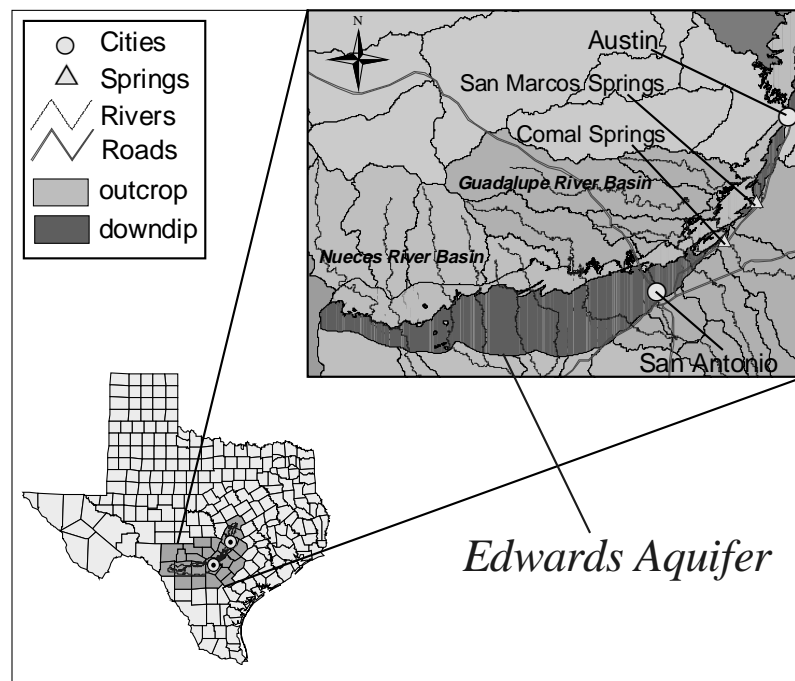


Figure 1.1 Edwards Aquifer Study Area

The Edwards Aquifer is one of the most productive aquifers in the world. The amount of water in the aquifer is estimated to be between 25 and 55 million AF (Maclay, 1989). Under normal conditions, the aquifer is able to provide an ample supply of water to meet the demands of the San Antonio region. There are hundreds of pumping wells in the city area and pumping rates have been steadily increasing over the last century to support population growth. The primary uses of well discharge during the period from 1981 to 1990 were municipal (56.6%) and agricultural (30.1%) (Wanakule and Anaya, 1993). Rising water demands have caused concerns about sustainable water supply and the threat of overdrafting the annual recharge to the aquifer. Water conservation regulations keyed to aquifer water levels have been adopted for San Antonio, New Braunfels, and San Marcos to reduce pumping during periods of low aquifer storage.

The karst characteristics of the Edwards Aquifer make it an extraordinary water resource. Extensive erosion of deposited limestone during the Cretaceous Period caused channelization in the subsurface formation. As a result, the aquifer behaves like a water distribution system with flow moving rapidly through cavities and conduits. The Edwards formation exhibits enhanced porosity and high transmissivity (Maclay and Land, 1988). Within the confined portion, water flows east and northeast towards natural discharge points including Comal and San Marcos Springs, which by themselves account for 355,000 AF of discharge annually. Because the karst aquifer is able to transfer large quantities of water quickly, water levels and spring flows are highly sensitive to recharge variability.

Groundwater divides separate the Edwards Aquifer into three portions. The central portion, which extends south from the Colorado River in Austin, is known as the Barton Springs segment. The portion of the aquifer that is located on the other side of the Colorado River is simply referred to as the northern segment. This study examines the San Antonio portion of the aquifer. In this area, the aquifer receives large amounts of recharge from streams and rivers which flow over exposed limestone formations that contain many faults and fractures. During dry periods, gauging stations below the limestone outcrop often record no flow because of extensive channel losses. The Nueces River Basin covers over half of the study area and contributes nearly 60% of the total annual recharge (Wanakule and Anaya, 1993). Precipitation over the outcrop area also supplies a minor portion of recharge through diffuse infiltration. However, rainfall plays a much larger role in that it is a primary factor driving flow rates in streams and rivers which supply most of the recharge. Consequently, changes in climate are highly correlated with recharge, water level, and spring flow variability.

While recharge is supplied through near-surface interactions within the water table portion of the aquifer, spring flows are maintained by hydraulic gradients that exist within the artesian zone, where Del Rio Clays overlying the Edwards limestones act as a confining unit. These springs stop flowing when the aquifer is still 90-95% full. During the drought of record (1947-1956), Comal Springs ceased to flow from June to November of 1956 (Eckhardt, 1995). Comal and San Marcos Springs are the two largest springs in Texas and their spring

flows are crucial to the region. They support downstream uses of water from the Comal, Guadalupe, and San Marcos Rivers. In addition, the springs provide a habitat for several endangered species. When Comal Springs went dry in 1956, an entire population of the fountain darter was eliminated and had to be reintroduced to the area. Increased pumping has had a negative impact on spring flows. The San Antonio Springs and San Pedro Springs, located in the city of San Antonio, have essentially stopped flowing except for very wet periods. Pumping has magnified the springs' susceptibility during times of drought.

1.1.2 Climate Change

Climate variability is generally natural in origin, resulting from subtle variations in the complex processes which drive the movement of heat and mass between the atmosphere, the oceans, and land surfaces. The El Niño-Southern Oscillation (ENSO), for example, is caused by weakening trade winds in the southern part of the Pacific Ocean (NOAA PMEL, 1997). Trade winds carry warmer air west, which causes rising sea temperatures and increased precipitation. During ENSO, the warming effect is reduced in the west, causing droughts in Australia and flooding in Peru. The Intergovernmental Panel on Climate Change (IPCC) has concluded that human activities are beginning to influence the global climate system (Houghton et al., 1996). Fossil fuel consumption, which has been steadily increasing since the pre-industrial period, is causing an overall increase in concentrations of greenhouse gases, including carbon dioxide (CO₂). Greenhouse gases trap the sun's heat and force a redistribution of the energy available near the earth's surface. The accumulation of greenhouse gases is expected to cause

significant changes over the next century. Surface temperatures are predicted to rise between 1.5° and 4.5°C and sea levels could increase from 15 to 95 cm. Because human influences are expected to follow a regular growth trend in the future, climate modifications caused by anthropological forcing are considered to be more permanent than those caused by natural variability.

The aspects of climate change that are most significant to the study region are rainfall variability and rising temperatures. The karst properties of the Edwards Aquifer make it particularly sensitive to variability in recharge. Since recharge is strongly influenced by precipitation and runoff, water levels and spring flows behave in an erratic manner from month to month and year to year. This variable response obscures increased evaporation losses caused by rising temperatures. However, evaporation rates are not offset by precipitation during extended dry periods. Under these conditions, the aquifer is less capable of sustaining spring flows and pumping will become more difficult. A repeat of the critical drought will certainly lead to greater environmental consequences than those experienced in the 1950s.

1.2 METHODOLOGY

This research aims to develop a better understanding of relationships between the hydrologic features of the Edwards Aquifer. The study considers climate, streamflows, recharge, pumping, spring flows, and water levels. The scope of work is outlined below.

- Develop a base map for the study area using Geographic Information Systems to assemble geospatial data from various sources

- Delineate watershed boundaries for streams and rivers that provide recharge to the aquifer
- Obtain historical climate records of precipitation and temperature for the region
- Estimate streamflows from precipitation and temperature using a soil-water balance
- Estimate aquifer water levels and spring flows from streamflows using a groundwater model
- Apply GCM scaling factors to precipitation and temperature and compare water levels and spring flows under $1xCO_2$ and $2xCO_2$ conditions

Chapter 2 describes the use of Geographic Information Systems (GIS) to create a digital base map that enables the user to assemble large amounts of information about the study area. The process of watershed delineation is described in detail. Drainage basins provide a framework for modeling hydrologic processes for the Edwards region because they are the primary source of water supply to the aquifer. All of the parameters and results of the study are defined in terms of drainage basins. Observed climate data are interpolated based on boundaries determined by watershed delineation. Rainfall and runoff interactions are modeled for each catchment area. Subsequently, water levels and spring flows are estimated using recharge functions that have been developed for each of the drainage basins. The base map consists of several layers describing the climate, terrain, soil, and geographic features of the study area. The data

dictionary provided in Appendix A describes all of the spatial data sets developed for this study.

Maps of historical average precipitation and temperature have been created using procedures described in Chapter 3. Spatial climate trends are more recognizable when the data is represented on a map. Mean annual precipitation in the study area, for example, increases from west to east which is strongly associated with different water uses in the region. Measured precipitation and temperature data were provided by the Vegetation/Ecosystem Modeling and Analysis Project (VEMAP) on a 0.5° by 0.5° grid covering the study region (Kittel et al., 1997). The climate data are interpolated to provide monthly values for each watershed. A computer program has been written that uses GIS to perform the necessary spatial analysis. All of the programs developed for this project are contained in Appendix B.

Chapter 4 describes the soil-water balance program that is used to model runoff generation in the catchment basins of the study area. The program is a modified version of a soil-water budget model developed by Reed, Maidment, and Patoux (1997). The program predicts streamflows given precipitation, minimum and maximum temperature, and soil-water holding capacity data. An accounting procedure is performed in which rainfall is distributed between soil moisture, runoff, and evaporation. The amount of rainfall that becomes streamflow is predicted using an exponential soil-saturation curve. When the soil's water holding capacity is exceeded, the surplus is also distributed to runoff. Evaporation is predicted using a temperature-based method. The objective of

calibration runs is to accurately reproduce a time-series of historical streamflow measurements. Streamflow plays a major role in linking climate to groundwater and spring flows.

A groundwater model developed by Watkins (1997) is used to assess the relationships between climate, runoff, and the availability of water from the Edwards Aquifer. The model considers pumping, recharge, water levels and spring flows. Each of the watersheds is treated as a rock-filled tank with uniform storage and transmissivity properties. The input to each tank is calculated using empirical recharge functions that were developed by Wanakule and Anaya (1993) using flow loss analysis. Estimated streamflows are multiplied by recharge ratios that vary over the course of the simulation. Movement of water within the aquifer is simulated based on the fundamental properties of continuity and momentum. The effects of varying streamflows and pumping on aquifer dynamics are evaluated. The groundwater model is described in Chapter 5.

Surface water and groundwater model runs under altered weather conditions are discussed in Chapter 6. Scaling factors for precipitation and temperature were developed by Kittel et al. (1996) and Valdés (1997) to simulate future climate trends. These factors are generated by complex programs that predict changes in various hydrologic parameters given increased concentrations of CO₂. General Circulation Models (GCMs) simulate global heat and mass transfer mechanisms between the land surface, the ocean, and the atmosphere. Seven different GCMs are considered in order to examine the range of model variability in predicted streamflows, water levels, and spring flows. Additional

runs are made under increased pumping scenarios to assess the impacts of growing water demands in the region.

1.3 LITERATURE REVIEW

This study draws upon a great deal of previous research regarding climate change, rainfall-runoff modeling, and groundwater simulation of the Edwards Aquifer. VEMAP is an ongoing study to examine the effects of climate variability. In the first phase of the study, seven different GCMs were run which simulated climate response to doubling atmospheric concentrations of CO₂ relative to global average levels in 1990 (Kittel et al., 1996). Each of the models were run under 1xCO₂ and 2xCO₂ scenarios to obtain scaling factors for climate. Differences in monthly mean temperature and change ratios for precipitation were obtained. These normal and altered climates were then used in ecosystem physiology models and life-form distribution models. In the second phase, a historical set of climate data was assembled for the conterminous U.S. (Kittel et al. , 1997). Precipitation and temperature data from over 10,000 measurement stations were interpolated to a 0.5° latitude/longitude grid.

Valdés (1997) evaluated monthly, seasonal, and annual scaling factors from VEMAP for the Edwards Aquifer region. This work determined that all seven of the GCMs predicted increased temperature for the study area, while mixed results were obtained for precipitation. It was noted that GCMs predict temperature changes more accurately than changes in rainfall. GCMs are also more appropriate for estimating climate on a global scale rather than a local scale. The study concluded that although GCMs may not provide accurate estimations

of local climate variables, the ability of these models to provide consistent results regarding temperature, along with their foundation in physical processes, lends itself to making assessments of relative trends in climate on a regional basis.

The interaction of the atmosphere, land surface, vegetation, and soils to generate runoff is a complicated process. Rainfall-runoff models of various complexities have been used to estimate streamflows given climate data. In common practice, runoff is predicted as a constant fraction of rainfall (Pilgrim and Cordery, 1993). Some relationships give consideration to the infiltration capacity of the soil. The Green-Ampt equation, for example, models the downward movement of a saturated wetting front that begins when the rainfall intensity exceeds the soil's maximum infiltration rate (Chow, Maidment, and Mays, 1988). Storm runoff is generated until the rainfall intensity decreases and ponding stops. Other models combine the concept of infiltration rates and scaling factors for precipitation by distributing a constant fraction of rainfall to runoff after a specified soil-water capacity is reached.

Reed, Maidment, and Patoux (1997) developed a soil-water accounting procedure to estimate runoff. It is based on the principle that runoff models are extremely sensitive to soil-moisture conditions at the beginning of a rainfall event (Coles et al., 1997). The soil-water balance program is part of a class of models referred to as simple "bucket" models. These models were originally developed in the 1940s by Thornthwaite (1948) to estimate soil moisture storage, evaporation, and runoff. Surface water interactions are often represented using a single soil layer as a basis. Soil properties such as rooting characteristics, soil

texture, and plant physiology are ignored (Alley, 1984). Using daily or monthly climate data, a simple mass balance is performed over an area of land that is characterized by horizontally averaged soil properties.

Watkins (1997) used a groundwater model to examine water management alternatives for the Edwards Aquifer. The program was a modified version of a lumped parameter model that was originally developed by Wanakule and Anaya (1993). The hydrologic system of the aquifer is conceptualized as a series of eight rock-filled tanks representing the region's major watersheds. By using state-space methodology, the model is able to simulate aquifer dynamics faster than conventional finite-difference models where the system is represented by a large number of cells. Edwards Aquifer simulations by Klemt et al. (1979), Maclay and Land (1988), and Thorkildsen and McElhaney (1992) using finite-difference models were slower and required input data for over 800 cells.

Groundwater models must consider the source of recharge to the formation. The Edwards Aquifer receives most of its recharge from channel losses in rivers and streams that flow over joints, faults, and sink holes in the outcrop area. Empirical functions were developed by Wanakule and Anaya (1993) which calculate recharge given streamflows at gauging stations located above the infiltration zone. Puente (1978) developed functions to estimate runoff in the infiltration zone by multiplying the streamflow at an upper gauge by a coefficient defined as the ratio of the ungauged and gauged drainage areas. Recharge was then calculated by subtracting streamflow at a lower gauge from the combined upper and intervening streamflows. HDR Engineering, Inc. (1993)

considered climate by estimating intervening runoff using the Soil Conservation Service (SCS) method for abstractions. This study employs the recharge functions developed by Wanakule and Anaya (1993), the groundwater model by Watkins (1997), and the soil-water balance program by Reed, Maidment, and Patoux (1997).

Chapter 2: Base Map Development

A base map of the Edwards Aquifer study region has been assembled using Geographic Information Systems (GIS). The base map consists of various data layers that provide information about particular features. Layers describing climate, terrain, and soil properties have been assembled, along with many others. The major difference between GIS and digital cartography is that GIS is capable of storing large amounts of data that characterize the geographic features of a region, in addition to depicting the location of those features. These data can be analyzed to determine how attributes of the features relate to each other (ESRI, 1997). For example, knowing the variation of precipitation over space, the average rainfall for a particular watershed can be determined by analyzing the data sets for precipitation and watersheds. This chapter discusses how GIS is used to assemble data in a common framework for examining the relationships between climate, surface water, and groundwater.

2.1 APPLICATION OF GIS

A major goal of the study is to develop a database to manage the large amount of information available for the Edwards Aquifer region. Using GIS, a digital base map is created which links descriptive and geographic data for the various features of the study area. Because information other than a feature's location is stored in the database, the map is able to communicate the variation of properties over space. In more specific terms, GIS is capable of not only displaying the location of the Nueces River Basin, but also of showing that it has

considerably more surface water runoff than the Frio River Basin to the east. In this example, the Nueces River basin is represented by a feature, or object, on the base map. Runoff is an attribute that is stored in the database and referenced by the object's unique identification number.

A more powerful function of GIS is its capability of performing operations on spatial data, using the base map as a reference. The spatial analysis capabilities of GIS are used to determine representative values of monthly climate variables for each watershed on the basis of delineated watersheds. Watershed boundaries are determined using a digital elevation model (DEM) to predict the flow of water over the landscape. Boundary lines are located along ridges where water flows in opposite directions on either side of the ridge. After the boundaries are located, precipitation and temperature data are interpolated for each watershed from a 0.5° by 0.5° grid of climate data. The average monthly values are calculated based on the portions of a watershed's area that are intersected by particular climate cells. The base map is an integral part of this study, because it is used for parameter calculations, as well as a spatial reference.

2.2 MAP PROJECTION

Flat maps provide a two-dimensional representation of the earth's curved surface. Projection is a mathematical transformation of a geographic location, defined by latitude and longitude, to a point on a map, defined by northing and easting. Projecting from a curved to a flat surface always introduces some level of distortion of the true distance between objects. There are different types of projection which are designed to minimize the distortion of shape, area, direction,

or distance. It is impossible to minimize all forms of distortion in a two-dimensional representation. Therefore, a suitable projection must be chosen which provides the least amount of error in the resulting surface, whether the error is in shape, area, direction, distance, or some combination thereof.

The projection chosen for this study is a modified version of the Texas Statewide Mapping System (TSMS). The Texas Geographic Information Council has established TSMS as a standard projection because it minimizes scaling errors over the large amount of area covered by the state (Smith and Maidment, 1995). Instead of using the Lambert Conformal Conic projection specified by TSMS, an Albers Equal Area projection with the same parameters as TSMS is used. The Albers Equal Area Projection eliminates the distortion of area which is particularly important for determining watershed areas for drainage basins. While scale is preserved in terms of area, shape is distorted to a greater extent than the unmodified TSMS. Projection parameters used in this study are provided in Table 2.1.

Table 2.1 Modified Texas Statewide Mapping System

Projection	Albers Equal Area
Datum	NAD 83
Ellipsoid	GRS 80
Map Units	Meters
Central Meridian	100° W
Reference Latitude	31° 10' N
Standard Parallel 1	27° 25' N
Standard Parallel 2	34° 55' N
False Northing	1,000,000
False Easting	1,000,000

2.3 WATERSHED DELINEATION

All of the parameters and results of this study have been defined in terms of drainage basins. Climate data is interpolated to determine average monthly values of precipitation and temperature for each watershed. The soil-water balance program then predicts evaporation, soil moisture, and runoff on a watershed-basis. Finally, the groundwater model treats each of the drainage basins as a rock filled tank with uniform properties such as storativity and transmissivity. The movement of water in the Edwards region is modeled according to the eight major drainage basins that recharge the aquifer. Consequently, it is essential that the locations and boundaries of the watersheds be accurate on the base map.

2.3.1 Digital Elevation Models

Watershed delineation in GIS involves the use of a digital representation of terrain called a Digital Elevation Model (DEM). As shown in Figure 2.1, the USGS provides DEMs for the study region in separate files according to 1° by 1° quadrangles. There are eight quadrangles that cover the study region. The extent of the coverage is 265 km east to west and 145 km north to south for a combined area of over 38,000 km². The USGS DEMs have a 1:250,000 scale, for which terrain elevations are recorded for ground positions on an evenly spaced grid at intervals of 100 m. A grid cell consists of a 100 m by 100 m area. Each of the 1° by 1° DEMs contain 1.44 million cells. The combined DEM for the study region contains over 11 million cells. As a result, computer processing of the DEM to

delineate watershed boundaries is very time and memory intensive. The quadrangles covering the study area are shown in Figure 2.1.

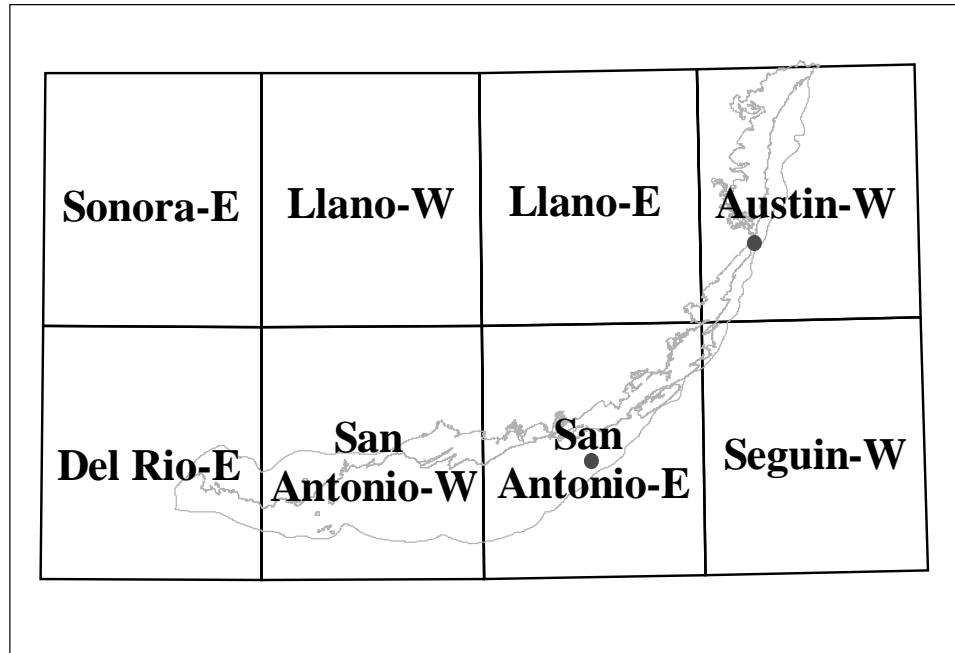


Figure 2.1 USGS 1:250,000 Quadrangles Covering the Study Region

DEMs obtained from the USGS are used to predict the movement of water over the landscape based on the principle that water always flows downhill. Processing of the DEM using GIS results in two grids that help define the extent of the drainage basin. The flowdirection grid consists of cells with values that correspond to the direction of steepest descent. This grid determines the path that water will follow. A second grid, called the flowaccumulation grid, is derived from the flowdirection grid. After the direction of flow is determined, the

accumulation of water along a particular flow path can be tracked. The value of each cell is the sum total of all the cells which flow into it. In other words, a cell with no other cells flowing into it is assigned a value of zero. If a cell has one upstream cell flowing into it, that cell is given a value of one. Figure 2.2 illustrates the relationship between a DEM, a flowdirection grid, and a flowaccumulation grid.

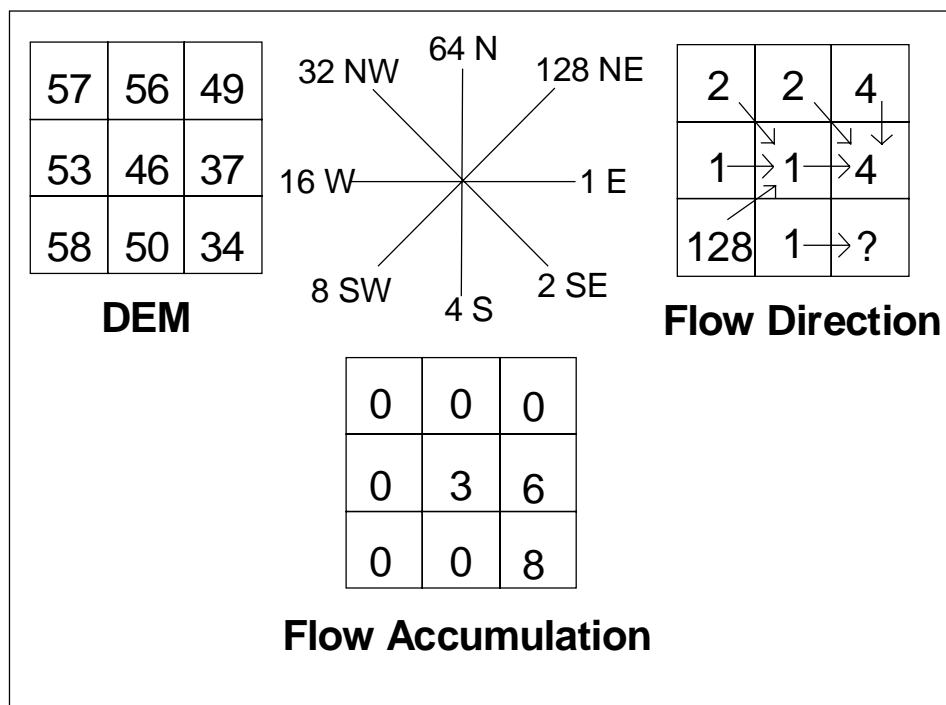


Figure 2.2 Watershed Delineation Grids

The DEMs used for this study are available through the USGS Earth Resources Observation System (EROS) Data Center web site (<http://edcwww.cr.usgs.gov/doc/edchome/ndcddb/ndcddb.html>). The data is not

provided in a format that is usable by GIS. It must first be reformatted using the following commands.

```
$gunzip del_rio-e.gz -v
```

```
$dd if=del_rio-e of=delrio.dem ibs=4096 cbs=1024 conv=unblock
```

```
Arc: demlattice delrio.dem delriogrid usgs
```

In the preceding example, the file **del_rio-e.gz** is downloaded and decompressed. It is then reblocked using the second command, which generates the file **delrio.dem**. In ARC/INFO, **delrio.dem** is converted into the grid **delriogrid** using the final command.

The resulting data is in a geographic coordinate system and needs to be projected to TSMS. This task is accomplished using a projection file. The projection file below was created in a text editor and is named **dem_tsms.prj**.

```
input
projection geographic
units ds
datum WGS72
parameters
output
projection albers
datum WGS84
units meters
parameters
27 25 0.000
34 55 0.000
-100 0 0.000
31 10 0.000
1000000.0
1000000.0
end
```

Once the projection file is created, the DEM grid is projected to TSMS in ARC/INFO using the command:

Arc: **project grid delriogrid delrio dem_tsms.prj**

This produces an output grid projected to TSMS called **delrio**.

Eight DEMs are needed to cover the study area. Before watershed delineation can be performed, the DEMs must be merged into a single grid:

Grid: **ed_dem=merge(delrio, sanant_w, sanant_e, llano_w, llano_e, austin, sonora, seguin)**

The resulting grid, **ed_dem**, requires 17 MB of computer memory. Figure 2.3 shows the variation of terrain in the study area. The minimum elevation is 90 m and the maximum elevation is 740 m.

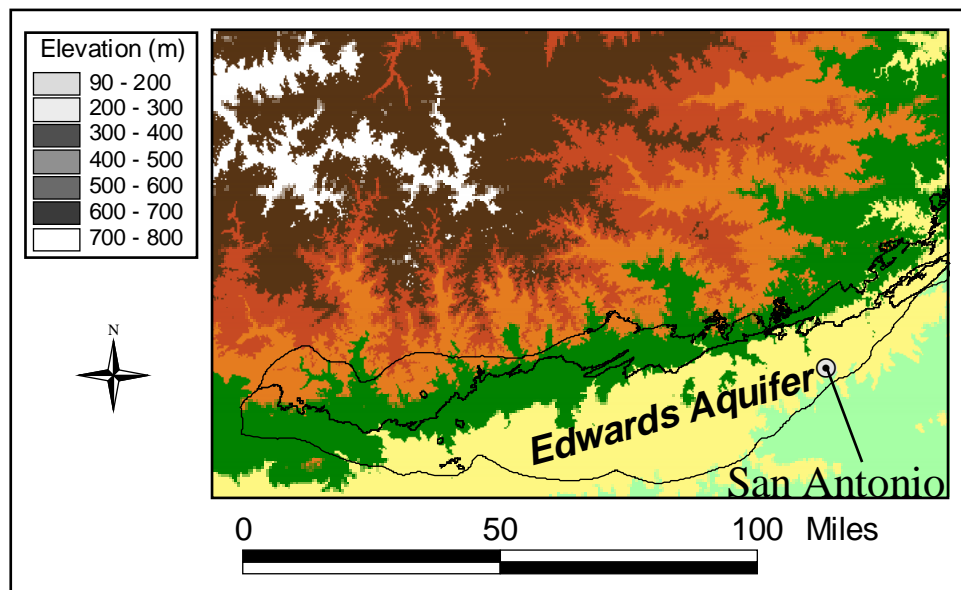


Figure 2.3 Topography of the Edwards Region

2.3.2 Burning In the Streams

Once a single DEM in the modified TSMS has been created, the watershed delineation process can begin. The first step is to *burn-in* digitized streams from the RF1 coverage. This procedure is not required for delineation, but research has shown that it improves the reliability of the watershed coverage by forcing the grid stream network to agree more closely with reality. In this process, all of the elevations except for those coinciding with digitized streams are artificially raised by an equal amount. Because the elevations in the *burned-in* streams remain the same, the flow of water is forced to follow the actual stream network after it “falls off” the artificially elevated land surface.

There are three primary steps to create a *burned-in* DEM. All of these steps involve raster (cell-based) data and are performed in the GRID module of ARC/INFO. The RF1 coverage consists of stream networks that are digitized from aerial photographs. It is in a vector (line-based) format and must first be converted to a grid. Subsequently, the DEM grid is modified to artificially raise each cell’s elevation value by an equal amount. The RF1 grid and the DEM grid are then merged together. Merging resets the cells in the DEM that coincide with the digitized stream cells to their original elevation value. This produces a new DEM, in which a trench of digitized streams has been *burned-in*, because the elevation of the area around them has been raised. The following command accomplishes the first step of converting the **RF1** coverage to a grid named **rivergrid**.

Grid: **rivergrid=linegrid(RF1)**

Rivergrid cells that do not coincide with digitized streams are given a null value, NODATA. The stream cells need to be assigned actual elevation values from the DEM. This is achieved by first resetting stream cell values to one and then multiplying by the elevation values of cells from the DEM. In order to change the **rivergrid** stream cells to unity, issue the command:

Grid: **unitgrid=rivergrid/rivergrid**

The next command changes the value of the stream cells in **unitgrid** to the elevation value from the DEM. Note that the NODATA cells outside of the digitized streams are ignored and remain unchanged.

Grid: **valugrid=unitgrid*ed_dem**

In the second major step, the elevation values in the DEM are artificially raised by an equal amount, 5000 m

Grid: **demplus=ed_dem+5000**

Finally, **demplus** and **valugrid** are merged. This returns the values of cells in the elevated DEM back to their true elevations.

Grid: **burndem=merge(valugrid, demplus)**

This completes the creation of the burned-in DEM. The flow path modeled by GIS will be modified so that water flowing into the artificial channels will not deviate from the path of the digitized streams. However, the flow of water over the landscape surrounding the digitized streams will not be affected. The *burn-in* procedure compensates for the resolution of the DEM. At the 1:250,000 scale, elevation values are recorded on a grid at 100 m intervals. The DEM does not capture terrain variations that occur within a 100 m by 100 m area.

As a result, changes in flow direction that occur inside of this area are not detectable. The RF1 coverages, on the other hand, are more precise because they are digitized on a continuous scale, in that the person digitizing from an aerial photograph can see beyond a single cell and knows the path of flow from a downstream perspective. Combining computational accuracy in determining the path of steepest descent on the grid with known flow paths from vector coverages results in delineated rivers and watersheds that agree better with reality. The RF1 coverage of rivers and streams in the Edwards region is shown in Figure 2.4.

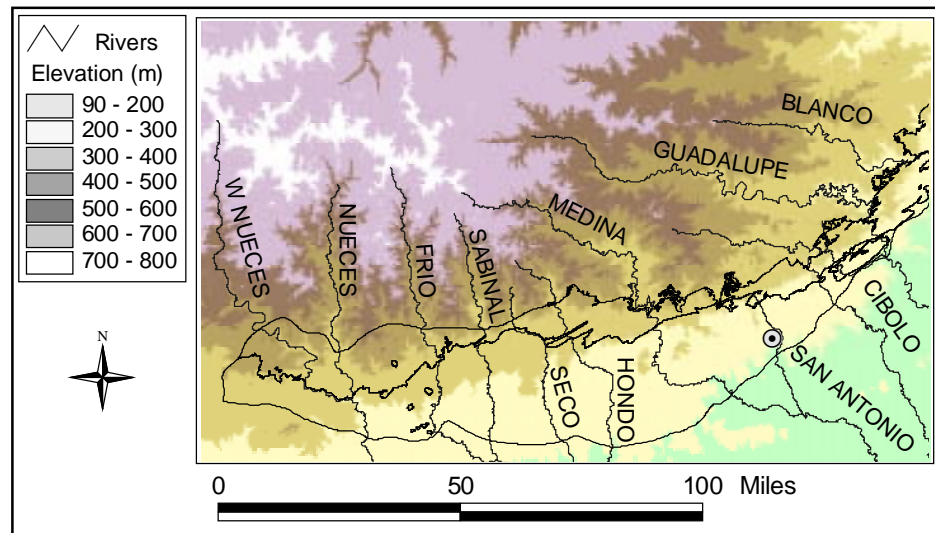


Figure 2.4 Rivers and Streams of the Edwards Region

2.3.3 Boundary Determination

Watershed delineation involves the determination of the area contributing streamflows to a particular point in a drainage basin. In this study, these points

are gauging stations that are located within the Edwards Aquifer recharge zone. These stream gauges are located at the outlet of drainage basins that were defined by Puente. The contributing area is based on the various flow paths that converge on the basin outlet at a specific stream gauge. The transport of water within a watershed is modeled using flowdirection and flowaccumulation grids generated from the DEM. There are six main steps, which are described in more detail below.

- Fill in artificial pits in the DEM
- Generate the flowdirection grid
- Generate the flowaccumulation grid
- Delineate stream networks
- Modify gauging station locations to coincide with streams
- Delineate the watersheds

Digital Elevation Models typically contain cells with elevations that are lower than the eight cells surrounding them. A flowdirection cannot be assigned to these cells because there is no path of steepest descent. These cells are called sinks because water that flows into them is trapped. This is not a valid condition considering that an actual land surface does not have discontinuities in elevation and water simply pools and then continues along a flow path. Sinks must be filled to ensure an accurate representation of water movement. The following command removes the nonexistent depressions in a DEM:

Grid: fill burndem_old burndem_new sink 100 #

After the sinks are filled, the flowdirection grid can be generated. Using the **flowdirection** command creates a new grid where each cell is assigned a value based on the direction of the neighboring cell with the lowest elevation. A cell is surrounded by eight other cells so there are eight directions in which water could go. As shown in Figure 2.2, the values assigned to a cell if the water goes East=1, Southeast=2, South=4, Southwest=8, West=16, Northwest=32, North=64, and Northeast=128. The following command generates the flowdirection grid.

Grid: **edfdr=flowdirection(burndem_new)**

The cells in a flowaccumulation grid have a value corresponding to the total number of cells that flow into them. It is generated using the **flowaccumulation** command:

Grid: **edfac=flowaccumulation(edfdr)**

Each cell in the **edfac** grid contains a tally of the number of upstream cells. This value can be used to calculate a drainage area. Each cell in a DEM is 100 m by 100 m, or 0.01 km². If 10,000 cells are upstream of a cell, that cell has a drainage area of 10,000 cells x 0.01 km²/cell=100 km². A boolean query can be used to define streams given a minimum drainage area. If the threshold accumulation value is set at 10,000 cells, the cell with a value of 10,000 would be assigned a one in the resulting grid, indicating that it was a stream cell. All of the cells feeding into this cell would not meet the stream definition criteria and would be assigned a zero. The following command performs this transformation:

Grid: **stream=con(edfac>10000,1)**

The outlet of each watershed is defined by the location of a stream gauge located at the downstream edge of the Edwards Aquifer recharge zone. The gauging stations were put in place to measure the amount of streamflow lost to infiltration. The locations were selected based on geologic and seepage studies. The USGS provides geographic coordinates for gauging stations, along with streamflow data, on its web site at <http://txwww.cr.usgs.gov/databases.html> (USGS, 1997). This information can be extracted by knowing a specific gauge number or a general location, such as the county in which the gauge is located. The USGS locational data are used to create a point coverage of gauges that define the outlets of the drainage basins. These data are provided in degrees, minutes, and seconds (DMS) format. They must be converted to decimal degrees (DD) before they can be used by ARC/INFO. This is accomplished using the following equation.

$$DD = Degrees + \frac{Minutes}{60} + \frac{Seconds}{3600} \quad (2.1)$$

A text file is then created that contains a unique identification number for each gauge followed by its geographic coordinates. A text file is provided as an example in Table 2.2.

Table 2.2 Station Coordinate File

1	29.472500	-100.236111
.	.	.
.	.	.
.	.	.
10	29.428333	-99.996944
end		

The word 'end' is a flag used by the program to indicate when all of the records have been read. This file is saved as **gauge.dat**. The actual coverage creation is performed in ARC/INFO using the **generate** command:

Arc: **generate stations**
Generate: **input gauge.dat**
Generate: **points**
Generate: **quit**

After the dialog is entered, two additional commands must be issued to create the coverage:

Arc: **build stations points**
Arc: **addxy stations**

The resulting data set is in geographic coordinates and must be projected to TSMS using the procedure outlined in Section 2.3.1.

Frequently, the locations of gauging stations cited by the USGS are offset slightly from the streams delineated by the DEM. This is a problem since the station locations are used to define the outlet, or pour point, of the stream network for each drainage basin. Consequently, the locations must be modified so that they coincide with the streams. This step is performed by comparing the **stream** grid and the **stations** coverage in ArcView. A new shapefile is created using a process called heads-up digitizing to place points on streams, as near as possible to the original gauge locations. The first step in heads-up digitizing is to use the menu option **View/New Theme** in ArcView and select the type of feature as shown in Figure 2.5. The new theme is a point coverage named **stations.shp**.

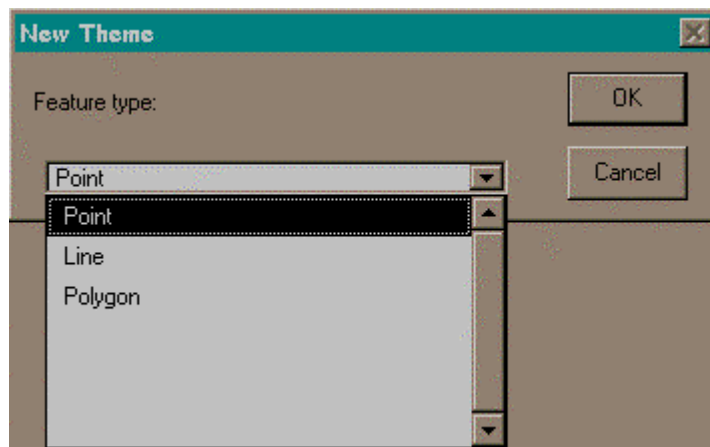


Figure 2.5 Creating a Point Coverage

Each of the stream gauges is assigned a number by editing the table for **stations.shp**. When the watershed delineation step is performed, the number specified for a stream gauge will be assigned to all of the cells that flow into the gauge. A new field named 'value' is created in the **stations.shp** attribute table. Open the attribute table and add the field using the menu item **Edit/Add Field**. The specifications for the new field are entered into the input box, as shown in Figure 2.6.

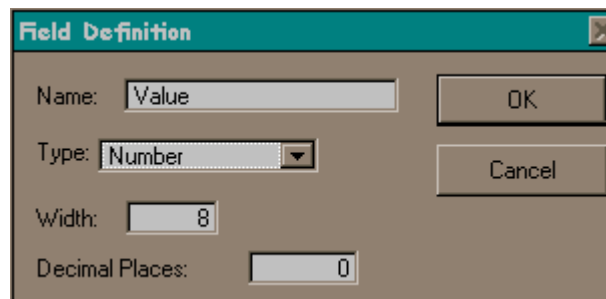



Figure 2.6 Field Definition

A point is added to the theme by clicking on the  button and then clicking after moving the crosshair cursor to the desired point on the map as shown in Figure 2.7.

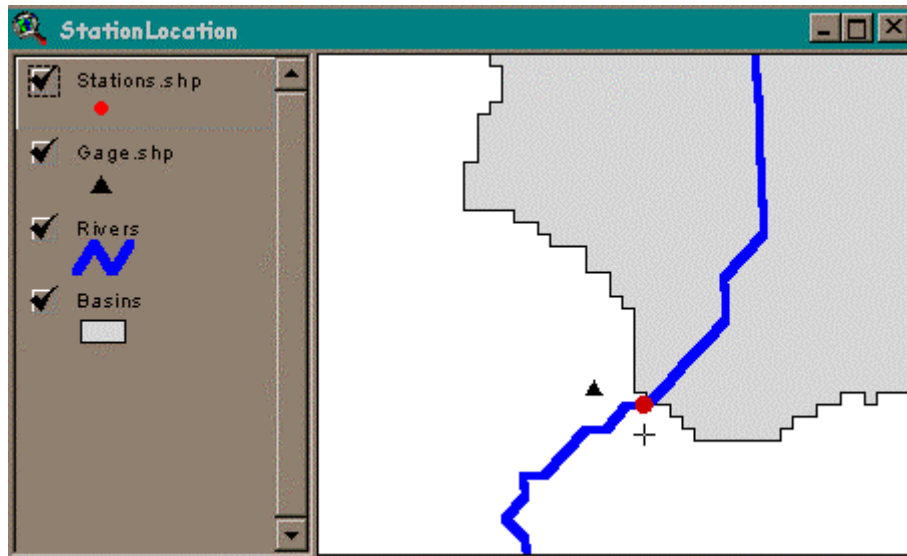



Figure 2.7 Modifying Gauge Locations

Edit the 'value' field in the new table to specify a number for each gauge. This number will be assigned to all of the cells in the gauge's drainage area when the watershed is delineated. To edit the table, click on the  button and type in the value for the selected record. Figure 2.8 shows a table being edited to assign numbers to stream gauges. This procedure is repeated to create a modified coverage of outlet points.

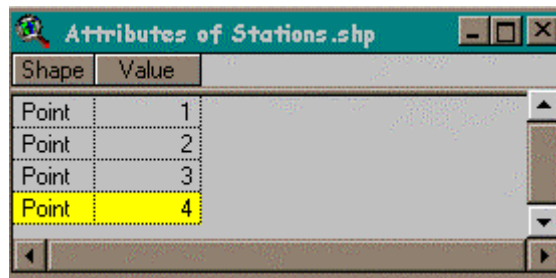


Figure 2.8 Editing the Attribute Table

The **stations.shp** theme must be converted to a grid before delineating the watersheds. This is performed by selecting the menu item **Theme/Convert to Grid**. A grid is defined by its extent and cell size. In most cases, the grids in a project should have a consistent resolution. All of the grids created in this study have the same extent and cell size as the original DEM. Grid specifications are entered into the Analysis Properties box, as shown in Figure 2.9.

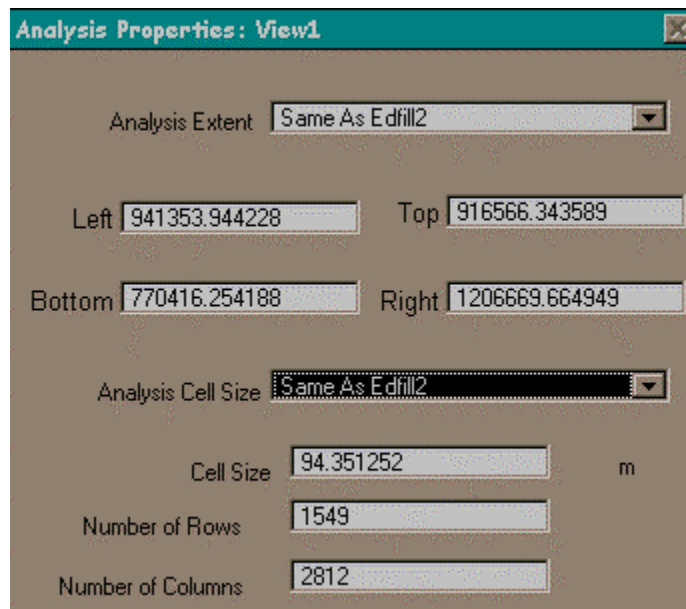


Figure 2.9 Setting the Grid Analysis Environment

Watershed delineation requires a flowdirection grid and an outlet grid. The **watershed** function determines all of the contributing area upstream of an outlet:

Grid: **basingrid=watershed (edfdr, stationgrid)**

Grid: **basins=gridpoly(basingrid)**

The second command transforms the grid from a raster (cell-based) format to a vector (polygon-based) format. Each of the drainage basins are assigned the number of the gauge at the outlet. This completes the watershed delineation process. Figure 2.10 shows the delineated watersheds for the Edwards region.

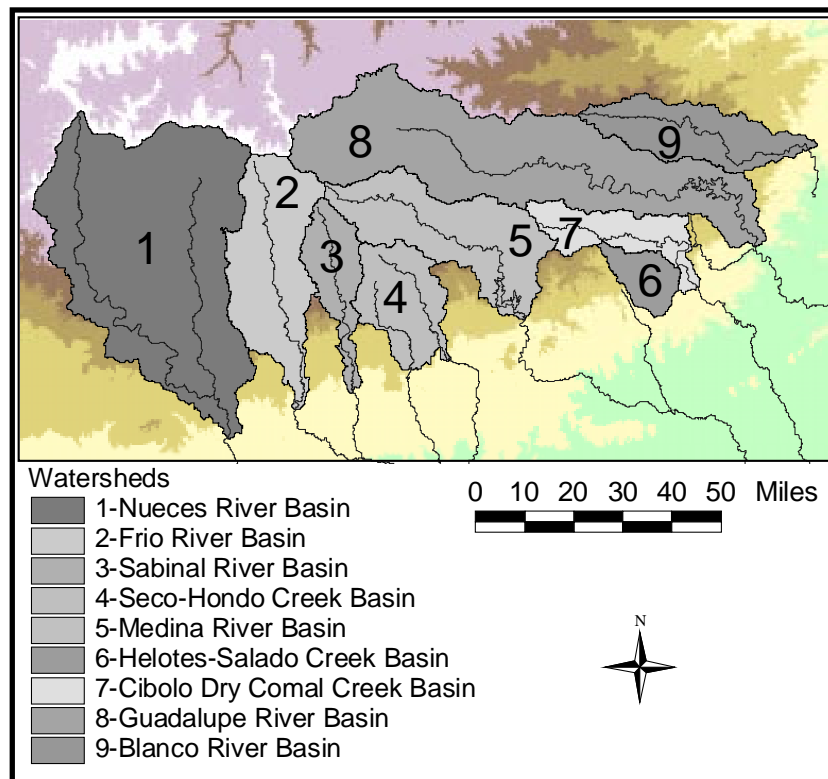


Figure 2.10 Watersheds in the Edwards Aquifer Region

2.3.4 Accuracy Considerations

Accurate representation of the drainage basins is important because their boundaries and total areas are used in subsequent calculations. The watershed boundaries are used to define zones for which average monthly precipitation and temperature are determined. Moreover, the area of a watershed is used by the soil-water balance program to transform water surplus values (mm/month) to streamflows (acre-ft/month) using the following equation:

$$\frac{acre \cdot ft}{month} = \frac{mm}{month} \cdot \frac{1}{10} \frac{cm}{mm} \cdot \frac{1}{30.48} \frac{ft}{cm} \cdot A_{basin} [mi^2] \cdot [5280 \frac{ft}{mi}]^2 \cdot \frac{1}{43560} \frac{acre}{ft^2} \quad (2.2)$$

To assess the validity of the delineated watershed coverage, the areas of the resulting drainage basins are compared to those cited in other references. These values were found to closely approximate data from other sources. Drainage areas for each of the watersheds are provided in Table 2.3.

Table 2.3 Watershed Area Comparison

Watershed	Gauge #	Drainage Area		% Differ
		Delineated	USGS	
Nueces River Basin	8192000	1842	1860	1.0%
Frio River Basin	8197500	641	631	1.6%
Sabinal River Basin	8198500	252	241	4.6%
Seco-Hondo Creek Basin	-----	352	-----	-----
Medina River Basin	8179500	653	634	3.0%
Helotes-Salado Creek Basin	8178700	139	137	1.5%
Cibolo-Dry Comal Creek Basin	8185000	273	274	0.4%
Guadalupe River Basin	8168500	1545	1520	1.6%
Blanco River Basin	8171300	410	412	0.5%

The data cited from the USGS are obtained from the stream gauge web site that was previously cited. The maximum percent difference between a

delineated watershed area and that cited by the USGS is 5% for the Sabinal River Basin. This level of accuracy is considered sufficient for modeling purposes. Once the watershed coverage is obtained, it can be used in the climate interpolation process, as described in the next chapter.

Chapter 3: Historical Climate

Climate is a primary driving force for surface and groundwater hydrology. Chapter 6 discusses the impact of climate change on the Edwards Aquifer. Historical precipitation and temperature records are described in this chapter. In order to predict the system's response to climate change, historical climate and its effects must first be understood. The data sets used were developed by the Vegetation/Ecosystem Modeling and Analysis Project (VEMAP) (Kittel et al., 1997). The precipitation and temperature records cover a 99 year period, from January 1895 to December, 1993. This chapter also discusses the interpolation of these data from a 0.5° by 0.5° grid to average monthly values for each drainage basin.

3.1 VEMAP CLIMATE DATA

Average monthly precipitation and temperature data were provided by VEMAP on a 0.5° latitude/longitude grid. The data for the Edwards Aquifer region were provided by VEMAP for the area from 28° to 32° north latitude and 97° to 101° west longitude. In order to decrease the amount of processing time needed to interpolate the data for the watersheds, only data covering the area from 28.5° to 31° north latitude and 97.5° to 101° west longitude are considered. The excluded area, on the north and east section of the grid, does not contain any part of the Edwards Aquifer. VEMAP coverage of the study region is illustrated in Figure 3.1.

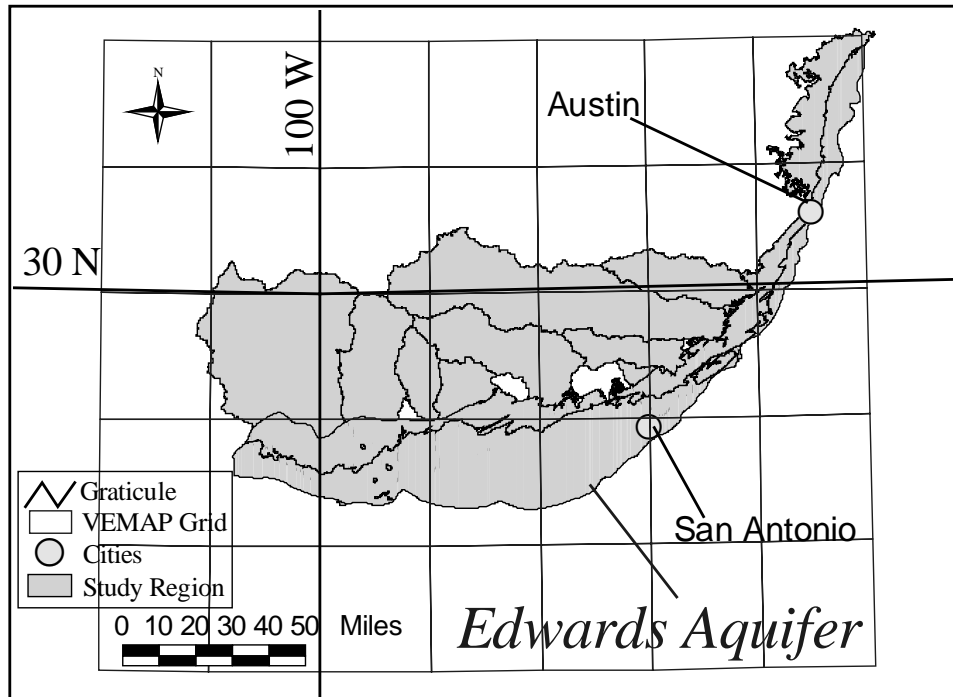


Figure 3.1 VEMAP Coverage of the 0.5° Cells in the Study Region

VEMAP is a two-phased study which examines the response of vegetation life-form distribution models and ecosystem physiology models to normal and altered climate forcing. In the first phase, a climate data set was developed that was not historical, but captured long term means for temperature, precipitation, solar radiation and humidity. This data set represented a “characteristic” year for use in the models. The goal of the second phase is to run the models using a long-term set of historical data. The records provided for the Edwards study were developed for this purpose.

3.1.1 Historical Precipitation

VEMAP interpolated observations from over 8,500 precipitation stations to a 0.5° by 0.5° grid for the contiguous U.S. The data set was developed using the Parameter-elevation Regressions on Independent Slopes Model (PRISM) (Daly et al., 1994). PRISM uses Digital Elevation Models (DEMs) to divide the landscape into regions of similar elevation and slope. The model considers the role that terrain plays in climate conditions. Statistical regression was used to interpolate observations from precipitation stations to grid points at other locations and elevations. As a qualitative analysis, the precipitation data provided by VEMAP are modified using a 12-month moving average over the period of record. Modified precipitation data for the area from 29° to 29.5° north and 98.5° to 99° west are presented in Figure 3.2.

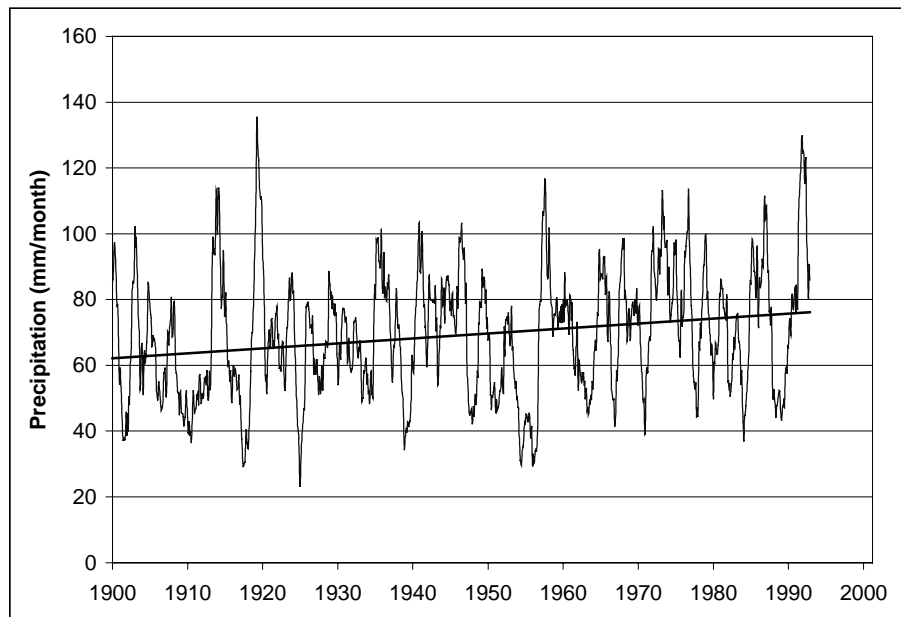


Figure 3.2 Historical 12-Month Moving Average Precipitation

The average precipitation for the area from 29° to 29.5° north and 98.5° to 99° west is 65 mm/month or 780 mm/year. The highest average monthly precipitation occurs in May, while the lowest occurs in January. These values are 189 mm/month and 42 mm/month, respectively. A trendline was included in Figure 3.2 for informational purposes. It is interesting to note that rainfall averages show an increasing slope of 1.8 mm/year², or approximately a 20% increase over the period of record, from 1895 to 1993.

3.1.2 Historical Temperature

Minimum and maximum temperature observations from 5,500 stations were used to create the VEMAP data set. The station records were adiabatically lowered to sea level and then interpolated to the VEMAP grid. The effect of temperature on elevation was then taken into account using a DEM. In order to display the temperature records (Figure 3.3), the data were modified using a 12-month moving average. A moving average has the effect of dampening temperature extremes. Modified temperature data for the area from 29° to 29.5° north and 98.5° to 99° west are presented in Figure 3.3.

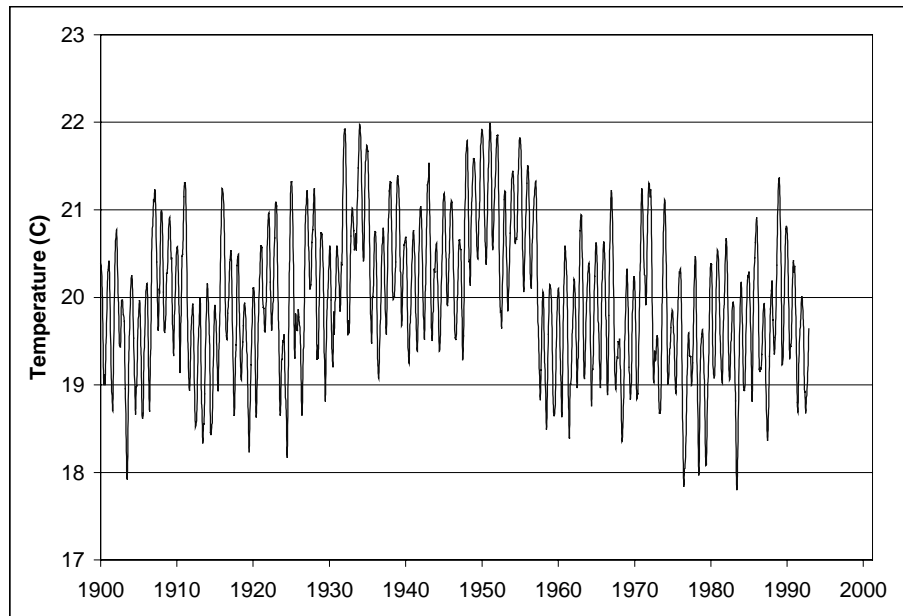


Figure 3.3 Historical 12-Month Moving Average Temperature

The average monthly temperature for the area from 29° to 29.5° north and 98.5° to 99° west is 19°C (67°F). The average maximum temperature occurs in August while the average minimum temperature occurs in January. These temperatures are 26°C (79°F) and 12°C (54°F), respectively. As a consistency check, these data were compared with normal daily mean temperature records for the city of San Antonio provided by the National Oceanic and Atmospheric Administration (NOAA) National Climatic Data Center (<http://www.ncdc.noaa.gov/ol/ncdc.html>) (NOAA NCDC, 1997). The average monthly temperature from 1961 to 1990 for the city of San Antonio was 20°C (69°F). There is a 3% difference between the average cited by NOAA and the 19°C (67°F) value calculated from the VEMAP data set.

3.2 CLIMATE MAPPING

The data provided by VEMAP comes in a raw text format that must be processed for use in the study. There were 63 files for each variable (precipitation, minimum temperature, and maximum temperature). Each file represents a 0.5° by 0.5° cell on the VEMAP grid. The files contain average monthly climate data for the 99-year time period between January 1895 and December 1993 (1,188 months). The files are not geographically referenced, but a file naming convention was defined in which file '1' was the upper left cell and file '63' was the lower right cell. The naming convention followed the grid from left to right, then top to bottom. These files were copied into an Excel spreadsheet and then save in a dBase format for use in ARC/INFO.

3.2.1 Processing Climate Data in ARC/INFO

A GIS representation of the VEMAP grid must be created to geographically reference the climate data. A grid is defined by its origin, cell size, and the number of rows and columns it contains. The origin is the lower left-hand corner of the grid, specified in geographic coordinates. In ARC/INFO, the **generate** command is used to create a coverage. This initializes the following dialog:

```
Arc: generate VEMAP
Generate> grid
Grid Origin Coordinate (X,Y): -101, 31
Y-Axis Coordinate (X,Y): 0, 31
Cell Size (Width, Height): 0.5, 0.5
Number of Rows, Columns: 7, 5
Generate> quit
```

After the dialog is entered, a polygon coverage consisting of 0.5° by 0.5° grid cells is created. The coverage must then be projected from a geographic coordinate system to TSMS using the procedure outlined in Chapter 2. After projecting, issue the **clean** command to generate polygon topology:

Arc: **clean VEMAP**

In the next step, the climate data is joined to the attribute table of the VEMAP coverage. There is a one-to-many relationship between a single cell of the VEMAP grid and multiple months of data. In order to join the climate table created in Excel to the VEMAP attribute table, the **joinitem** function must be used. **Joinitem** requires a key field which has the same name and definition in both tables. The unique identification numbers (IDs) in the ARC/INFO generated coverage do not coincide with the VEMAP naming convention. Consequently, a linking table must be created which cross references the coverage unique IDs with the VEMAP cell numbers. This table is created in Excel and saved in a dBase format. An example of a linking table is provided in Table 3.1.

Table 3.1 Linking Table from Excel

VEMAP_ID	FILE_ID
1	1
6	2
11	3
*	*
*	*
*	*
31	61
2	62
7	63

The coverage attribute table and the climate data table are joined through the linking table. ARC/INFO does not recognize the dBase file format from Excel. The climate data and linking table files must be converted to an INFO format using the following command:

Arc: **dbaseinfo precip.dbf ppt**

This creates the INFO file **ppt** from the dBase file **precip.dbf**.

The climate table can now be joined to the geo-referenced grid using a two-step process. The **joinitem** command is used to first join the linking table to the coverage attribute table. The same command is then used to combine the attribute and climate tables. The dialog is summarized below.

Arc: **joinitem VEMAP.pat linktable VEMAP.pat VEMAP_ID VEMAP_ID**

Arc: **joinitem VEMAP.pat ppt VEMAP.pat FILE_ID FILE_ID**

The previous two commands modified the polygon attribute table (PAT) for the VEMAP coverage to first add the linking table and then the precipitation table. Spatial and temporal variation of climate can now be displayed in ArcView.

3.2.2 Climate Variability

Mean precipitation and temperature data were calculated for each VEMAP grid cell. The calculations were joined to the attribute table of the VEMAP coverage following the previously described procedure. Spatial climate trends are more observable when the data is presented on a map. Maps of historical average precipitation and temperature data for the period from 1895 to 1993 are presented in Figure 3.4.

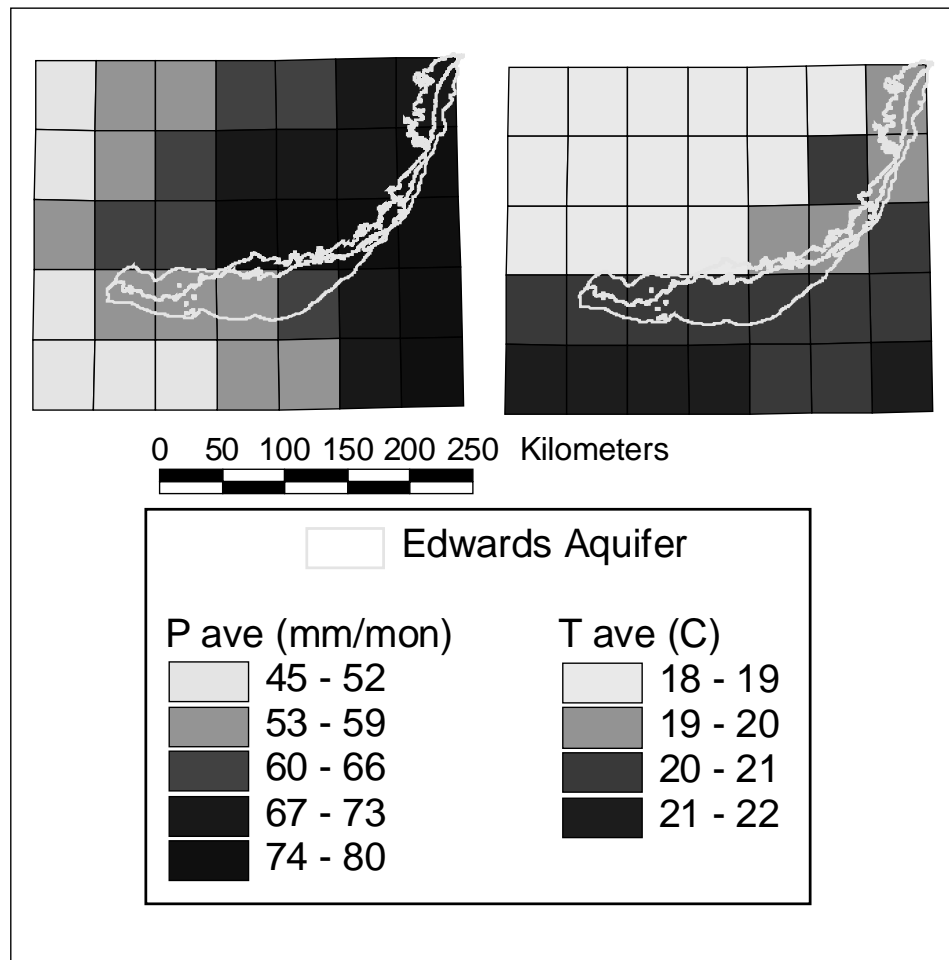


Figure 3.4 A Map of Historical Average Climate Data from 1895 to 1993

A close correspondence exists between climate conditions within the 0.5° by 0.5° grid cells and the climate conditions for the entire study area. The average precipitation of 65 mm/month and average temperature of 19°C are closely matched for many of the cells. Precipitation shows an increasing trend from west to east. Temperature appears to increase to the south. Precipitation has a higher spatial variability than temperature. This makes sense considering that

precipitation is a highly random event while temperature change is strongly driven by a continuous diurnal and seasonal cycle.

3.3 CLIMATE INTERPOLATION

In order to model climate effects on surface and subsurface water availability, the VEMAP data were interpolated to the Edwards Aquifer watersheds. This step is necessary because the groundwater simulation program is a lumped parameter model. Input data, aquifer properties, and results are all defined on a watershed basis. A script was written in Avenue to calculate average monthly climate values for each drainage basin using time-series data provided for 0.5° by 0.5° grid cells covering the study region. Avenue is an object oriented programming language that is native to ArcView. The script is generic in that it can be used to calculate statistics for any property over a user-specified period of time. In this project, the program was used to generate tables of precipitation, and minimum and maximum temperatures from January 1975 to September 1990 to cover the same time period as the measured streamflow data set that was used in the project.

The interpolation of climate data from the VEMAP grid to the watersheds involves raster (cell-based) analysis in ArcView. Two base map layers are used in the calculations, the VEMAP coverage is designated as the value theme. The value theme is converted to a grid in which the cells contain the climate data to be interpolated. The watersheds coverage is designated as the zone theme. In grid terminology, a zone is a collection of cells containing the same value. In this case, each of the basins is assigned a unique ID. The objective of zonal analysis

is to identify the cells in the value theme that intersect the cells in a zone theme. The mean of the values in the intersecting cells is then calculated. A single mean is calculated for each watershed. A one-to-one relationship exists between a basin's unique ID and a calculated mean for that basin. The unique IDs and their corresponding means are written to a separate table. The calculation of a zonal average is illustrated in Figure 3.5.

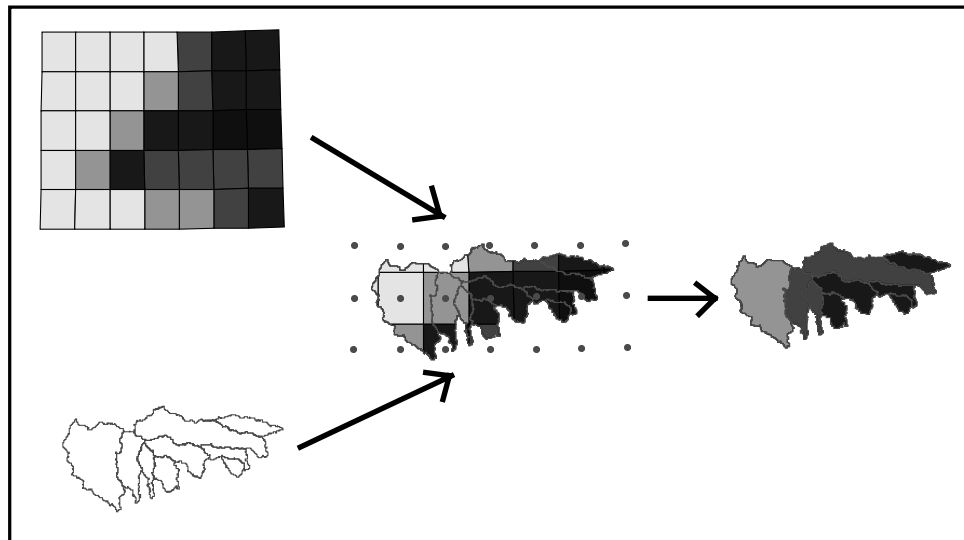


Figure 3.5 Zonal Mean Calculation

The ZoneMean program (Appendix B) was developed using average monthly precipitation data. Precipitation data was used for the purpose of deriving a constant scaling factor for predicting runoff from rainfall. This effort is described in Chapter 4. For each watershed, it is assumed that the rainfall at a given point is the same as that at the nearest data point on the VEMAP climate grid (Chow, Maidment, and Mays, 1988). The average precipitation is,

$$\bar{P} = \frac{1}{A} \cdot \sum_{n=1}^N A_n P_n \quad (3.1)$$

where A is area, N is the total number of data points, and P is precipitation.

The ZoneMean script automates the interpolation procedure allowing more efficient processing of time-series data. The script requires a zone theme, a value theme, and a table to which the results will be written, upon running, a message box will appear prompting the user to enter a zone theme and value theme, as shown in Figure 3.6.



Figure 3.6 Specifying a Zone and Value Theme

The next message box asks for a table to which the calculated means for each basin will be written. This table must be created prior to running the script. It should contain a single field named 'Grid_code' which contains the unique IDs assigned to each watershed. This table can be created in Excel, saved as a dBase file, and then imported into ArcView using the menu option **Project/Add Table**. After the output table is specified, another message box appears requesting the name of the field in the zone theme that contains unique IDs for the watersheds. This field should reference the watersheds in a manner identical to the output table.

The user is asked to specify the fields in the value theme that contain the climate data for the first time step and the last time step. The program then loops through each month, performing the following actions during an iteration:

- Generate a grid of a single month's climate values.
- Execute the ZonalStatsTable request to create a table containing statistics for a particular month.
- Find the field in the statistics table that contains the mean values for each watershed.
- Add a new field to the output table and write the name of the month and its values to this field.

Grid analysis properties must be set for the ZoneMean program to generate monthly climate grids. A grid is defined by its extent and cell size. In most cases, the grids in a project should have a consistent resolution. The VEMAP data are provided on a 0.5° by 0.5° grid. This resolution is too low to accurately capture the spatial extent of the watershed boundaries. Consequently, the VEMAP data are resampled to a cell size of 100 m. Each 100 m cell is assigned the same value as the 0.5° by 0.5° VEMAP cell in which it is contained. The 100 m cell size was chosen to be consistent with the DEM grid that was used to delineate the watersheds. If the cell size is larger, the grid fails to duplicate the watershed boundaries and climate statistics will be less accurate. Figure 3.7 compares the boundaries that result from different cell sizes.

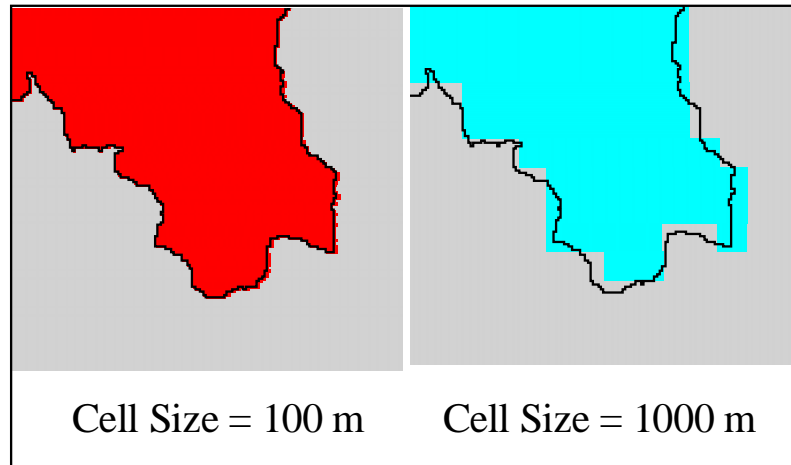
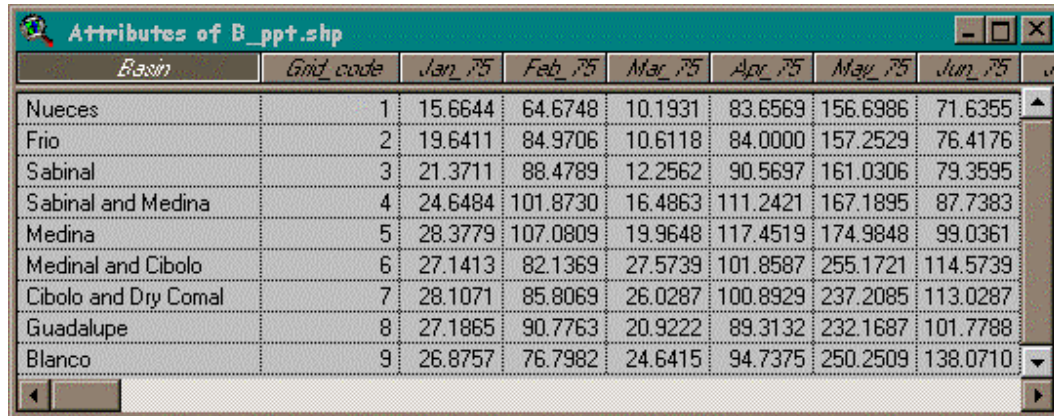


Figure 3.7 Boundary Approximation from Different Cell Sizes

As shown in Figure 3.7, specifying a smaller cell size improves the accuracy of the areal average calculation by creating an area consisting of grid cells that closely approximates the watershed area. A drawback to the greater accuracy achieved with smaller cell size is longer computational times. Using a computer with a 133 MHz Pentium processor, the ZoneMean program took three hours to process the 228 months of data for the period of time between January 1975 and December 1993 with a 100 m cell size. Average precipitation and temperature data were needed for this time period to coincide with historical streamflow time-series provided by Wanakule and Anaya (1993) that were used in the study. An example of the average monthly precipitation values that are determined for each watershed is provided in Table 3.2.

Table 3.2 Average Monthly Precipitation Interpolated for each Watershed



<i>Basin</i>	<i>Grid_code</i>	<i>Jan_75</i>	<i>Feb_75</i>	<i>Mar_75</i>	<i>Apr_75</i>	<i>May_75</i>	<i>Jun_75</i>
Nueces	1	15.6644	64.6748	10.1931	83.6569	156.6986	71.6355
Frio	2	19.6411	84.9706	10.6118	84.0000	157.2529	76.4176
Sabinal	3	21.3711	88.4789	12.2562	90.5697	161.0306	79.3595
Sabinal and Medina	4	24.6484	101.8730	16.4863	111.2421	167.1895	87.7383
Medina	5	28.3779	107.0809	19.9648	117.4519	174.9848	99.0361
Medinal and Cibolo	6	27.1413	82.1369	27.5739	101.8587	255.1721	114.5739
Cibolo and Dry Comal	7	28.1071	85.8069	26.0287	100.8929	237.2085	113.0287
Guadalupe	8	27.1865	90.7763	20.9222	89.3132	232.1687	101.7788
Blanco	9	26.8757	76.7982	24.6415	94.7375	250.2509	138.0710

The ZoneMean program interpolates grid-based climate data for each of the watersheds. After the tables of historical precipitation and temperature are generated, the soil-water balance program can be run to predict streamflows. The use of climate data for rainfall-runoff modeling is described in Chapter 4.

Chapter 4: Climate and Surface Water

The relationship between climate change and water availability from the Edwards Aquifer is strongly influenced by surface interactions. Precipitation, evaporation, and runoff all determine the partitioning of water between the surface, subsurface, and atmosphere. It is impossible to ignore the role that surface water plays in linking climate to groundwater and spring flows. A soil-water balance program developed by Reed, Maidment, and Patoux (1997) is used to simulate the movement of water within the surface region. The objective of the soil-water balance program is to match observed streamflow data. The output from the program becomes the input for the groundwater model. As described in Chapter 5, recharge to the Edwards Aquifer is calculated as a function of surface flows. Thus, the soil-water balance program provides the necessary link between climate and groundwater.

A climate-based runoff model must consider the manner in which factors such as precipitation, temperature, and soil moisture drive the partitioning of water between different media. Relationships involving these factors are developed to predict evaporation, runoff, and indirectly, recharge. In the soil-water balance program, evaporation is a function of temperature and soil moisture (Section 4.3). Runoff is predicted using precipitation and soil moisture (Section 4.4). For both of these relationships, the influence of soil moisture depends on the extent of saturation. Therefore, soil-water holding capacity must be estimated (Section 4.2). The model is calibrated by adjusting constants which

control the effect that precipitation and temperature have on the system. The goal is to optimize the match between predicted and observed inflows.

4.1 SOIL-WATER BALANCE MODEL

The soil-water balance (Reed, Maidment, and Patoux 1997) is essentially an accounting procedure for the water that is introduced to a drainage basin by precipitation. The objective of the model is to accurately reproduce a time-series of historical streamflow measurements from gauging stations which are located at the upstream boundary of the Edwards Aquifer recharge zone. Losses due to infiltration are believed to be minor in the areas above the recharge zone. In these upstream areas, precipitation (P) is distributed between near-surface soil moisture (w), evaporation (E), and rainfall excess, which eventually becomes runoff (Q). A mass balance is performed to determine the amount of water passing into and out of a watershed.

$$\frac{dw}{dt} = P - E - Q \quad (4.1)$$

In the preceding equation, precipitation is the only variable for which measured data is available. Soil moisture, evaporation, and runoff must be estimated using relationships based on available climate data from VEMAP (Kittel et al. 1996). These relationships are described in later sections.

4.1.1 Assumptions

The program to be used in this study is part of a class of models referred to as simple “bucket” models. These models are used to estimate runoff and evaporation for large areas when data regarding humidity, root zone properties,

leaf area indexes, and other types of information are not available or cannot be utilized for some reason. The input data for this project are limited by the availability of scaling factors for simulating future climate scenarios. The original version of the model predicted evaporation based on observed net radiation data. Because $2\times\text{CO}_2$ scaling factors are unavailable for net radiation, an alternative relationship that calculates evaporation as a function of temperature is used.

Soil-water balancing is performed on a monthly time scale. The use of this time scale involves the implicit assumption that rain falls continuously at a low intensity throughout the month. As a result, correction factors must be applied to avoid under-predicting runoff. A monthly time step ignores the fact that precipitation is episodic in nature and runoff is generated when the rainfall intensity exceeds the maximum infiltration rate of the soil. These conditions produce storm runoff over periods of minutes or hours. Another time-scale consideration is that there is a lag between rainfall (surplus generation) and streamflow measurement, when runoff actually reaches a gauging station. Thus, rainfall measured at the end of one month may not reach a stream gauge until the following month. The average extent of an Edwards Aquifer watershed can be represented by a 30-mile square area. As such, significant delays can occur between rainfall and runoff.

Soil that plays an active role in near-surface hydrology is assigned a single property specifying the infiltration capacity for a drainage basin. As a result, soil properties are averaged over space and depth. The estimation of an average water-holding capacity for each watershed is described in Section 4.2. Losses of

soil moisture from percolation to the water table are not considered. Moreover, soil-moisture gain from snowmelt is ignored. In effect, a mass balance is performed over a patch of soil, in which moisture is increased by precipitation and decreased through evaporation and runoff. These assumptions simplify the model in terms of computer and data requirements. They may also introduce a significant amount of error. Model accuracy is discussed in Section 4.5.

4.1.2 Methodology

The soil-water balance program performs an accounting procedure for soil moisture within each drainage basin. Calculations are made on a pseudo-daily basis by dividing VEMAP precipitation data by the number of days in a given month. Daily climate conditions are simulated because relationships used to predict evaporation involve the estimation of solar radiation based on Julian day numbers. For each daily time step, the new soil moisture (w_t) is calculated using the following equation:

$$w_t = w_{t-1} + P - E - Q \quad (4.2)$$

Evaporation (E) and runoff (Q) are predicted using functions developed in later sections.

Initial conditions and constraints are established for soil moisture. In the first time step, soil moisture is set to zero for each watershed. This value is increased during subsequent iterations as an optimal solution is sought (Section 4.5). However, the reason that initial conditions are set at a minimum is because budgeting calculations are started in January or August. The lowest average monthly precipitation occurs during these months and it is assumed that

lack of rainfall causes dry soil conditions. Another condition is established to ensure that mass entering the system equals the mass exiting the system. To close the mass balance, it is assumed that the soil moisture in the first computational time period is the same as the last. Realistically, soil moisture can accumulate or be lost from watershed storage. This assumption is seasonal in nature, however. Soil moisture follows a consistent cycle over the course of a year. Soil that is dry in the summer is replenished by rainfall during the following spring. The final constraints are that soil moisture cannot fall below zero or exceed a drainage basin's water holding capacity (w^*) in a given time period. Soil moisture in excess of the water holding capacity becomes runoff.

The soil-moisture budgeting procedure is summarized below:

1. Set initial soil moisture to zero ($w=0$)
2. For each modeled year:
3. For each month:
4. Calculate E (Section 4.3) and Q (Section 4.4)
5. $w_t = w_{t-1} + P - E - Q$
6. If $w_t < 0$, set $w_t = 0$
7. If $w_t > w^*$, $Q = Q + w_t - w^*$
8. If $w_t > w^*$, set $w_t = w^*$
9. At the end of the year, if $w_{12} \neq w_1$ then go to 3.

The model can be modified to run for any number of months. Although the initial soil moisture is set to zero, it is allowed to vary during the simulation and is not required to have the same value at the beginning of every year. The input data to the model consists of precipitation, minimum and maximum temperature, water holding capacity, and watershed area. VEMAP climate data is interpolated to a drainage basin using the areal averaging procedure described in Chapter 3. Watershed area is determined by delineating drainage basins from a

DEM, as discussed in Chapter 2. Water holding capacity is estimated using the United States Department of Agriculture (USDA) State Soil Geographic Data Base (STATSGO). The procedure used to derive an average water holding capacity for each watershed is explained in the next section.

4.2 SOIL-WATER HOLDING CAPACITY

In the soil-water balance program, the land within a given drainage basin is described using a single property, water holding capacity. This property is the total depth of storage available to water, and is defined as the field capacity minus the plant wilting point. If the amount of water available to soil moisture exceeds the water holding capacity in a given month, the excess is distributed to runoff. An areal average procedure is used to determine water holding capacity values for each drainage basin. Unlike VEMAP climate data, this property is not available on an evenly spaced grid. In the STATSGO database, soil properties are geographically referenced using map units (United States Department of Agriculture 1991). A map unit is linked to several tables which contain information about soil properties. This section describes the Avenue script that is used to extract data from STATSGO tables and determine an average water holding capacity for a map unit. The areal average procedure described in Chapter 3 can then be used to interpolate these values to each watershed.

4.2.1 STATSGO Soils Data

The STATSGO database consists of three tables that group soils according to geographically referenced surface units and vertically distributed layers. The

broadest soil classification is the map unit. The map unit table contains locational information. There are 6,032 map units in the state of Texas and each map unit can contain up to 21 components. A component is defined by a distinct set of vertical soil layers. While the locations of map units are specified by STATSGO, the locations of components are not. A map unit has a specified percentage of its total area occupied by each of its components. The attributes of the component table include USDA soil texture classifications, hydrologic soil groups, and other information pertinent to agriculture. Each component can have up to six vertical layers. Among its many attributes, the layer table specifies the property of interest to this study, water holding capacity. Unfortunately, water holding capacity is defined on a layer-basis. All three STATSGO tables must be utilized to calculate an average water holding capacity for a map unit.

4.2.2 Average Available Water Capacity

The WHCcalc program (Appendix C) was written to derive average water holding capacities for each map unit. The program is a script written in Avenue to read data from the component and layer tables of the STATSGO database. Average available water capacity is calculated using the data, and the result is written to the map unit table. The map unit table provides a geographic reference that can be used to interpolate water holding capacities for each watershed.

The component and layer tables both contain information that is needed to calculate water holding capacity. The attributes that must be retrieved from the component table are:

- Muid-the unique ID for a map unit

- Seqnum-the number that specifies a particular soil component
- Comppct-the percentage of the map unit occupied by a component

The attributes that must be retrieved from the layer table are:

- Muid-same as above
- Seqnum-same as above
- Layernum-the number that specifies a particular layer
- Awcl-a lower limit on estimated water holding capacity
- Awch-an upper limit on estimated water holding capacity
- Laydepl-the soil depth at the top of the layer, in inches
- Laydeph-the soil depth at the bottom of the layer, in inches

The available water capacity (AWC) is similar to porosity. While porosity represents the volume of void space per total volume of soil, AWC indicates the maximum amount of water that could be stored in a two-dimensional soil profile. For example, an AWC value of 0.2 inches of water per inch of soil would mean that 20% of the soil's bulk volume is void space that is available to store water. After all of the data is obtained for a map unit, the water holding capacity is calculated using the equation,

$$w^* = \sum_m \frac{comppct}{100} \cdot \sum_n \frac{1}{2} \cdot (awcl + awch) \cdot (ldeph - ldepl) \quad (4.3)$$

where m is the number of components in a map unit and n is the number of layers in a component. Since $muid$ is known, the estimated available water capacity can then be written to the map unit table. The spatial distribution of water holding capacity is shown in Figure 4.1.

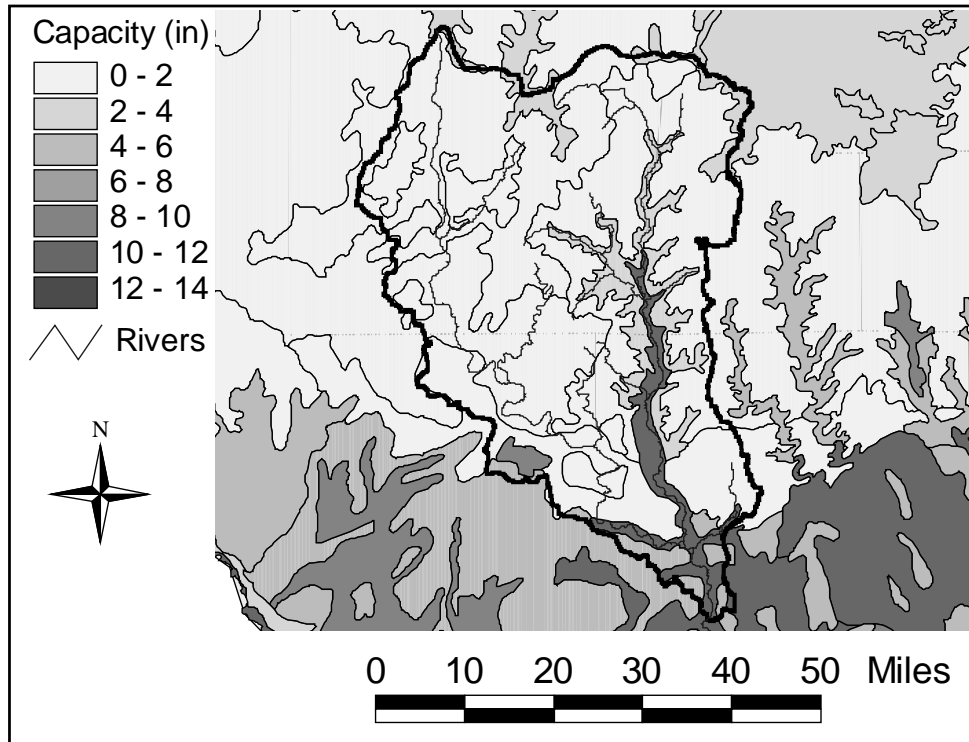


Figure 4.1 Water Holding Capacity in the Nueces River Basin

4.3 EVAPORATION

There are many different methods that can be used to estimate evaporation. The variety of methods reflects the complex interactions that occur in the near-surface zone. Soil, vegetation, and atmospheric factors must all be considered. The most physically realistic functions for estimating evaporation involve an extensive set of input data. As an example, the widely accepted Penman equation considers net radiation, relative humidity, wind speed, and soil heat flux. In a climate-change study, it is difficult to quantify how these factors

would be affected if atmospheric concentrations of CO₂ were doubled. Consequently, only scaling factors for temperature and precipitation are available. The temperature-based Hargreaves equation is used since temperature is closely related to net radiation (Shuttleworth 1993). Given saturated soil conditions, net radiation becomes the dominant control on the evaporation rate.

A conventional two-stage approach is used to predict evaporation. First, the potential evaporation rate is calculated. This is the reference crop evaporation, defined as the quantity of water evaporated from an ideal grass crop with unlimited moisture supply. Potential evaporation is then multiplied by scaling factors which account for non-ideal conditions, such as unsaturated soil and crops other than grass. The most general form of the equation is,

$$E = f \cdot E_p \quad (4.4)$$

where E is evaporation, E_p is the potential evaporation, and f is a scaling factor.

The reference crop evaporation is calculated using the following equation,

$$E_{rc} = 0.0023 \cdot S_o \cdot \delta_T \cdot (T + 17.8) \quad (4.5)$$

where E_{rc} is reference crop evaporation (mm/day), S_o is the water equivalent of extraterrestrial solar radiation (mm/day), and T is temperature in °C. δ_T (°C) is calculated with mean monthly climate data from VEMAP, using the following equation,

$$\delta_T = (\bar{T}_{\max} - \bar{T}_{\min}) \quad (4.6)$$

where \bar{T}_{\max} is the mean maximum temperature (°C) and \bar{T}_{\min} is the mean minimum temperature (°C) for a given month. The extraterrestrial solar radiation (S_o) is calculated from,

$$S_0 = 15.392 \cdot d_r \cdot (\omega_s \cdot \sin \Phi \sin \theta + \cos \Phi \cos \theta \sin \omega_s) \quad (4.7)$$

where d_r is the relative distance between the earth and the sun given by

$$d_r = 1 + 0.033 \cdot \cos\left(\frac{2\pi}{365} \cdot J\right) \quad (4.8)$$

where J is the Julian Day Number. ω_s is the sunset hour angle (in radians) from

$$\omega_s = \arccos(-\tan \Phi \tan \theta) \quad (4.9)$$

Finally, Φ is the latitude of the study area and θ is the solar declination (in radians) given by

$$\theta = 0.4093 \cdot \sin\left(\frac{2\pi}{365} \cdot J - 1.405\right) \quad (4.10)$$

Simply using potential evaporation would result in greatly over-predicted rates. The calculated values are diminished using scaling factors to account for non-ideal conditions. There are two factors used. The first factor is the crop coefficient (K_c). This is a complex factor which considers the amount of resistance a particular crop introduces to restrict evaporation. Different plant species exert varying amounts of control over the amount of moisture that is released to the atmosphere. Moreover, taller plants have a stronger limiting influence than shorter plants. Vegetation characteristics are highly variable in the Edwards Aquifer region. As a result, K_c is used as a calibration parameter. The second factor is a soil-moisture extraction function (K_s). This factor is also related to vegetation resistance, in that soil moisture controls the amount of water available to plants. Evaporation restrictions are minimal when the moisture level increases to the soil's water holding capacity (w^*). Plants are able to extract

water freely under saturated conditions. Water accessibility begins to decrease as soils dry. When the soil moisture reaches the wilting point, $K_s = 0$. The value of K_s is given by

$$K_s = \frac{w}{w^*} \quad (4.11)$$

The complete equation used to predict evaporation is,

$$E = K_c \cdot K_s \cdot E_p \quad (4.12)$$

Having developed a function that predicts evaporation under varying climate conditions, attention can now be turned to the estimation of runoff.

4.4 RUNOFF

Several different methods were investigated to estimate streamflows given VEMAP precipitation data. These methods fall into two separate groups. In the first group, runoff is calculated as a constant fraction of rainfall. In the second group, a soil-water balance procedure is used to distribute rainfall between soil moisture, evaporation, and runoff. Using monthly precipitation under-predicts runoff because these data do not capture short-term storm events. To compensate, an exponential soil-saturation curve is introduced to force a portion of monthly precipitation to be distributed to runoff. The modified soil-water balance method produced a better fit with observed data than the constant coefficient method. However, the benefit of constant coefficient methods lies in their simplicity. As a preliminary approach, an attempt is made to establish a direct relationship between rainfall and runoff. Subsequently, the exponential correction function that is used in the soil-water balance is described.

4.4.1 Constant Runoff Coefficient Method

A single factor relating rainfall to runoff can be established by fitting a straight line to observed data. Straight lines were fitted to graphs of monthly precipitation and streamflow for each of the drainage basins for the period from January 1975 to September 1990. In general, there was a poor correlation between the two parameters and it was decided that direct rainfall-runoff relationships were too general for the Edwards Aquifer region. It was evident that a significant amount of rainfall fails to become streamflow. This observation should be considered in light of the fact that the aquifer receives the majority of its recharge from channel losses in the streams. If the rainfall is not becoming runoff, and also not becoming recharge through percolation, a large amount of water must be lost to evaporation and changes in near-surface soil moisture. Examination of the rainfall-runoff plots revealed trends indicating that evaporation and soil moisture should be considered. Similar patterns were observed between the different watersheds. A graph of rainfall versus combined streamflows for Nueces River Basin gauges 8190500 and 8190000 is provided in Figure 4.2.

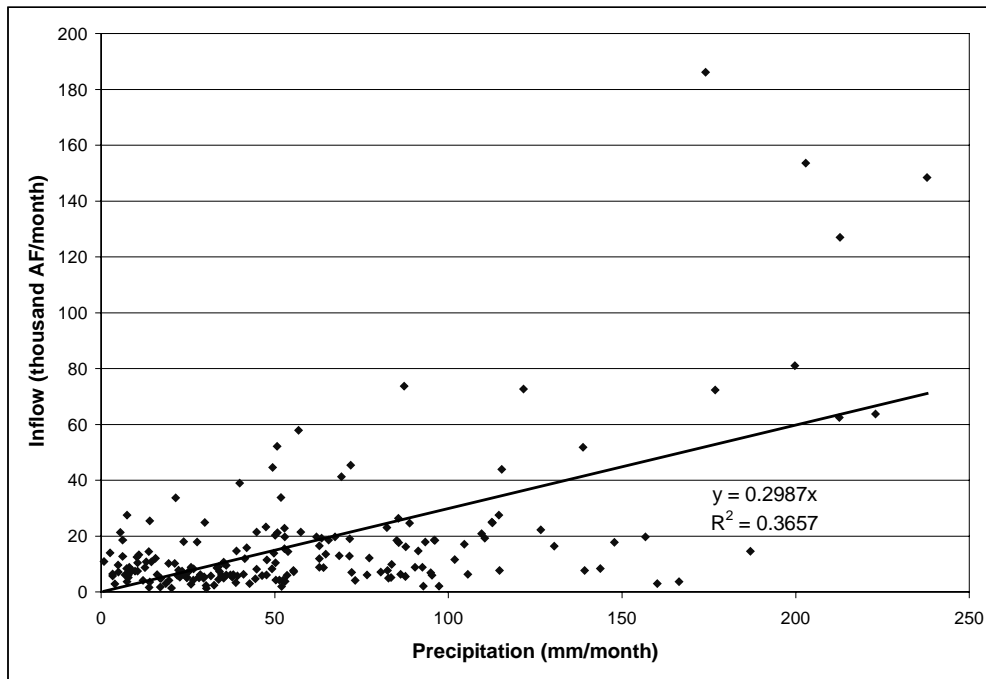


Figure 4.2 Nueces River Basin: Rainfall versus Combined Streamflows from Gauges 8190500 and 8190000 (1975-1990)

One of the drawbacks of using monthly precipitation data to predict streamflow is that it does not consider that rainfall is a periodic event. Looking at Figure 4.2, there are no months where there was zero precipitation. However, examining the daily precipitation data collected at several gauging stations revealed many instances where significant rainfall occurred after an extended number of days where zero precipitation was recorded. A large cluster of data points are observed in which increased monthly rainfall did not result in increased monthly inflows. One explanation for this could be that previous dry periods had left the soil moisture low and the intensity of rainfall during the month failed to exceed the soil's infiltration capacity. Another explanation could be that warmer

temperatures and drier conditions caused greater losses of precipitation to evaporation. Regardless of these hypotheses, the low R-squared value indicates that there is only a weak correlation between monthly precipitation and monthly inflows. An improved fit is achieved by considering the effects of soil moisture and evaporation.

4.4.2 Soil Saturation Curve Method

Conventional soil-water balance models predict surplus when monthly precipitation exceeds evaporation and the soil's water holding capacity is reached (Alley 1984). When this constraint is placed in the model, the watersheds fail to produce any runoff. This incorrect result is caused by the fact that the average water holding capacity for the Edwards Aquifer drainage basins is 89 mm while the average monthly precipitation is only 65 mm. The basins' water holding capacities are never reached. While the constant coefficient method over-predicts runoff, the traditional "bucket" model predicts no runoff whatsoever. A simple moisture accounting procedure based on monthly data ignores short-lived storm events in which the soil's maximum infiltration rate is exceeded by the rainfall intensity.

An exponential soil-saturation curve was introduced by Reed, Maidment, and Patoux (1997) to compensate for the time-scale limitations of monthly data. This function causes an initial abstraction to be removed from the budgeting calculations and automatically distributes a portion of rainfall to runoff. In the absence of excess soil moisture, the following function allocates water for runoff.

$$Q = \alpha \cdot P \quad (4.13)$$

where Q is stream flow, P is precipitation and α is the soil-saturation curve function defined by

$$\alpha = \left(\frac{w}{w^*} \cdot A^{\left(1 - \frac{w}{w^*}\right)} \right) \quad (4.14)$$

where w is soil moisture, w^* is water holding capacity, and A is a constant that is used to calibrate the predicted runoff with observed values. In the next section, the procedure used for calibration is described and the relative accuracies of the soil-water balance model and the constant coefficient method are compared.

4.5 MODEL CALIBRATION AND VALIDATION

The predicted streamflows from the soil-water balance program are used as the input to the groundwater model. The groundwater model was calibrated with measured aquifer levels in a previous study. The input to the groundwater model was a data set of observed streamflows from gauging stations at the upper boundary of the recharge zone. The soil-water balance program was modified in this study to include a calibration mechanism. Three different versions of the soil-water balance program were developed for use in calibration, validation, and climate change modeling (Appendix B). The calibration version is considered in this discussion. The objective of the calibration process for the soil-water balance program was to match predicted streamflows with the set of observed values used in the groundwater model. The data was divided into two sets, one for calibration and another for validation. The model parameters, A and K_c , were first adjusted to obtain the best fit with gauged streamflows from August 1982 to July 1990. Adjusted parameters were then used with measurements taken between August

1975 and July 1983 for model verification. The verification runs actually produced higher correlation values than the calibration runs. These results are described below.

4.5.1 Calibration Procedure

Model calibration is performed using two parameters. The crop coefficient (K_c) inhibits evaporation while the soil-saturation parameter (A) automatically distributes a portion of rainfall to runoff. A separate set of parameters were determined for each drainage basin. For calibration runs, the soil-water balance program requires the user to input a range of values for A and K_c and a watershed for which measures of accuracy will be calculated. The user also specifies parameter intervals. The program iterates over each interval, starting at the specified lower bounds for A and K_c and stepping up to the higher bounds. Rough runs are first performed using large parameter ranges to identify general trends in the level of accuracy. The program is then run with smaller ranges to identify local optima.

Three different measures are used to assess the accuracy of the model for each watershed. The program calculates a correlation coefficient (R-squared), the sum of root-mean-square (RMSE) errors, and the sum of mass discrepancies (SMD) for each combination of values of A and K_c . The program reports the parameter values that give the highest R-squared value and the lowest RMSE value. Initially, only R-squared and RMSE were considered. However, it was determined that the local optima for these measures occurred over different ranges of A and K_c . Using parameters that produce high R-squared values caused the

program to over-predict streamflows while low RMSE parameters produced the opposite effect. The SMD measure is used as a compromise to find the best combination of parameters that meets the constraint that the total difference between observed and predicted streamflow values approaches zero. The calibration procedure can be stated mathematically as

$$\text{maximize } R - \text{squared} = \frac{[n \cdot (\sum_{t=1}^n O^t \cdot P^t) - (\sum_{t=1}^n O^t) \cdot (\sum_{t=1}^n P^t)]^2}{[n \cdot \sum_{t=1}^n (O^t)^2 - (\sum_{t=1}^n O^t)^2][n \cdot \sum_{t=1}^n (P^t)^2 - (\sum_{t=1}^n P^t)^2]} \quad (4.15)$$

$$\text{and minimize } RMSE = \frac{\sqrt{\sum_{t=1}^n (O^t - P^t)^2}}{\sum_{t=1}^n O^t} \quad (4.16)$$

$$\text{subject to } SMD = \sum_{t=1}^n (O^t - P^t) \cong 0 \quad (4.17)$$

where O^t is the observed streamflow and P^t is the predicted streamflow at time step t and n is the total number of months simulated (Ye 1996).

4.5.2 Validation Results

The optimum values for A and K_c determined for the soil-water balance program are compared to the best-fit rainfall-runoff coefficients (M) for each of the watersheds in Table 4.1. The accuracy measures R-squared, RMSE, and SMD are provided.

Table 4.1 Calibration Factors and Associated Accuracy Measures
for Simulated Streamflows (1975-1990)

Watershed	Soil-Water Balance Program					Constant Coefficient (M)			
	A	K _c	R ²	RMSE	SMD	M	R ²	RMSE	SMD
Nueces	0.28	0.99	0.41	0.14	0	0.29	0.39	0.11	-9
Frio	0.64	0.79	0.39	0.13	0	0.22	0.34	0.13	-23
Sabinal	0.45	0.70	0.38	0.19	0	0.09	0.27	0.21	-93
Seco-Hondo	0.13	0.75	0.47	0.21	0	0.16	0.29	0.25	-250
Helotes	0.07	0.76	0.57	0.15	0	0.02	0.36	0.18	-32
Cibolo	0.12	0.99	0.20	0.19	0	0.03	0.09	0.15	36
Blanco	0.27	0.52	0.46	0.13	0	0.16	0.32	0.14	-65

After the best parameter values are found, the model is run using climate data for the period from January 1975 to September 1990. This run is performed to generate the input data set of streamflows for the groundwater model. Using the extended set of climate data, the model obtained the values R-squared = 0.42 and RMSE = 0.15. These measures were obtained by combining the results for all of the watersheds and calculating aggregated values for R-squared and RMSE. The soil-water balance model obtained better results than the constant rainfall-runoff coefficient method in all cases. The average value of accuracy measures obtained by the constant coefficient method was R-squared = 0.29 and RMSE = 0.17. These differences are illustrated in Figures 4.3 and 4.4, which show the predicted and observed streamflows obtained by the soil-water balance model and the constant coefficient method, respectively.

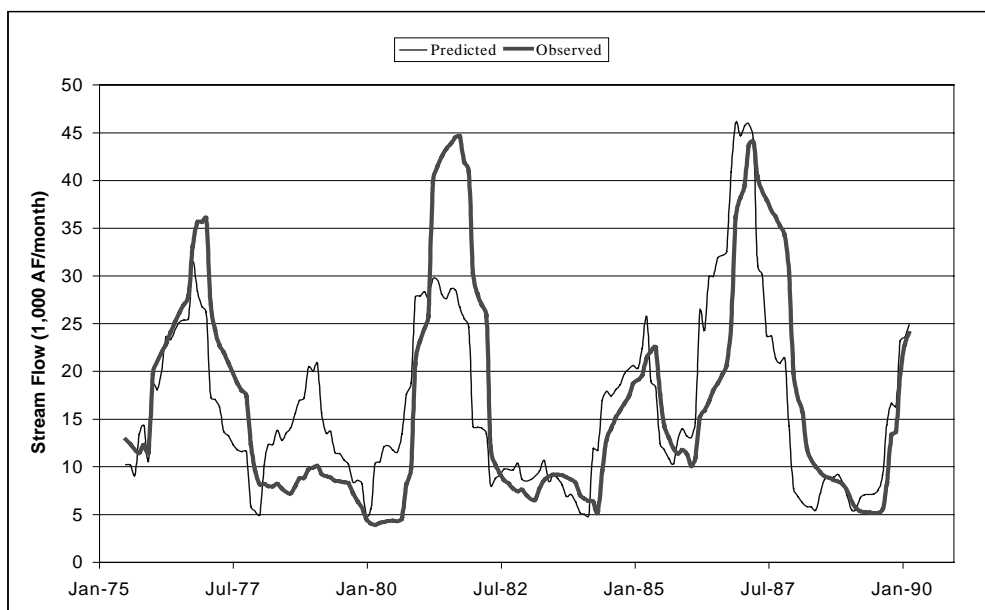


Figure 4.3 12-Month Moving Average Streamflows for the Nueces River:
Observed and Predicted by the Soil-Water Balance Model

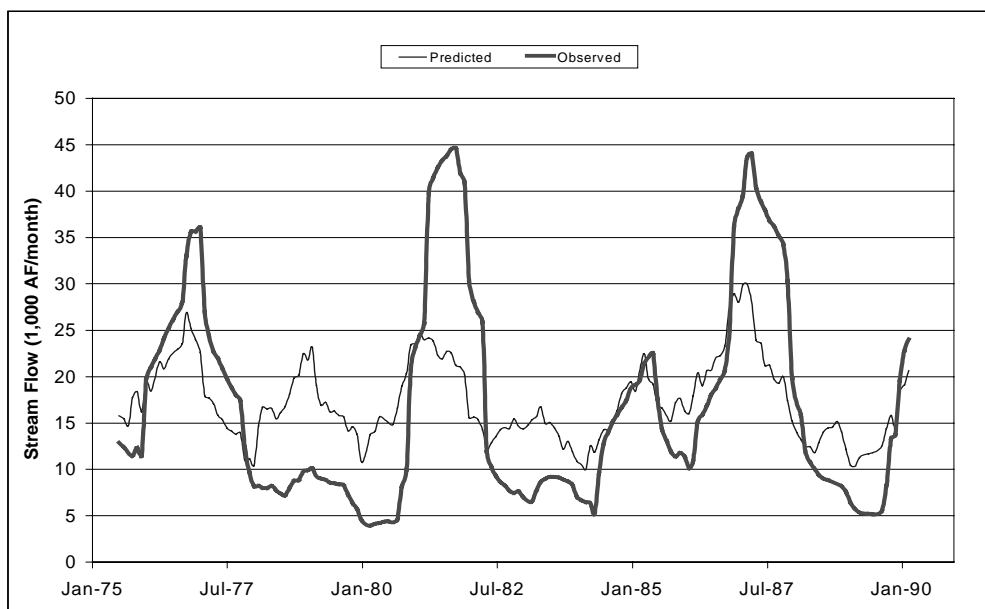


Figure 4.4 12-Month Moving Average Streamflows for the Nueces River:
Observed and Predicted by the Constant Coefficient Method

The soil-water balance model is able to capture streamflow extremes more effectively than the constant coefficient method. Assessing the results for all of the watersheds, the soil-water balance model still tends to under-predict streamflows to a small degree. This becomes an issue when the data are used as input to the groundwater model. Lower streamflows produce lower water levels and spring flows. This is discussed in the next chapter. In comparison to other tributaries in the Edwards region, the Nueces River has higher flow rates. To present results for drainage basins with low to moderate flow rates, Figures 4.5 and 4.6 present predicted streamflows for the Helotes-Salado Creek Basin and the Blanco River Basin, respectively.

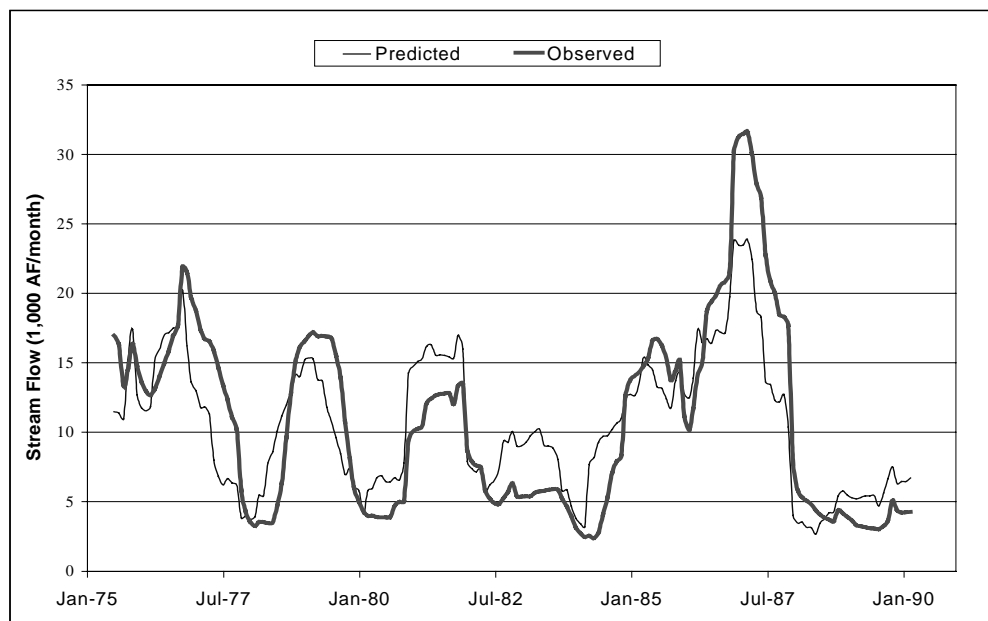


Figure 4.5 12-Month Moving Average Streamflows for the Blanco River

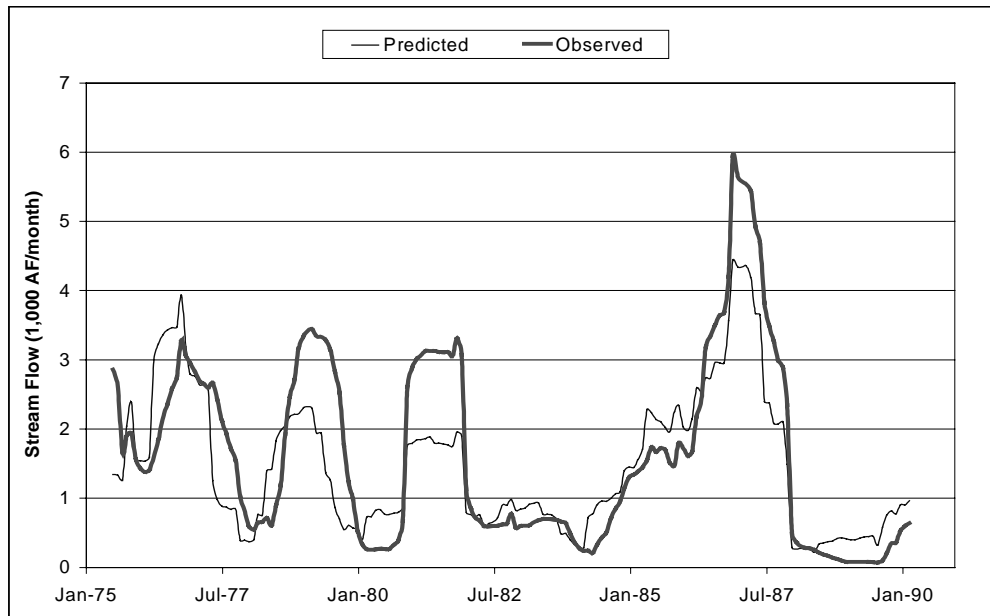


Figure 4.6 12-Month Moving Average Streamflows for Helotes-Salado Creek

The results for drainage basins with low and moderate flow rates are similar to those for the Nueces River Basin. Rainfall is a dominant factor even when soil moisture and evaporation are taken into account. An interesting example of problems inherent to rainfall-runoff modeling can be seen by comparing the simulated and observed streamflows for the period between July 1977 and January 1980. Observed streamflows in the Helotes-Salado Creek and Blanco River Basins peak sharply in response to increased rainfall. Flow rates in the Nueces River Basin, however, indicate a minimal response. The predicted streamflows rise sharply in all three watersheds. Apparently, differing conditions in the Nueces River Basin were not captured by the model. Perhaps daily climate and streamflow data would improve the resolution and allow for more accurate results. Once the streamflow data set is obtained, the groundwater

model can be used to simulate the interaction between surface water and groundwater. This is the topic of discussion in Chapter 5.

Chapter 5: Surface Water and Groundwater

The purpose of this study is to examine the effects of climate change on water levels and spring flows for the Edwards Aquifer. Streamflows are estimated from precipitation and temperature using the soil-water balance program described in Chapter 4. The soil-water balance program provides a link between climate and surface water. Relationships between surface water and groundwater are simulated using a lumped parameter model provided by Watkins (1997) that predicts recharge to the aquifer based on streamflows within the recharge zone. The groundwater program is provided in Appendix B. As a lumped parameter model, the program treats each of the watersheds as a rock-filled tank with uniform properties. The input to each tank is calculated using empirical recharge functions that were developed using flow loss analysis (Wanakule and Anaya, 1993). This chapter provides an overview of the tank model, followed by a discussion of water movement within the aquifer. The recharge functions and program methodology are also described. The tank model completes the link between climate, surface water, and groundwater.

5.1 TANK MODEL OVERVIEW

The Edwards Aquifer tank model is designed to accurately predict water levels and spring flows with minimal input data and shorter run times (Watkins, 1997). The program is a modified version of a groundwater model developed by Wanakule and Anaya (1993). It is a lumped parameter model, in which the system consists of a small number of elements with uniform properties. The

lumped parameter model (also known as the tank model) considers each watershed as an elementary control volume. The input to the model consists of monthly time-series data for the combined inflows from gauges located at the upstream boundary of the Edwards Aquifer recharge zone along with intervening runoff inside the zone. In accordance with USGS recharge estimation methods, intervening runoff is assumed to be proportional to upper gauged flows (Puente, 1978). The soil-water balance program is calibrated to match the input data for each watershed. Water can leave a tank by flowing into another tank, by feeding spring flows, or by being pumped out. The state variable for a tank is its water level. Water level represents the potential to drive flow through the system and is directly related to the storage in each tank. The groundwater model has been calibrated based on water levels in observation wells near the lower boundary of the recharge zone along with measured flows from Comal and San Marcos Springs. A map showing the locations of the gauging stations along with Comal and San Marcos Springs is provided as Figure 5.1. Table 5.1 lists the watersheds and their associated stream gauges and observation wells.

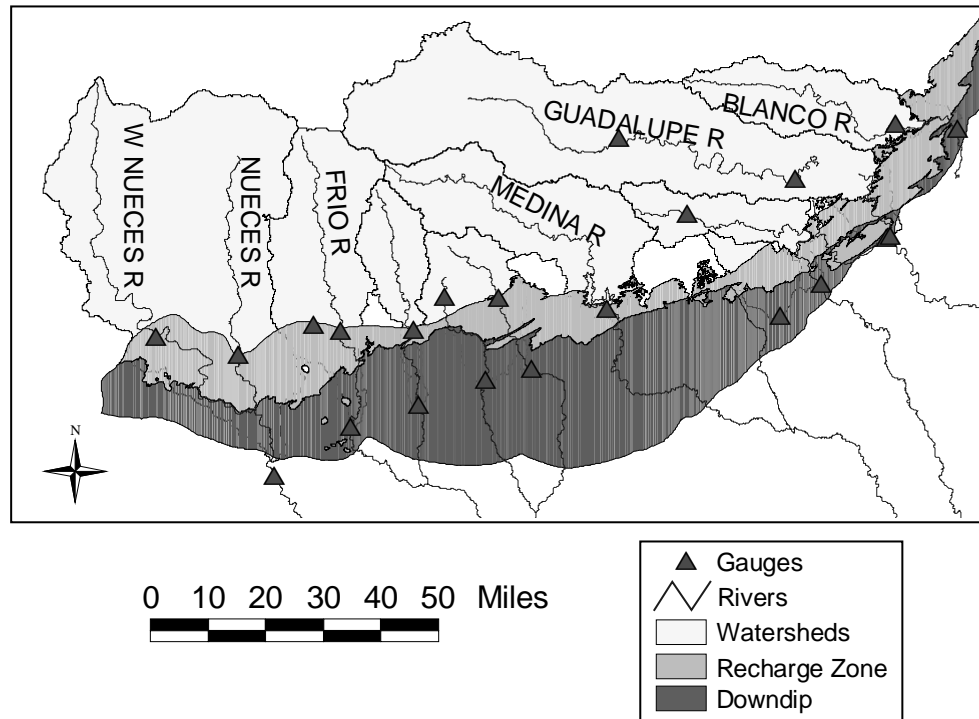


Figure 5.1 Watersheds and Associated Gauges

Table 5.1 Watersheds and Associated Gauges and Wells

Drainage Basin	Upper Gauge	Lower Gauge	Observation Well
Nueces River Basin	08190500 08190000	8192000	YP 69-50-302 (H-5-1)*
Frio River Basin	08196000 08195000	08197500	YP 69-43-804
Sabinal River Basin	08198000	08198500	YP 69-45-401 (I-4-4)*
Seco-Hondo Creek Basin	08201500 08200000	08202700 08200700	TD 69-47-302 (I-3-148)*
Medina River Basin	08179500	08179500	TD 68-41-301 (J-1-82)*

Drainage Basin	Upper Gauge	Lower Gauge	Observation Well
Helotes-Salado Creek Basin	08181400	08178700	AY 68-37-203 (J-17)*
Cibolo-Dry Comal Creek Basin	08183900	08185000	DX 68-23-302 (G-49)*
Guadalupe River Basin	08167000 08167500	08168500 08169000	
Blanco River Basin	08171000	08171300	LR 67-09-110

* Old Well Number

The tank model simulates the flow of water through the aquifer using the fundamental principles of continuity and momentum. The governing equation for a tank is

$$S \cdot \frac{dh}{dt} = R - P - \sum T(h_1 - h_2) \quad (5.1)$$

where R is recharge, P is pumpage, S is storativity, T is transmissivity, and h_1 and h_2 are the water levels in the tank and the next tank downstream as shown in Figure 5.3. This equation is discretized over a monthly time step and individual tanks. The hydraulic properties, storativity and transmissivity, are dependent on water levels. Consequently, their values change throughout the simulation. This results in a non-linear, non-stationary system. Recharge is predicted from surface flows and pumpage is estimated based on monthly pumping data from 1978-1989. The model is developed in more detail in Section 5.4.

5.2 WATER MOVEMENT

The Edwards Aquifer receives the majority of its recharge through channel losses in rivers and streams. There are three river basins that pass through the study area. These are the Nueces, San Antonio, and Guadalupe Rivers. The

Nueces River Basin covers over half of the study area and supplies almost 60% of the recharge to the aquifer. In addition to the larger tributaries, there are several smaller rivers and creeks, including the Blanco, Frio, Medina, and Sabinal Rivers, and the Seco and Hondo Creeks. These water bodies lose major portions of their flow to the aquifer through joints, faults, and sink holes. While the principal direction of surface flow is south and southeast, water lost to the aquifer is redirected. Within the confined portion of the aquifer, water flows to the north and northeast. The aquifer discharges flow through several springs, the largest of which are Comal and San Marcos Springs. Analyses of tritium content in the spring flows indicate that water may spend up to twenty years traversing the aquifer (HDR Engineering, Inc., 1993). Figure 5.2 illustrates the movement of subsurface water.

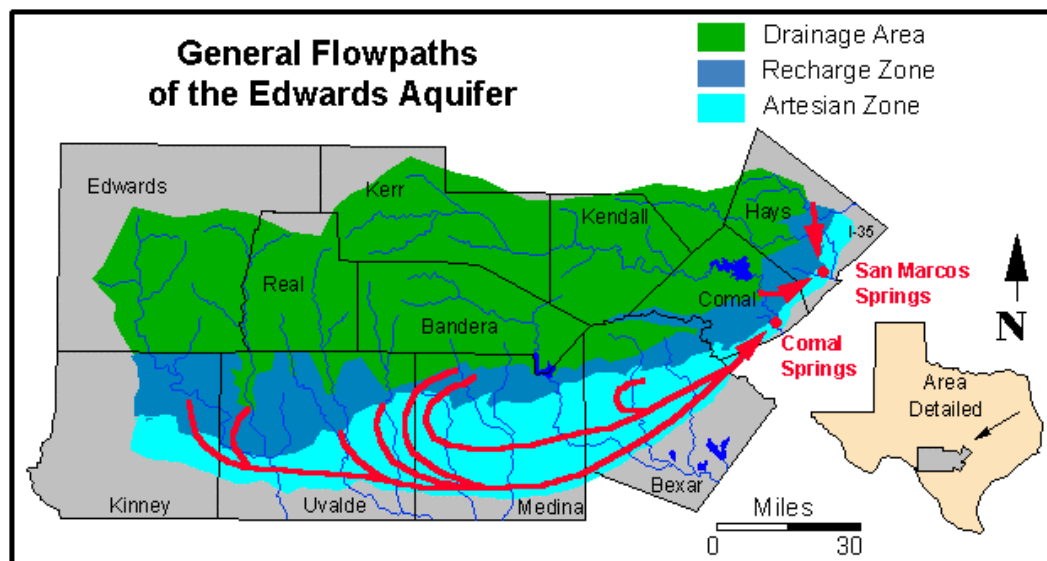


Figure 5.2 Movement of Water Within the Edwards Aquifer
(© Copyright Eckhardt, 1995)

There are nine drainage basins that intersect the Edwards Aquifer recharge zone. Eight of the basins are considered by the model. Although the Guadalupe River crosses the infiltration area, seepage studies have indicated that its recharge contribution is minimal (Puente, 1978). The other watersheds are conceptualized as a series of rock-filled tanks. The tanks are connected according to the flow pattern within the aquifer. Channel losses from streams and rivers are assumed to enter a tank and flow directly to the next tank. The only outlets considered are Comal and San Marcos Springs. Flow patterns and the configuration of tanks are shown in Figure 5.3.

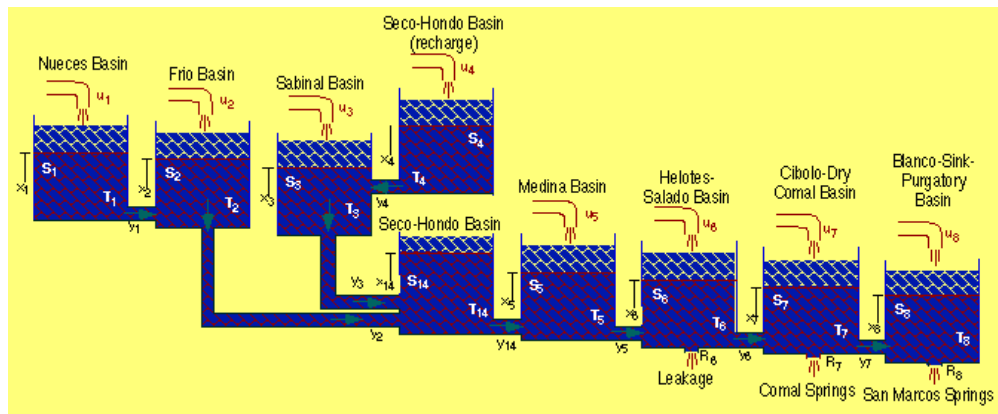


Figure 5.3 Tank Configuration (© Copyright Wanakule and Anaya, 1993)

In addition to the natural discharge of water through spring flows, the Edwards Aquifer also loses water from pumping. Pumping affects water levels within the formation which, in turn, affects spring flows. Pumping rates are taken as a fixed output in the tank model. Pumpage data for the period between 1978 and 1989 were provided by the Texas Water Development Board (TWDB). Analysis of the data provides some insights regarding pumping's effects on water

availability. During 1989, a record high 542,400 AF of water was pumped from the aquifer. The USGS estimates that the aquifer receives an annual recharge of 651,700 AF (Wanakule and Anaya, 1993). Pumping rates are greatest in the eastern portion of the region, where the water is mainly used for municipal purposes. In addition, a large seasonal demand for water is observed in the western areas, where the water is used in agriculture. As it stands, the model does not include a mechanism for testing pumping scenarios. However, modification of the program for these purposes would be relatively simple. For example, the observed pumping rates could be reduced by a percentage if water levels dropped below specific requirements. The exploration of management alternatives is becoming a necessity as pumping rates approach the rate of natural recharge to the Edwards Aquifer.

5.3 RECHARGE FUNCTIONS

The recharge functions used by the tank model provide a mechanism for simulating the interactions between surface water and groundwater. Recharge to the Edwards Aquifer is derived primarily from channel losses in rivers and streams that flow over the outcrop area. Consequently, recharge estimation methods have historically focused on measured streamflows at locations above and below the recharge zone. The amount of recharge can be inferred by using the following mass-balance equation,

$$R = Q_U + Q_I - Q_L \quad (5.2)$$

where Q_U and Q_L are upper and lower gauged streamflows, respectively, and Q_I is the intervening runoff from precipitation.

Much like recharge, intervening runoff is difficult to quantify and must be estimated. Two methods have been previously used for this purpose. The standard USGS method assumes that rainfall and runoff conditions are the same in the recharge zone as they are in the catchment area above the upper gauge (Puente, 1978). Based on this assumption, the intervening runoff is calculated using a scaling factor based on the ratio of the intervening area (A_I) to the catchment area (A_U),

$$Q_I = Q_U \cdot \frac{A_I}{A_U} \quad (5.3)$$

The inflow values used to calibrate the soil-water balance model are the sum of upper gauged streamflows and intervening runoff. The intervening runoff is calculated using the USGS method described above. Instead of assuming that the estimated intervening runoff is accurate and simply subtracting lower gauged streamflows to obtain recharge, Wanakule and Anaya (1993) developed empirical functions by plotting inflow against recharge ratios defined by,

$$RR = \frac{Recharge}{Inflow} = \frac{Q_U + Q_I - Q_L}{Q_U + Q_I} \quad (5.4)$$

where RR is a recharge ratio. Recharge can be estimated without measured streamflows at the downstream gauge using the following equation:

$$R = RR \cdot Inflow \quad (5.5)$$

Wanakule and Anaya (1993) developed recharge functions for each drainage basin using regression analysis with observed data. Their analysis indicated that as streamflow decreases, the volume of recharge decreases, but the

percentage of streamflow lost increases. During dry periods, sometimes flow at an upper gauge is completely lost to the aquifer ($RR = 1$), and there is no flow at the lower gauge. In most cases the recharge ratio is calculated using a non-linear relationship based on inflows but in some basins, water level was also considered due to the presence of a shallow water table. Recharge in the Medina River basin is estimated using a completely different method because of Medina Lake. In this area, recharge to the aquifer is supplied by seepage losses. Recharge is calculated based on the volume of water contained in Medina Lake. The derivation of functions used to estimate recharge is described in more detail in Wanakule and Anaya (1993). For this study, their functions are used without modification.

5.4 METHODOLOGY

The tank model is used to simulate the movement of water for the Edwards Aquifer. Its primary function is to estimate flows into and out of a given tank during a monthly time step. The concepts that form the basis of mass transfer mechanisms are illustrated in Figure 5.4, which depicts a series of three connected tanks with piezometric heads that coincide with water levels in observation wells for separate drainage basins.

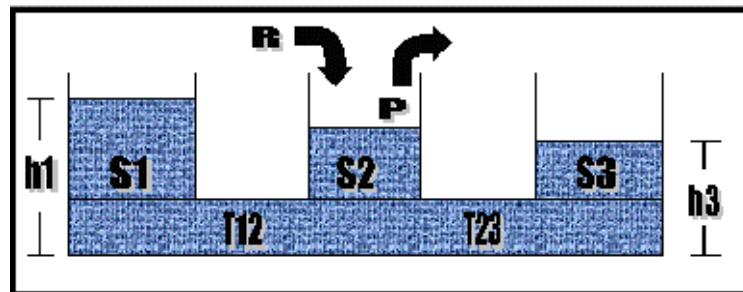


Figure 5.4 Groundwater Transport Simulated with a Tank Model

The variables shown in Figure 5.4 are piezometric head (h), recharge (R), pumping (P), transmissivity (T), and the storage coefficient (S).

Groundwater movement is simulated based on the laws of continuity and momentum. According to the law of mass conservation, the flow into a tank must equal the flow out of a tank. If the system is not at steady-state, the change in the volume of water stored in a tank must also be considered. Assuming an incompressible fluid, the continuity equation can be written as,

$$Q_{in} - Q_{out} = \frac{\partial V}{\partial t} \quad (5.6)$$

where Q_{in} is the volume of water flowing into a tank, Q_{out} is that flowing out of a tank, and $\frac{\partial V}{\partial t}$ is the change in volume of water stored with time (Wang and Anderson, 1982).

The water flowing into a tank may be underflow from another tank or recharge. The tank may lose water to pumping, spring flows, or underflow. Flows between tanks are controlled by their water levels, also known as heads. According to Darcy's Law, water will flow in the direction of decreasing potential, as given by

$$Q_{12} = -T \cdot (h_1 - h_2) \quad (5.7)$$

where T, the transmissivity, is directly related to hydraulic conductivity, and h_1 and h_2 are the water levels in the tank and its adjoining neighbor. The negative sign in this equation indicates that the volume of water in tank one will decrease if it has a higher potential than tank two.

In addition to being tank dependent, water level is also time dependent. To account for transient conditions, the rate of release of water from tank storage

must be estimated. The rate of release is dependent on the potential for flow. The storage coefficient is used to characterize the behavior of an element given a head gradient,

$$S = \frac{\partial V}{dh} \quad (5.8)$$

where $\frac{\partial V}{dh}$ is the change in volume of water stored with a given head differential.

The rate of release from storage can therefore be written as,

$$\frac{dV}{dt} = S \cdot \frac{dh}{dt} \quad (5.9)$$

The following equations were formulated for the tank model by Wanakule and Anaya (1993). Storativity and transmissivity are the only parameters used to characterize the hydraulic properties of the system. They are both dependent on water levels. Transmissivity is calculated using the equation,

$$T = K_T \cdot \frac{(h_1 + h_2)}{2} \quad (5.10)$$

where K_T is a parameter used to calibrate the model. Thus, transmissivity is a link characteristic that is based on the average water levels in adjoining tanks. The function used by the model to calculate storativity is given by,

$$S = K_S \cdot n \cdot h_l^{(n-1)} \quad (5.11)$$

where K_S and n are parameters used to calibrate the model. The storativity parameter is associated with an individual tank.

Watkins (1997) modified the program to solve Aquifer flow equations are using a form of finite-difference method based on Gauss-Seidel iteration and Successive Over Relaxation (SOR). The problem is discretized over time and

space by determining the movement of water for a single tank over a monthly time step.

A mass balance equation can be formulated for a tank by considering the transfer of water between tanks and changes in storage during each time step. By also accounting for recharge and pumping, the continuity equation for two adjacent tanks is,

$$S \cdot [h_i^t - h_i^{t-1}] = T \cdot (h_{i-1}^{t-1} - h_i^{t-1}) + T \cdot (h_{i+1}^{t-1} - h_i^{t-1}) + R_i^{t-1} + P_i^{t-1} \quad (5.12)$$

where i is the tank index and t is the time index. This equation can be rearranged to solve for the water level in the selected tank,

$$h_i^t = \frac{1}{S} \cdot [S \cdot h_i^{t-1} + T \cdot (h_{i-1}^{t-1} - h_i^{t-1}) + T \cdot (h_{i+1}^{t-1} - h_i^{t-1}) + R_i^{t-1} + P_i^{t-1}] \quad (5.13)$$

In the actual program, the general tank equation is modified to account for boundary conditions and spring flows. If the adjoining tank ($i-1$) is actually a boundary, the value of h_{i-1}^{t-1} is represented by the linear equation

$$h_{i-1}^{t-1} = \alpha_i + \beta_i \cdot h_i^{t-1} \quad (5.14)$$

where α and β are calibration parameters. A constant flux boundary is simulated by setting $\alpha_i = 0$, and a constant head boundary is simulated by setting $\beta_i = 0$. Spring flows are also modeled by using a linear relationship. If the adjoining tank ($i+1$) is actually a spring, the third term on the right-hand side of the mass balance equation is modified in the following manner,

$$T \cdot (h_{i+1}^{t-1} - h_i^{t-1}) = -SprK_i \cdot (h_i^{t-1} - SprElev_i) \quad (5.15)$$

where $SprK$ is a calibration coefficient relating spring flow to water level in a tank and $SprElev$ is the spring elevation (ft.) (Ye, 1996). The term is negative,

indicating that the tank loses water if its water level exceeds the elevation of the spring.

The tank model repeats the procedure below for each tank and each time step:

1. Read in initial water levels, stream flows, and pumping rates
2. Read in tank parameters
3. Set $h_i^t = h_i^{t-1}$
4. Calculate T's based on h_i^t , h_{i-1}^t , and h_{i+1}^t
5. Calculate S based on h_i^t
6. Calculate R based on streamflows and h_i^t (recharge function)
7. Calculate Spring flows based on h_i^t
8. Calculate a revised h_i^t using tank continuity equation.
9. If the difference between new h_i^t and old $h_i^t > 0.1$ then go to 4.

The groundwater simulation program was calibrated by Watkins (1996). The program is run in this research without modification using previously compiled data sets for initial water levels, pumping rates, and tank parameters. Documentation for the program is provided in Watkins (1996). A data set of simulated streamflows is created using calculated values from the soil-water balance program. The groundwater model is then run with the simulated streamflow data and with observed streamflow data that was collected by Wanakule and Anaya (1993). The results from these runs are compared in the next section.

5.5 RESULTS

The groundwater model was run with observed streamflow data, as well as predicted values from the soil-water balance model. The objective was to

evaluate whether aquifer water levels and spring flows predicted using climate-modeled streamflows are comparable to those predicted using actual measurements. The accuracy of the predicted values was evaluated by comparing them to well data provided by the Texas Natural Resource Conservation Commission (TNRCC) and spring flow data from USGS. The groundwater model predictions were relatively accurate compared to measured aquifer water levels and spring flows for the period between 1975 and 1990. Using the observed streamflows as input achieved an average R-squared of 0.80. The streamflows predicted by the soil-water balance resulted in an average R-squared of 0.70. This is notable, considering that the aggregate R-squared value for the streamflows predicted by the soil-water balance was 0.42. The reason for the major difference in the level of accuracy stems from the fact that runoff is strongly influenced by random storm events while aquifer water levels are not. Changes in the amount of water stored in the formation are more gradual due to slower hydraulic response times. The relative influence of precipitation on streamflows and water levels is illustrated in Figure 5.5.

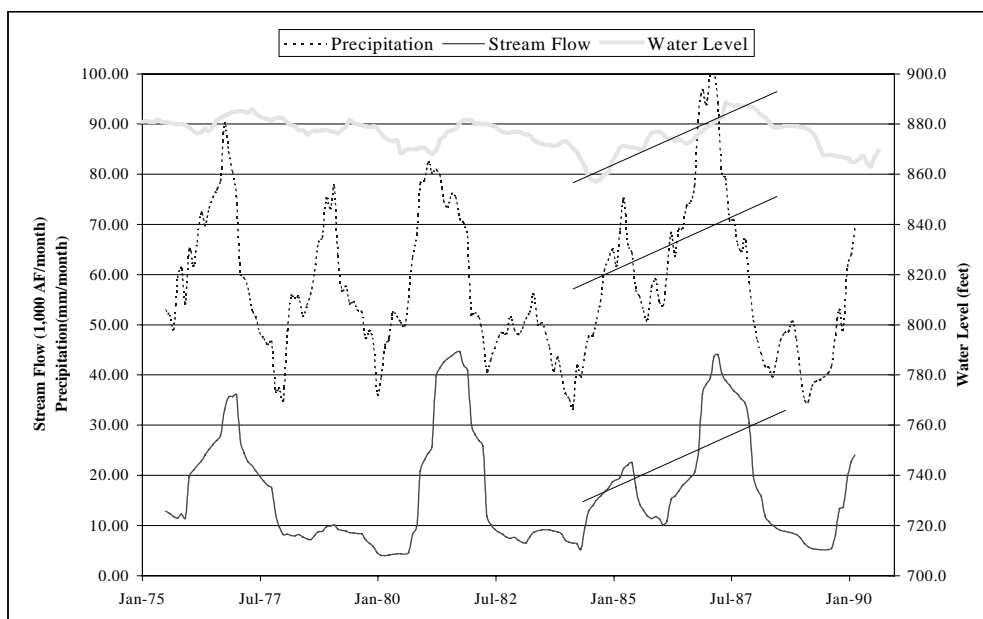


Figure 5.5 Relationship Between Precipitation, Streamflows and Water Levels for the Nueces River Basin

The straight lines are included to highlight the increasing trends in streamflows and water levels caused by changes in precipitation. Water levels also indicate a time lag between climate forcing and aquifer response. This delay would probably be more apparent if values were available on a daily time-scale. However, the relatively short delay time can be attributed to the karst characteristics of the Edwards Aquifer. In alluvial aquifers, the effects of climate change would be more gradual, and less apparent.

As discussed in Chapter 4, the soil-water balance model tended to under-predict streamflows to a small degree, even when a modeling constraint was included to ensure that the total difference between observed and predicted streamflow values approached zero. This trend was reflected in the water levels

and spring flows predicted by the groundwater model. These trends are apparent in Figures 5.6 and 5.7, which show the observed and predicted water levels of the Edwards Aquifer in proximity to the Nueces River Basin and the Helotes-Salado Creek Basin, respectively.

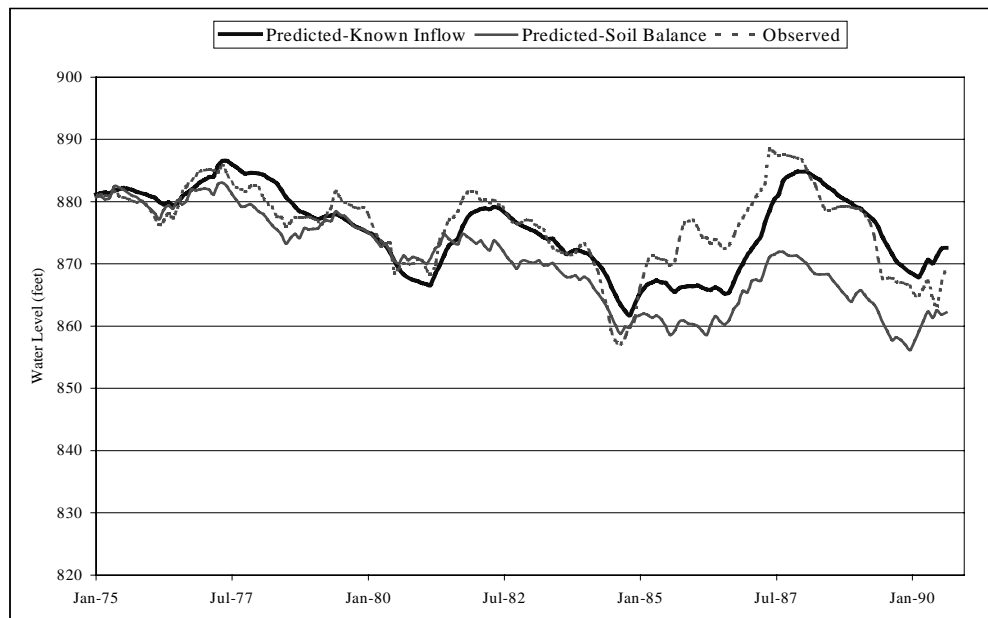


Figure 5.6 Nueces River Basin: Observed and Predicted Water Levels

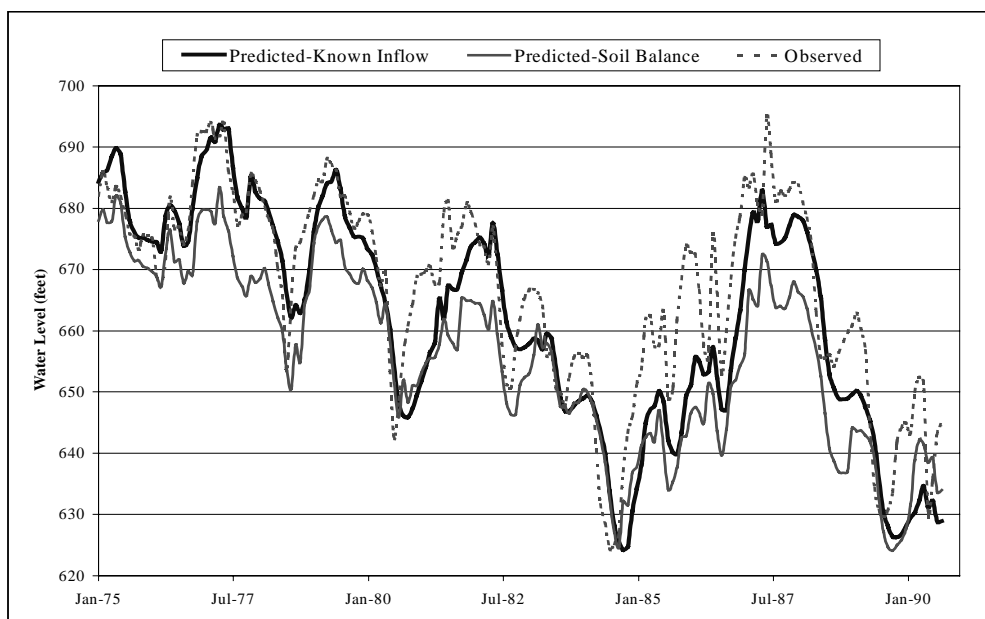


Figure 5.7 Helotes-Salado Creek Basin: Observed and Predicted Water Levels

The Nueces River Basin water levels are somewhat higher than those for the Helotes-Salado Creek Basin. Both of the figures were placed on relative scales to show fluctuations in water levels during the period of record. The region encompassing the Helotes-Salado Creek Basin is heavily pumped to provide municipal water supply for San Antonio. Human influence may be a factor in the increased level of variability in water levels. The potential for recharge increases during periods when the aquifer is depleted, as evidenced by the increased percentage of channel losses that occur during dry periods. According to this hypothesis, climate effects would be magnified by increased pumping of the aquifer. When rainfall is low for an extended duration, changes in aquifer levels are more a reflection of pumping rates. The recharge potential, however,

increases during this time. When wet climate conditions return, the aquifer receives more recharge and water levels are quickly replenished.

Increased pumping has had a marked effect on spring flows in the Edwards region. Comal and San Marcos Springs, the largest springs in Texas, have experienced decreased flow rates. Some of the smaller springs that once had continuous flows are now intermittent. San Antonio and San Pedro Springs, which are located in San Antonio, now stop flowing on a regular basis during certain parts of the year. Spring flows predicted with observed and climate-based streamflows are plotted against actual values for Comal Springs in Figure 5.8.

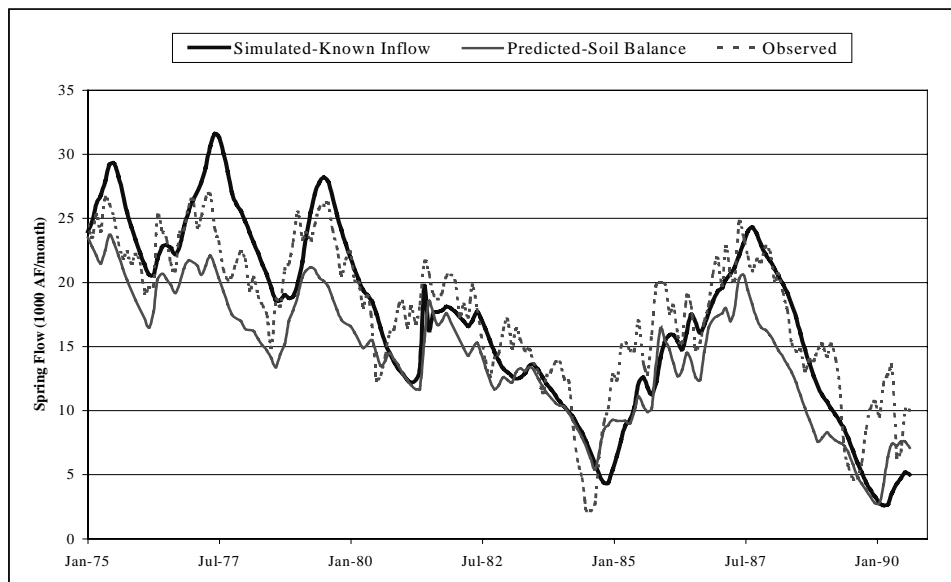


Figure 5.8 Comal Springs: Observed and Predicted Spring Flows

The figure clearly shows lower spring flow estimates resulting from the soil-water balance predicted streamflows. However, the model slightly over-predicted spring flows when observed streamflows were used as input. A

decreasing trend in actual spring flows is also evident. Like spring flows, aquifer water levels have been reduced by increased pumping. Figure 5.9 shows pumping rates and observed water levels for the Helotes-Salado Creek Basin near San Antonio from January, 1975 to September, 1990.

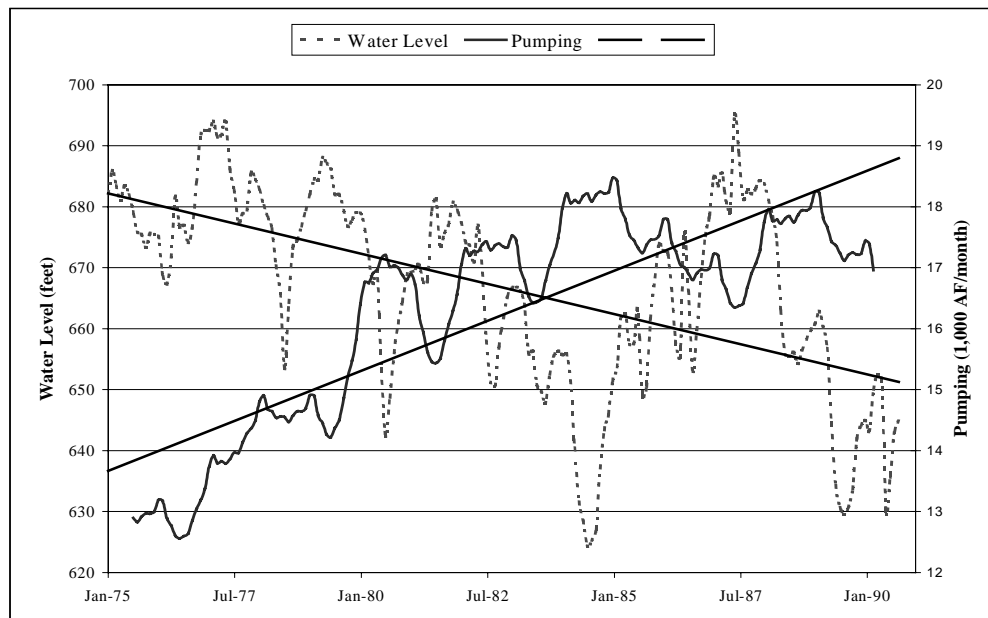


Figure 5.9 Relationship Between Pumping Rates and Water Levels for the Helotes-Salado Creek Basin

This chapter has discussed climatological and anthropogenic influences on the Edwards Aquifer. Chapter 6 will examine the effects of altered climate forcing using scaling factors for precipitation and temperature under 1xCO₂ and 2xCO₂ scenarios.

Chapter 6: Climate Change

Global mean temperatures have increased significantly during the last century. Projected growth of emission rates for greenhouse gases, primarily carbon dioxide (CO_2), will contribute to a temperature rise of 1.5° to 4.5°C by the year 2100. The objective of this study is to examine how future changes in climate will affect water availability in the Edwards Aquifer region. Kittel et al. (1996) and Valdés (1997) used general circulation models (GCMs) to generate scaling factors for precipitation and temperature that simulate the impacts of doubled atmospheric concentrations of CO_2 (2xCO_2) on regional hydrology. The concentration of CO_2 is doubled relative to global averages observed in 1990. Climate models provide a physically-based prediction of how precipitation, temperature and other factors could change under 2xCO_2 conditions. Scaling factors from seven different GCMs are applied to observed climate data and changes in streamflows are predicted using the soil-water balance program. Subsequently, the groundwater model is run using the modified streamflows. This chapter discusses how climate change will influence streamflows, water levels, and spring flows in the study area.

6.1 METHODOLOGY

Scaling factors for precipitation and temperature are provided by VEMAP (Kittel et al., 1996) and Valdés (1997). The scaling factors were derived from the results of GCM runs conducted under normal atmospheric CO_2 concentrations (1xCO_2) and 2xCO_2 conditions and specify change ratios for precipitation

(P_{2xCO_2}/P_{1xCO_2}) and differences for temperature ($T_{2xCO_2}-T_{1xCO_2}$) in °C. Climate change scenarios represent a possible future in which the atmospheric concentration of CO₂ is instantaneously doubled relative to 1990 levels and climate is then allowed to reach a new equilibrium (CSIRO 1996). The estimated values of precipitation, temperature, and other variables under altered CO₂ conditions are generated by GCMs for geographic locations on an evenly spaced grid. These values are then compared to their historical averages (1895-1993). Temperature scaling factors are calculated by subtracting the historical mean from the GCM-generated value at a particular point. Precipitation scaling factors are calculated by dividing the GCM-generated value by the historical average. Scaling factors are essentially measures of climate sensitivity to modified atmospheric concentrations of CO₂.

VEMAP provided 2xCO₂ scaling factors for precipitation and temperature on a monthly, seasonal, and annual basis. For this study, only the annual scaling factors are used. In the future, other researchers will most likely expand this work to include monthly and seasonal scaling factors. The seven GCMs that are considered are listed below:

- Canadian Climate Centre (CCC) (Boer et al., 1992)
- Goddard Institute for Space Studies (GISS) (Hansen et al., 1984)
- Geophysical Fluid Dynamics Laboratory (GFDL)
- R15 runs without Q-flux corrections (Manabe and Wetherald, 1987)
- R15 runs with Q-flux corrections (Manabe and Wetherald, 1990, Wetherald and Manabe, 1990)

- R30 runs with Q-flux corrections (Manabe and Wetherald, 1990, Wetherald and Manabe, 1990)
- Oregon State University (OSU) (Schlesinger and Zhao, 1989)
- United Kingdom Meteorological Office (UKMO) (Wilson and Mitchell, 1987)

Two sets of scaling factors were provided for use in this work. Valdés (1997) provided the results from GFDL R30 10-year equilibrium simulations for $1\times\text{CO}_2$ and $2\times\text{CO}_2$ scenarios. In addition, results were obtained from the VEMAP Phase I database for each of the seven climate models (Kittel et al., 1996). Rather than just using the single set of scaling factors generated by the GFDL R30 10-year simulation runs, results from all of the GCMs provided by the VEMAP Phase I database are considered. Seven sets of scaling factors are used to examine the range of model variability in predicting streamflows, water levels, and spring flows. Differences for temperature predicted by the seven GCMs are shown in Figure 6.1 and change ratios for precipitation are shown in Figure 6.2. Values of the scaling factors for temperature are provided in Table 6.1 and those for precipitation are provided in Table 6.2.

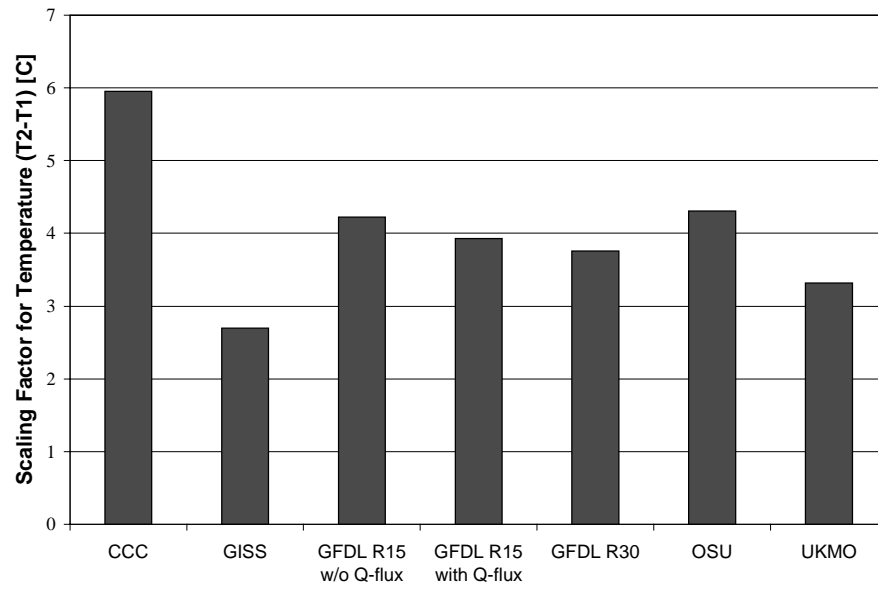


Figure 6.1 Annual Scaling Factors for Temperature from GCMs

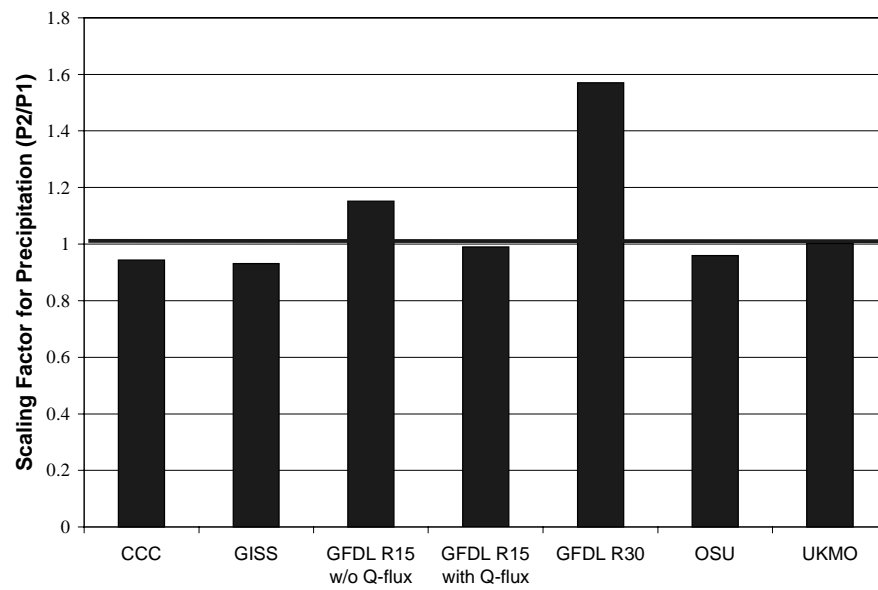


Figure 6.2 Annual Scaling Factors for Precipitation from GCMs

Table 6.1 Annual Scaling Factors for Temperature (°C)

GCM	Temp (T2-T1)
CCC	5.953
GISS	2.700
GFDL R15 w/o Q-flux	4.223
GFDL R15 with Q-flux	3.927
GFDL R30	3.753
OSU	4.305
UKMO	3.318
AVERAGE	3.704
AVERAGE w/o R30	4.071

Table 6.2 Annual Scaling Factors for Precipitation

GCM	Precip (P2/P1)
CCC	0.943
GISS	0.931
GFDL R15 w/o Q-flux	1.152
GFDL R15 with Q-flux	0.990
GFDL R30	1.570
OSU	0.959
UKMO	1.002
AVERAGE	1.078
AVERAGE w/o R30	0.996

The average increase in temperature predicted by the models is 4°C with a range from 2.7 to 6.0°C. The average change ratio for precipitation is 1.08 with a range from 0.93 to 1.57. The precipitation scaling factor from GFDL R30 is considerably higher than those obtained from the other models. If GFDL R30 scaling factors are omitted from the calculation of the mean, the temperature increase is 3.7°C with a range from 2.7 to 6.0°C and the average change ratio for precipitation drops to 1.00 with a range from 0.93 to 1.15. The models produced varying results regarding climate variability. For example, while all of the models

predicted increased temperature, mixed results were obtained for precipitation. In general, GCMs predict temperature changes more accurately than changes in rainfall. According to Valdés (1997), greater seasonal variability in rainfall is forecast by the models. Precipitation tends to increase in the summer and decrease in the spring. Rainfall decreases more frequently in the study region, but extreme wet conditions may also occur. Although monthly and seasonal variability is not considered in predicting streamflows, spring flows, and water levels, it affects annual scaling factors, producing mixed results for rainfall change ratios. Sub-annual variability causes average annual change ratios to be greater than unity for three of the models. The differences provided for each of the seven GCMs are applied to historical time series for temperature, and precipitation data are multiplied by change ratios. The soil-water balance program and groundwater model are then run using the modified data sets. Trends in water availability for 1xCO₂ and 2xCO₂ conditions under normal and increased pumping scenarios are discussed in the next section.

6.2 RESULTS

The soil-water balance program was modified to allow the user to specify scaling factors for precipitation and temperature. Three different versions of the program are included in Appendix B. These versions are used for calibration, validation, and climate change modeling. Using the third version, the program was run with annual average scaling factors from seven different GCMs. After completing the seven model runs, it was determined that the variability in streamflows predicted with 2xCO₂ climate factors covered a consistent range of

outcomes. The GFDL R30 scaling factors produced streamflows that were significantly higher than those predicted by the other models. In contrast, the streamflows predicted using CCC scaling factors were always lower relative to the results from the other simulations. The ratios of average streamflows from 1975-1990 predicted under $2xCO_2$ climate scenarios to the $1xCO_2$ average for the Nueces River Basin in Figure 6.3. Values of the average ratios ($2xCO_2/1xCO_2$) for streamflow are provided in Table 6.3.

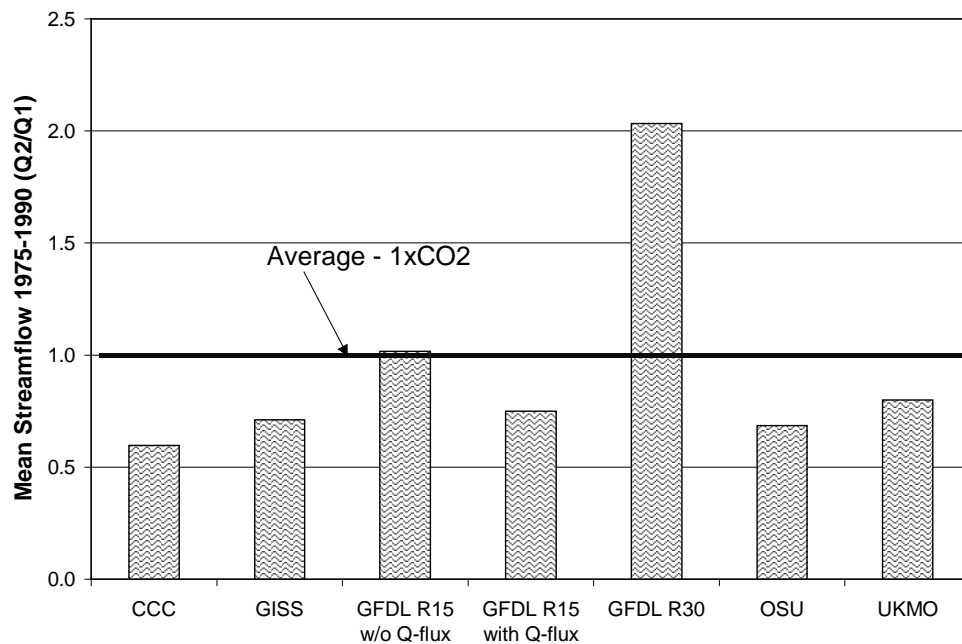


Figure 6.3 Average Streamflow Scaling Factors for the Nueces River Basin from 1975-1990 Predicted from GCM Climate Scenarios

Table 6.3 Annual Scaling Factors for Streamflow in the Nueces River Basin

GCM	Flow (Q2/Q1)
CCC	0.597
GISS	0.711
GFDL R15 w/o Q-flux	1.017
GFDL R15 with Q-flux	0.750
GFDL R30	2.034
OSU	0.684
UKMO	0.800
AVERAGE	0.942
AVERAGE w/o R30	0.760

As shown in Figure 6.3, all of the scaling factors except those for GFDL R30 predicted streamflows that were at or below the average for the 1975 to 1990 period under a 1xCO₂ scenario. Average streamflows dropped from 16,700 AF/month under normal climate conditions to 10,000 AF/month predicted by the CCC model. The average change ratio for streamflow predicted by the models is 0.94 with a range from 0.60 to 2.0; omitting the GFDL R30 results reduces the average to 0.76 and the range varies from 0.6 to 1.0. Climate change essentially forces a redistribution of water resources for the area. Higher temperatures cause more evaporation losses. If these losses are not supplemented by rainfall, runoff decreases. Streamflow trends are more closely correlated with precipitation change ratios than with predicted temperature differences. The unusual results from the GFDL R30 runs are caused by a simulated 57% increase in precipitation.

Modified streamflow data sets from the 2xCO₂ scaling factor runs were used as input to the groundwater model to identify trends in aquifer responses to climate change. Model variability in predicted water levels and spring flows

followed the same trends observed in the soil-water balance program. Figure 6.4 shows average water levels for the Nueces River Basin from 1975-1990 and Figure 6.5 shows these results for the Helotes-Salado Creek Basin. Table 6.4 provides the average change in water levels (ft.) for the Nueces River Basin and the Helotes-Salado Creek Basin from 1975-1990 compared to the annual average for 1975.

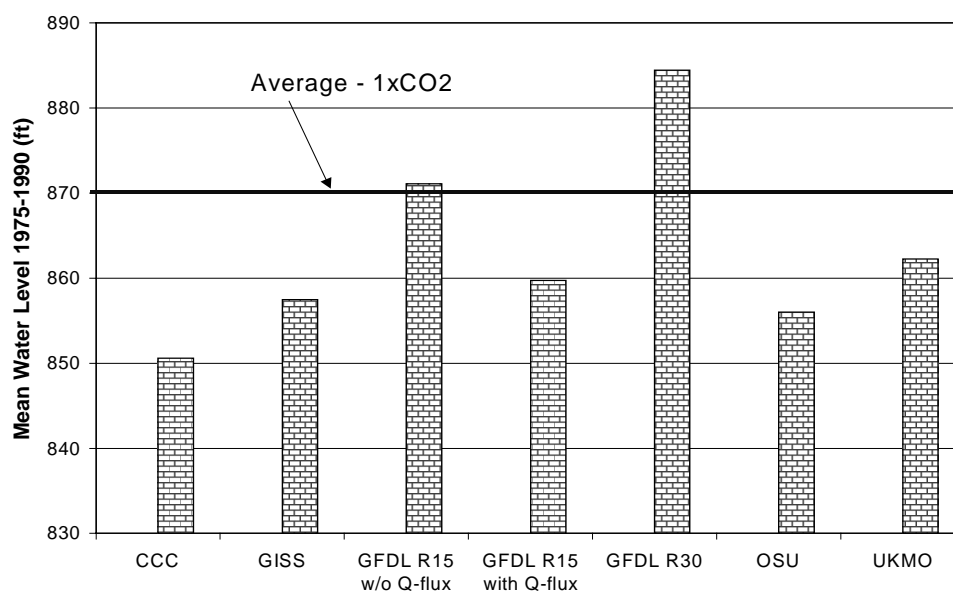


Figure 6.4 Average Water Levels for the Nueces River Basin from 1975-1990 Predicted from GCM Scaling Factors

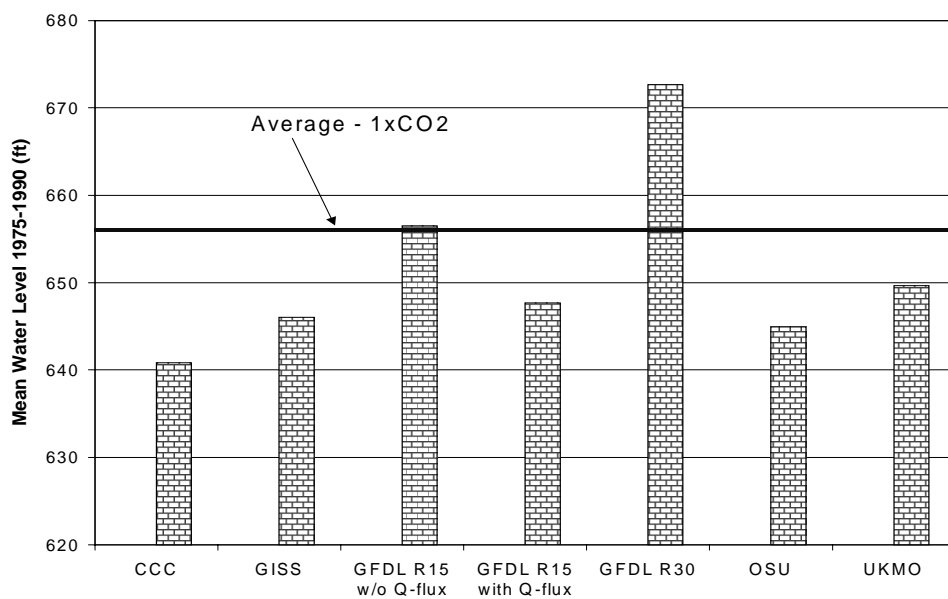


Figure 6.5 Average Water Levels for the Helotes-Salado Creek Basin from 1975-1990 Predicted from GCM Scaling Factors

Table 6.4 Average Change in Water Levels (ft.) from 1975 to 1990

GCM	Nueces Average=880.7 ft.	Helotes-Salado Average=679.4 ft.
CCC	-56.9	-53.1
GISS	-44.3	-47.6
GFDL R15 w/o Q-flux	-20.3	-36.1
GFDL R15 with Q-flux	-40.0	-45.4
GFDL R30	-1.6	-15.9
OSU	-47.1	-48.7
UKMO	-35.6	-43.3
AVERAGE	-35.1	-41.5
AVERAGE w/o R30	-40.7	-45.7
1xCO ₂	-20.3	-36.1

The water levels for the Nueces River Basin are measured using USGS observation well YP 69-50-302, which was formerly numbered H-5-1. Since the Edwards Aquifer gets nearly 60% of its recharge from the Nueces River Basin, these results are indicative of variability in water supply under 2xCO₂ conditions. Higher average water levels correspond to higher streamflows and spring flows. The average decrease in water levels under 2xCO₂ for the Nueces Basin (1975-1990) is 35.1 ft. The water levels for the Helotes-Salado Creek Basin are measured by observation well AY 68-37-203, which was formerly numbered J-17. Comal Springs become intermittent when the level of the J-17 well drops below 620 ft. (Eckhardt, 1995). The average water levels predicted using the seven different GCM scaling factors are higher than 620 ft. However, water levels fall below 620 ft. temporarily during the modeled time period (Figure 6.7). The average decrease in water levels under 2xCO₂ climate scenarios for the Helotes-Salado Creek Basin is 41.5 ft. Figure 6.6 illustrates water level variability over time under 1xCO₂ and 2xCO₂ for the Nueces River Basin. These

results are presented for the Helotes-Salado Creek Basin in Figure 6.7. The lines representing the results from different GCM scaling factors are placed in order from highest to lowest average water levels. The results for normal ($1\times\text{CO}_2$) climate conditions are depicted with a heavier line. Water level variability predicted by the scaling factors from GFDL R15 without Q-flux corrections is very similar to that for $1\times\text{CO}_2$ conditions. Consequently, this line is hard to differentiate from the heavier line for normal climate conditions.

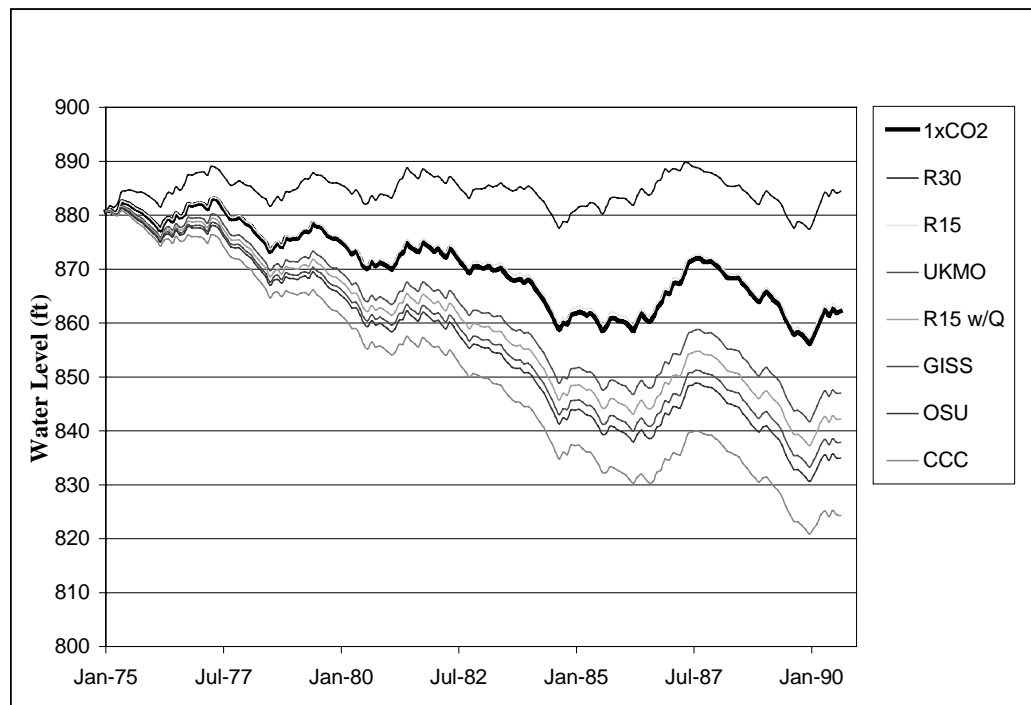


Figure 6.6 Water Level Variability for the Nueces River Basin from 1975-1990 Predicted from GCM Scaling Factors (Legend Ordered by Decreasing Average Water Level)

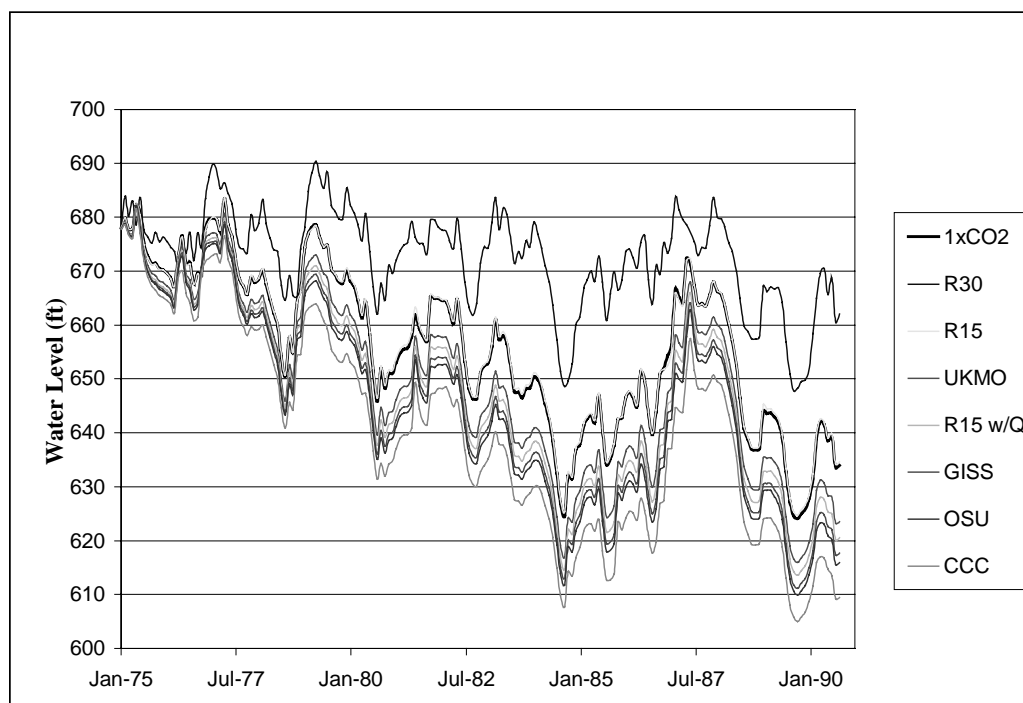


Figure 6.7 Water Level Variability for the Helotes-Salado Creek Basin from 1975-1990 Predicted from GCM Scaling Factors (Legend Ordered by Decreasing Average Water Level)

Water levels predicted using GFDL R30 scaling factors were noticeably offset from the other model results. Six out of the seven GCMs predicted water levels at or below those observed under normal climate conditions. Since the GFDL R30 results do not agree with trends predicted by the other models, and because a 57% increase in precipitation is somewhat questionable, subsequent figures do not include statistics from this particular model. However, the results are considered to be significant, in that water availability in the Edwards region could increase given the possibility of a substantial increase in future rainfall. The range of outcomes for water levels from the majority of the GCMs

considered in this study is shown for the Nueces River Basin in Figure 6.8 for the Helotes-Salado Creek Basin in Figure 6.9, and for the Blanco River Basin in Figure 6.10. The shading that represents model variability extends slightly above the line for 1xCO₂ conditions in all cases. This is difficult to differentiate because the second highest water levels, predicted by the GFDL R15 model, approximate those forecast for normal climate conditions.

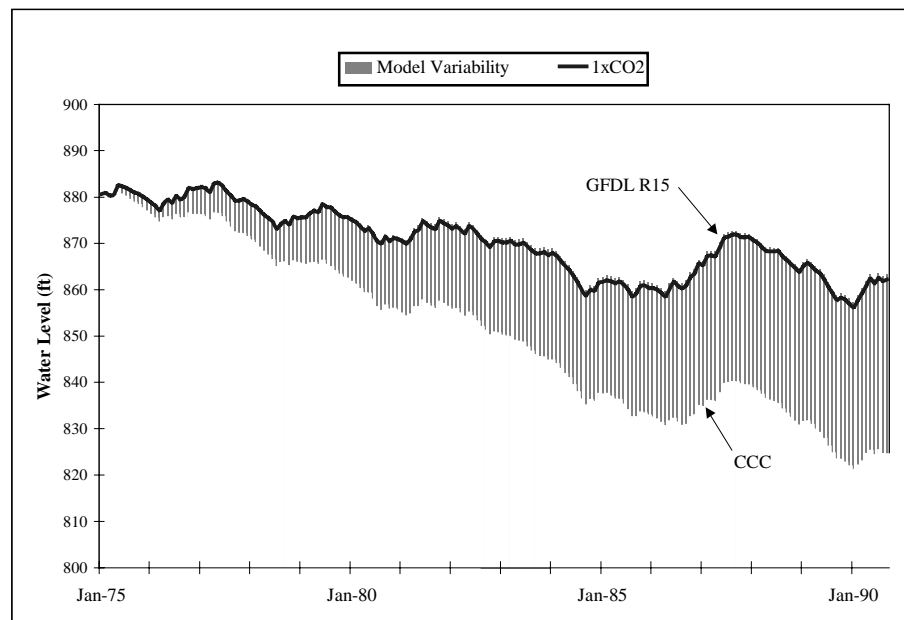


Figure 6.8 Range of Water Level Predictions for the Nueces River Basin

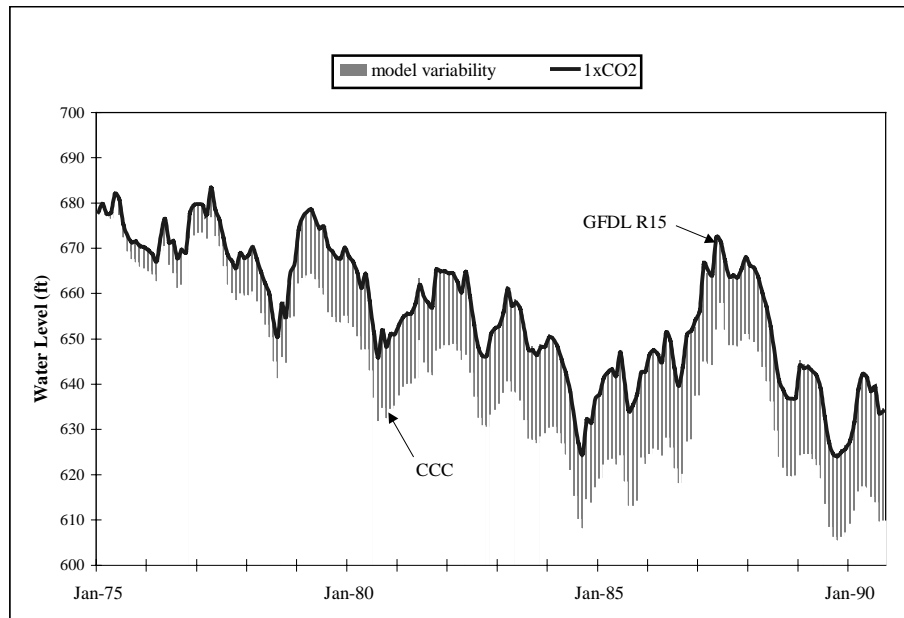


Figure 6.9 Range of Water Level Predictions for the Helotes-Salado Creek Basin

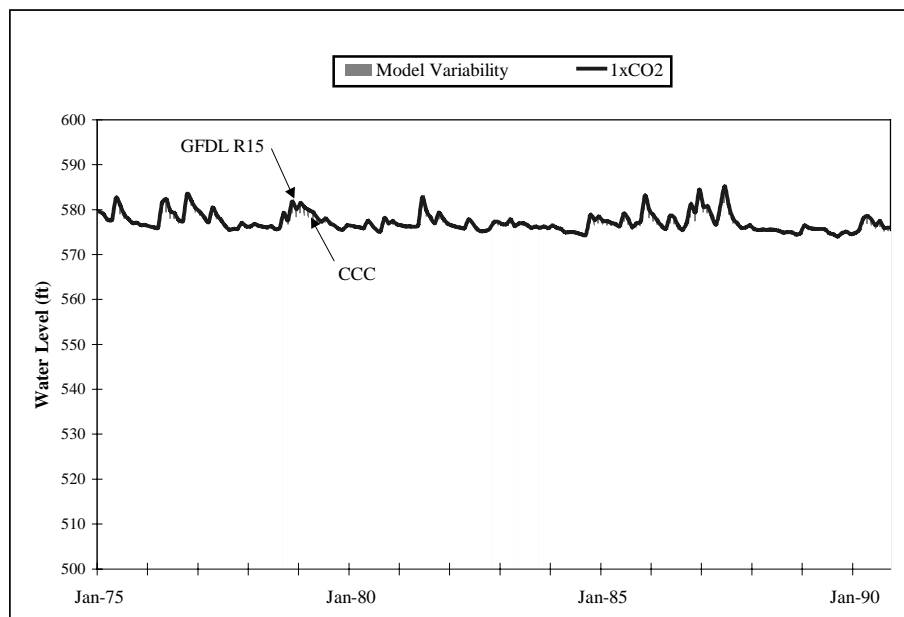


Figure 6.10 Range of Water Level Predictions for the Blanco River Basin

The effects of climate change appear to grow over time for the Nueces River Basin and the Helotes-Salado Creek Basin. However, the Blanco River Basin showed a very limited response to modified climate forcing under $2xCO_2$ conditions. Faulting and complex flow patterns cause some portions of the formation to exhibit greater variability in water levels. In general, regions with lower water level variability are less susceptible to climate change. This is also true for spring flows. San Marcos Springs are not as sensitive as Comal Springs to changes in aquifer water levels. San Marcos Springs receive a large portion of their water supply from local sources of recharge. Comal Springs, on the other hand, are recharged by water originating from farther reaches of the aquifer, as evidenced by analyses of tritium content. Tritium levels in spring flows are indicative of the amount of time the water spent in the subsurface. Comal Springs flows are highly correlated to fluctuations in observed water levels in observation well J-17 (Helotes-Salado Creek Basin). Figure 6.11 compares average spring flows from 1975-1990 predicted under $2xCO_2$ climate scenarios with the $1xCO_2$ average for Comal Springs. These results are presented for San Marcos Springs in Figure 6.12. Values of the average ratios ($2xCO_2/1xCO_2$) for Comal and San Marcos Springs are presented in Table 6.5 and Table 6.6, respectively.

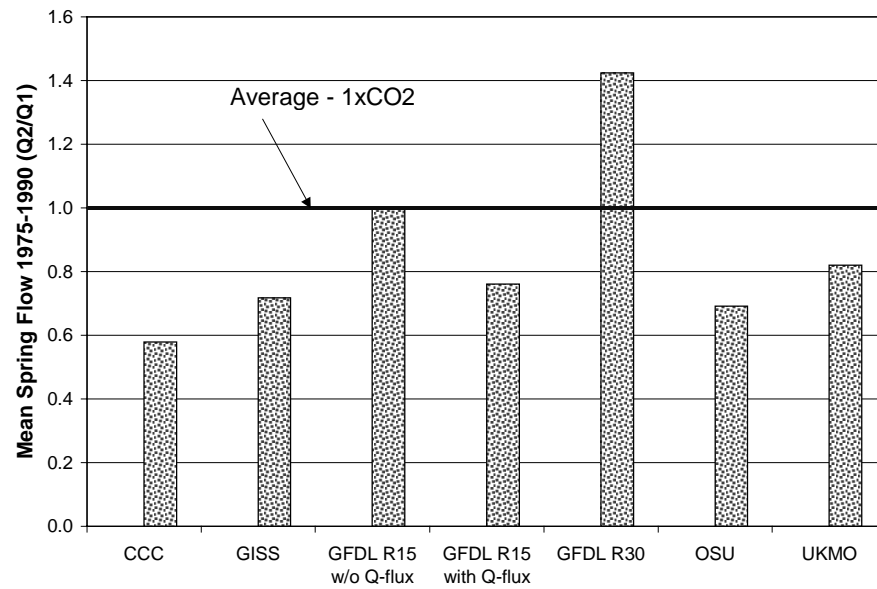


Figure 6.11 Average Scaling Factors for Spring Flows from Comal Springs Predicted from GCM Climate Scenarios (1975-1990)

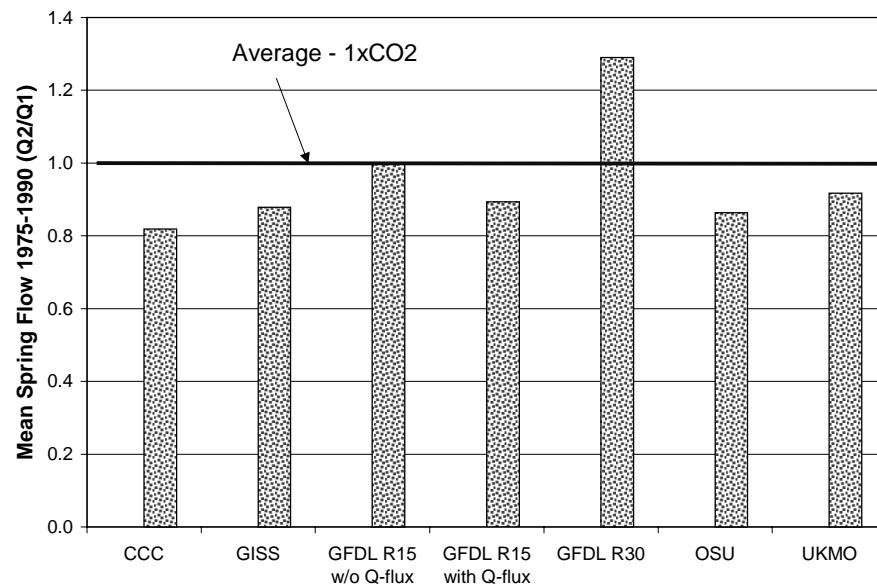


Figure 6.12 Average Scaling Factors for Spring Flows from San Marcos Springs Predicted from GCM Climate Scenarios (1975-1990)

Table 6.5 Annual Scaling Factors for Spring Flows from Comal Springs

GCM	Flow (Q2/Q1))
CCC	0.579
GISS	0.718
GFDL R15 w/o Q-flux	1.000
GFDL R15 with Q-flux	0.762
GFDL R30	1.424
OSU	0.692
UKMO	0.819
AVERAGE	0.856
AVERAGE w/o R30	0.762

Table 6.6 Annual Scaling Factors for Spring Flows from San Marcos Springs

GCM	Flow (Q2/Q1))
CCC	0.818
GISS	0.878
GFDL R15 w/o Q-flux	0.999
GFDL R15 with Q-flux	0.894
GFDL R30	1.290
OSU	0.864
UKMO	0.917
AVERAGE	0.951
AVERAGE w/o R30	0.895

The majority of GCMs predicted decreased spring flows under 2xCO₂ climate scenarios. Omitting the results from GFDL R30, the average change ratio for spring flow from Comal Springs is 0.76 with a range from 0.58 to 1.00. Average spring flows for Comal Springs dropped from 14,400 AF/month under normal climate conditions to 8,300 AF/month predicted by the CCC model. San Marcos spring flows had a weaker response, dropping by 1,400 AF/month, using CCC scaling factors. The average change ratio for spring flow from San Marcos Springs, without considering GFDL R30, is 0.90 with a range from 0.82 to 1.00.

The GFDL R30 model predicted significantly higher streamflows in the future. The range of outcomes predicted by the majority of GCMs is shown for Comal Springs in Figure 6.13. The results for San Marcos Springs are shown in Figure 6.14.

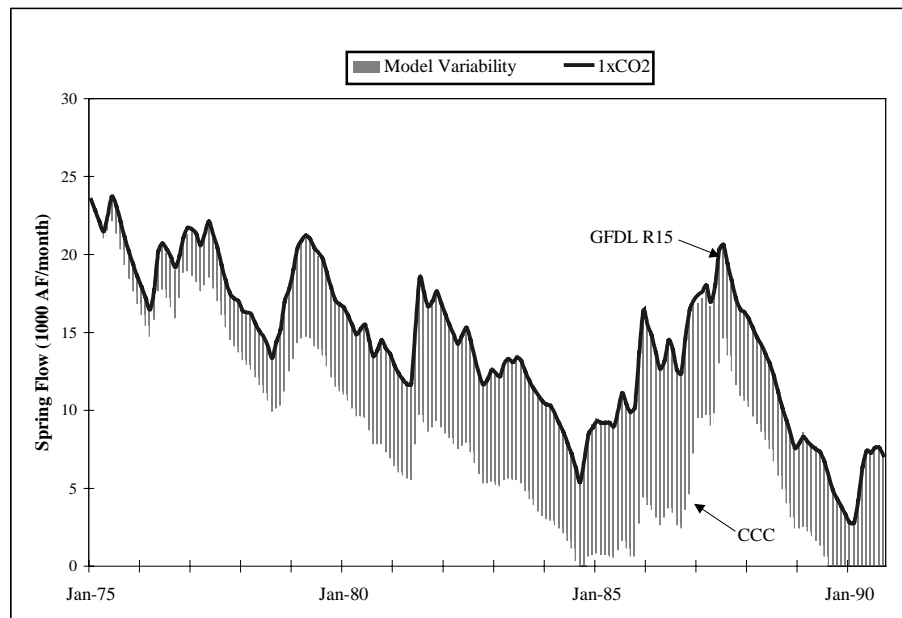


Figure 6.13 Range of Spring Flow Predictions for Comal Springs

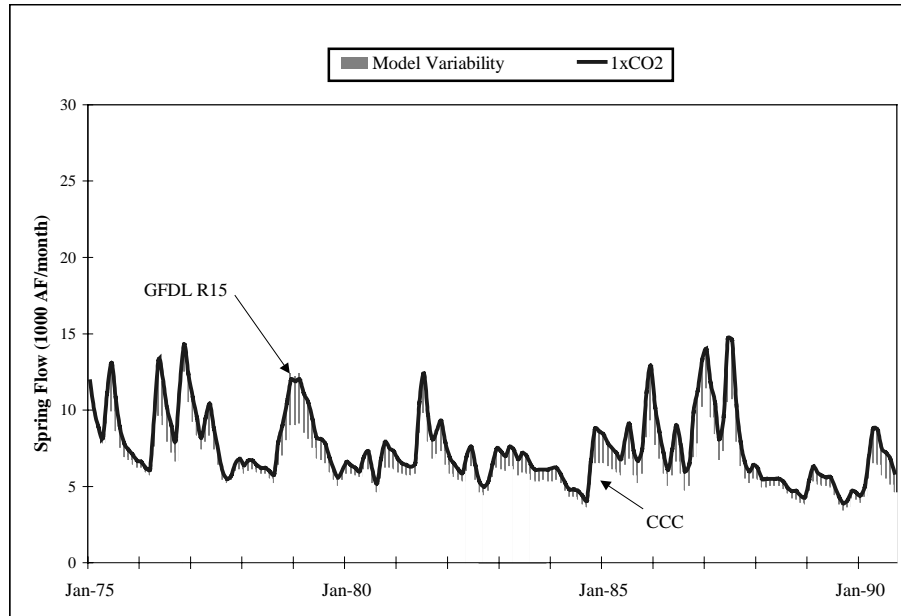


Figure 6.14 Range of Spring Flow Predictions for San Marcos Springs

The behavior of Comal Springs follow the trend of increased climate sensitivity given a higher variability in flow rates. However, flow rates from Comal Springs decrease even under normal conditions. Pumping has had a negative impact on the amount of water available to the springs. The groundwater model was run with increased pumping scenarios to examine the effects of increased pumping on water levels and spring flows. In Chapter 5, observed decreases in water levels for the Helotes-Salado Creek Basin were shown to be closely correlated with increased removal of water from the aquifer. A straight line was fitted to observed pumping rates for this basin to forecast changes over time. The following equation was used to predict pumping for the year 2000:

$$\bar{P} = 0.3285 \cdot Y - 635 \quad (6.1)$$

where \bar{P} is predicted pumping (1000 AF/month) and Y is the year. This function estimates pumping to reach 22,000 AF/month by the year 2000. This is a 35% increase over average pumping rates in 1975.

An alternate pumping scenario was created by scaling observed pumping using a constant factor. Since the Helotes-Salado Creek Basin is heavily pumped to provide drinking water for the growing population of San Antonio, a more conservative growth rate of 25% was assumed for pumping throughout the Edwards region during the period from 1975 to 2000. The historical time series for pumping was multiplied by this scaling factor and the groundwater model was run under different climate scenarios using the modified data set. The influence of increased pumping on water levels for index well J-17 (Helotes-Salado Creek Basin) is shown in Figure 6.15. Figure 6.16 shows spring flows for Comal Springs predicted for 2xCO₂ conditions with increased pumping.

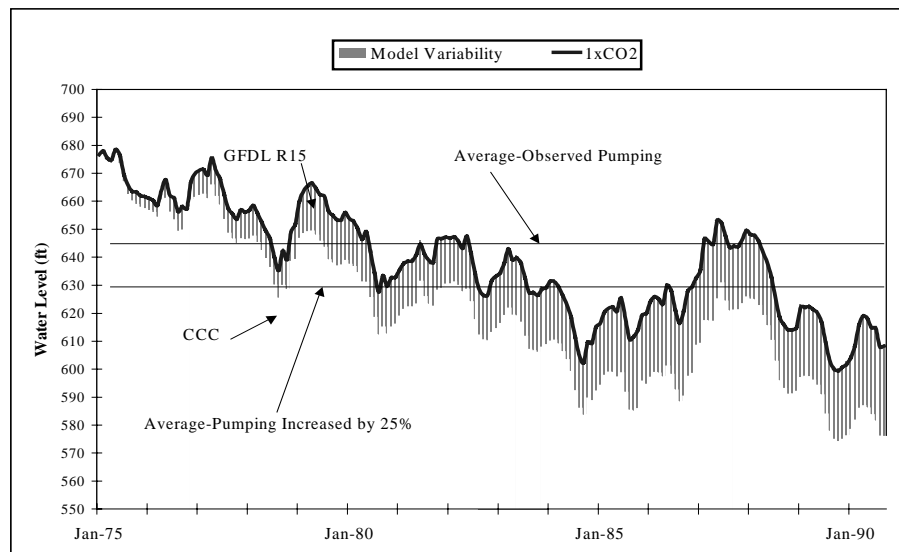


Figure 6.15 Index Well J-17 Water Levels Predicted Under Increased Pumping

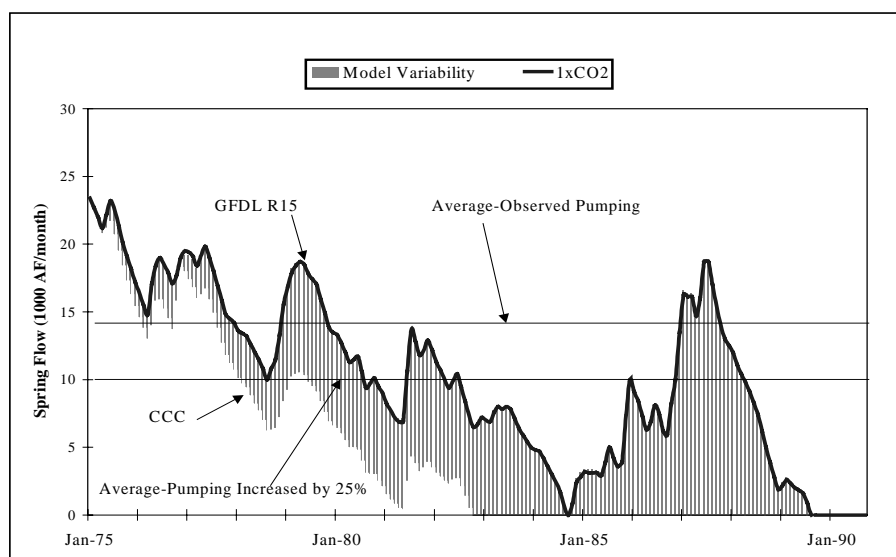


Figure 6.16 Spring Flows for Comal Springs Predicted Under Increased Pumping

Historical precipitation data for the Edwards area indicate that the last three decades have had higher than average precipitation (Figure 3.2). Water levels and spring flows respond to climate change on a much faster time scale, however. A repeat of the drought of record would most likely have a substantial negative impact on water resources. Although GCM predictions for precipitation have a greater level of uncertainty, temperatures will undoubtedly rise over the next century. Unless increased evaporation is offset by rainfall, significant drops in water levels would occur during an extended dry period. Moreover, the Edwards region is experiencing population growth which has led to greater pumping of the aquifer. As shown in Figures 6.15 and 6.16, the combined effects of climate change and pumping will severely limit water supply in the study area. Conclusions are provided in the next chapter.

Chapter 7: Conclusions

This conclusion provides a brief summary of the important features of this study and represents the combined efforts of Dr. David Maidment and myself.

–Kris Martinez, 1998

7.1 SUMMARY OF RESULTS

The objective of this study is to evaluate how climate change would affect water availability for the Edwards Aquifer region. Surface water and groundwater models are run under normal and altered climate scenarios which simulate precipitation and temperature changes under current and doubled atmospheric concentrations of CO₂. The results indicate that gradually rising CO₂ levels will bring about a warmer climate in the study region. Higher temperatures will have a negative impact on water availability, as shown in Table 7.1

Table 7.1 Effects of Climate Change in the Edwards Aquifer Region

Variable	Average	Low	High
Annual Temperature (Future – Present)	+4.0°C	+2.7°C	+6.0°C
Annual Precipitation Ratio (Future/Present)	1.00	0.93	1.15
Annual Streamflow Ratio (Nueces River)	0.76	0.60	1.00
1975-1990 Water Level (Nueces Basin)	-20.4 ft	-36.6 ft	0.0 ft
1975-1990 Water Level (Helotes-Salado Basin)	-9.6 ft	-17.0 ft	0.0 ft
Comal Spring Annual Flow Ratio	0.76	0.58	1.00
San Marcos Spring Annual Flow Ratio	0.90	0.82	1.00

The extent of climate change was estimated using General Circulation Models (GCMs) in a previous study by the National Center for Atmospheric Research (Jenne, 1992). The study used five different GCMs, developed by research centers in the United States, Canada, and the United Kingdom, to obtain

scaling factors which measure climate sensitivity to CO₂ concentrations. There was a consensus among the models that increased levels of CO₂ will produce a warmer climate in Central Texas with an increase in the mean annual temperature of approximately 4.0°C (7.2°F) with a range from 2.7 to 6.0°C (4.9 to 10.8°F). The majority of the GCMs predict normal precipitation. Although rainfall will remain unchanged, increased temperature will lead to greater evaporation losses with the end result being a diminished water supply. A temperature increase of the magnitude predicted by the GCMs would have a marked effect on the Edwards region.

The results are complicated by the fact that one of the GCMs predicted a 57% increase in rainfall under doubled CO₂ concentrations. An experiment by Manabe and Wetherald (1990) in which the Geophysical Fluid Dynamics Laboratory (GFDL) R30 model was run with Q-flux corrections produced a precipitation change ratio of 1.57. Two other experiments using a different version of the GFDL model (R15) forecast increasing precipitation of up to 15% [e.g., Manabe and Wetherald (1987) and Manabe and Wetherald (1990)]. The reason for the large discrepancy between the separate experiments is unclear. However, when a precipitation change ratio of 1.57 is applied to historical climate data and the surface and groundwater models are run, the results show a significantly higher level of water availability in the region. The disparate scaling factor generated by the GFDL R30 model requires further investigation. The summary provided in Table 7.1 does not include GFDL R30 predictions.

The consequence of a warmer climate is that evaporation is increased and streamflow is decreased relative to current conditions. Future average flows in the Nueces River are predicted to be reduced to 76% of their current levels, with a range from 60-100%. Reduced streamflows lead to reduced groundwater recharge and thus to reduced aquifer water levels. Water levels in the San Antonio portion of the aquifer measured by the J-17 Index Well dropped 36 ft during the 1975-1990 period. Lowered water levels were primarily the result of increased pumping but model runs indicate that climate change would magnify these effects, decreasing levels by an additional 10 ft. Over the modeled time frame, the J-17 water level repeatedly fell below levels associated with intermittent spring flows for Comal Springs, under altered climate conditions. The portion of the aquifer in proximity to the Nueces River Basin, measured by the H-5-1 Index Well, were impacted less by pumping and more by climate change. Although levels dropped approximately 20 ft during the 1975-1990 time period, model runs estimate an additional 20 ft decrease would have occurred if atmospheric concentrations of CO₂ were doubled.

The discharges from the two main springs are also reduced. The model data indicate that mean annual flow in Comal Springs would be reduced to 0.76 of current levels with a range of 0.58 to 1.00, and that in San Marcos Springs to 0.9 of current levels with a range from 0.82 to 1.00. While there is still a significant amount of uncertainty surrounding these predictions, the results from all seven of the GCMs indicate that the Edwards region will experience a much warmer climate in the future. According to the models, the drying effects of increased

temperatures will not be offset by precipitation. As a result, streamflows, aquifer water levels, and spring flows will be reduced if atmospheric CO₂ concentrations double relative to current levels. This is a significant conclusion because it suggests that the negative effects of greater water demands in the region will be magnified by the natural forces of climate change. Further research is necessary to determine rational alternatives to reconcile the increased need for water to support human activities with the likelihood of decreased supply.

7.2 STUDY LIMITATIONS

This study has many limitations. The scaling factors that were used to analyze climate change were annual factors applied uniformly to all months of the year. A more detailed impact study could use monthly scaling factors derived separately for each month. A limited historical period from 1975 to 1990 was used to study effects on the aquifer, because this was the period for which recorded streamflows were available at all required locations to compare to simulated values. The climate data developed in this study range from 1895 to 1993, and examination of a longer period is necessary to judge the impacts during critical periods such as the 1950's drought. The groundwater model used in this research is a simplified tank model and more complex and accurate groundwater models are available, such as the GWSIM IV model from the Texas Water Development Board (TWDB). A standard approach to estimating groundwater recharge from streamflow was employed in this study but it is possible that refinements in this method could lead to improved predictions. A significant uncertainty in the current study is the degree of discrepancy found between the

effects of climate change on precipitation in the region for the GFDL R30 model and the six other global climate models whose results were used. The reasons for the changes in precipitation need to be more closely examined and understood.

Perhaps the greatest limitation of this study is that while the evidence for increasing content of greenhouse gases in the atmosphere is unambiguous, prediction of how long it will take before the concentration of carbon dioxide doubles in the atmosphere is quite uncertain. The effects of climate change will not be felt abruptly, but will be an added effect applied slowly year by year, whose impact may be difficult to identify independently of the great climatic variations through time which occur naturally.

7.3 CONTRIBUTIONS

A major accomplishment of this work has been to integrate climate, surface water, and groundwater modeling. Scaling factors for climate scenarios are provided by VEMAP (Kittel et al., 1996) and Valdés (1997). The rainfall-runoff model provided by Reed, Maidment, and Patoux (1997) is modified to use a temperature-based method for estimating evaporation. This allows the model to estimate streamflows using precipitation and temperature, which are the only parameters for which $2\times\text{CO}_2$ scaling factors are provided. The groundwater recharge functions of Wanakule and Anaya (1993) are used for calculating recharge given streamflows at gauging stations located above the Edwards Aquifer outcrop. A groundwater model provided by Watkins (1997), which uses these recharge functions, is employed in this research to provide a mechanism for estimating water levels and spring flows. The rainfall-runoff model is calibrated

to match observed streamflows using historical climate data. The rainfall-runoff and groundwater models are then run consecutively with normal and altered precipitation and temperature data to predict streamflows, water levels, and spring flows. This study successfully links models to describe the influence of climate on surface and subsurface water availability.

A great deal of information about the Edwards Aquifer has been assembled within a GIS framework. A digital base map is developed which includes layers describing climate, terrain, soils, and other meaningful characteristics. Geographical features, such as cities, counties, roads, and rivers are also depicted. The base map shows the locations of pertinent gauging stations, along with Comal Springs and San Marcos Springs. The spatial analysis capabilities of GIS are used to create an accurate representation of the drainage basins that provide recharge to the aquifer. A program has been written to interpolate historical climate data from a 0.5° by 0.5° grid to provide monthly time-series data for each of the watersheds. Another program has been written to derive an average soil-water holding capacity for a drainage basin using STATSGO soils data. All of the programs developed for the study are provided in Appendix B. A data dictionary is included as Appendix A which describes all of the information that has been brought together to complete this work.

Appendix A

Data Dictionary

The data dictionary lists the spatial information that was assembled for this study. Included in the index are coverages, shapefiles, grids, and tables. Scripts and programs used in the project are contained in Appendix C. The following conventions are used:

Pnt	Point Coverage
Arc	Arc Coverage
Ply	Polygon Coverage
Grd	Grid
Tbl	Table

All coverages and grids are in the Texas Statewide Mapping System projection, unless otherwise noted.

Name	Class	Attributes	Values	Description
Average	Tbl	precipitation (mm/month) temperature (°C) runoff (acre-ft/month) water level (ft)	floating point	Average values for basins (1975-1990)
Basins	Ply	grid code	1 Nueces 2 Frio 3 Sabinal 4 Seco-Hondo 5 Medina 6 Helotes-Salado 7 Cibolo 8 Guadalupe 9 Blanco	Edwards Aquifer watersheds
B_wlvl	Tbl	water level (ft)	floating point	Average monthly water levels for basins (1975-1990)
Cities	Ply			Cities in the study area (polygon)
Citypnt	Pnt			Cities in the study area (point)
Comp	Tbl	seqnum	integer	STATSGO component number
Counties	Ply	county name		Counties in the study area
Edfill2	Grd	elevation	floating point	Digital Elevation Model (DEM) for the study area
Edwards	Ply	aquifer	0 nodata 1 outcrop 2 downdip	Edwards Aquifer
Gage	Pnt	gauge number		USGS stream gauges
Grid	Arc	latitude/longitude on 10 minute grid		
Huc	Ply	HUC code		USGS Hydrologic Unit Codes (HUCs) major and minor river basins
Latlong	Arc	latitude/longitude on 5° grid		
Layer	Tbl	water holding capacity (in)	floating point	Soil-water holding capacity for each layer
Mapunit	Tbl	muname		STATSGO map unit name

Name	Class	Attributes	Values	Description
Ppttbl	Tbl	precipitation (mm/month)	floating point	Average monthly rainfall for basins (1975-1990)
Rainave	Tbl	precipitation (mm/month)	floating point	Average rainfall for basins (1975-1990)
Raingrd	Ply	precipitation (mm/month)	integer	VEMAP monthly rainfall (1975-1990)
Rivers	Arc			USGS Reach File 1 (RF1) rivers and streams
Roads	Arc			Streets and highways
Spflwtbl	Tbl	spring flow (1000 acre-ft/month)	floating point	Comal and San Marcos Springs monthly
Springs	Pnt			Comal and San Marcos Springs
Statsgo	Ply	water holding capacity (in)	floating point	Soil-water holding capacity for each map unit
Surptbl	Tbl	streamflow (1000 acre-ft/month)	floating point	Average monthly streamflow for basins (1975-1990)
Tempave	Tbl	temperature (°C)	floating point	Average temperature for basins (1975-1990)
Texas	Ply	county name		Counties of Texas
Tmaxtbl	Tbl	temperature (°C)	floating point	VEMAP monthly maximum temperature (1975-1990)
Tmintbl	Tbl	temperature (°C)	floating point	VEMAP monthly minimum temperature (1975-1990)
Usgs	Ply			USGS 1:250,000 quadrangles
Vemap	Pnt			Centroids of VEMAP grid cells
Wlvtbl	Tbl	water level (ft)	floating point	Average monthly water level for basins (1975-1990)

Appendix B

Programs and Scripts

Program Name	Language	Function
Calbrate.for	FORTRAN 77	Calibration version of soil-water balance used to find parameter values that achieve best match between observed and predicted streamflows from August 1982-July 1990 (96 months)
Output.inc	FORTRAN 77	Groundwater model sub-program that writes Edwards Aquifer water levels and spring flows to sim.out
Read.inc	FORTRAN 77	Groundwater model sub-program used to read in streamflows, pumping rates, initial water levels, and other parameters
Sim.f	FORTRAN 77	Groundwater model used to estimate Edwards Aquifer water levels and spring flows given streamflows
ToGrnd.for	FORTRAN 77	Final output version of soil-water balance used to write file togrnd.txt to be used as input in groundwater model
Validate.for	FORTRAN 77	Validation version of soil-water balance used to check the accuracy of the program against observed streamflows from August 1975-July 1983(96 months)
WHCcalc.ave	Avenue	Calculates the soil-water holding capacity for each map unit
ZoneMean.ave	Avenue	Calculates the mean of a value theme variable for each feature in a zone theme

Calbrate.for

PROGRAM CALIBRATE ! Original program by Reed, Maidment, and Patoux (1997)

```

      IMPLICIT NONE
      REAL P(8,8,13), TMAX(8,8,13), TMIN(8,8,13)
      REAL STMAX(8), AREA(8)
      REAL SURP_OBS(8,8,13), SURP_PRD(8,8,13)
      REAL EVAP_BDG(8,8,13), EVAP_PRD(8,8,13)
      REAL ST(8,8,13), DST(8,8,13)
      REAL ST_TEMP, SATUR, DIFF
      REAL DIST, SIGMA, PHI, OMEGA, PI
      REAL SORAD, T_AVE, E_POT, EVVAL, EVAPTOT
      REAL A, C, RC, DSURP, SURPTOT, RUNOFF
      INTEGER NDAYS(12), D, MNTH, YR, JDAY
      INTEGER I, K, TANK, TK
      LOGICAL CONVERGE

! *****
! CALIBRATION VARIABLES
! *****

      REAL SMIN, SMAX, SINT, AMIN, AMAX, AINT, S, T
      REAL N, SUMX, SUMY, SUMXSQ, SUMYSQ, SUMXY, RSQ, NUM, DEN
      REAL E, ERROR, SUMOBS, BIGDIF, BIGDIFE, BIGDIFR
      REAL ABESTR, CBESTR, ABESTE, CBESTE, MAXRSQ, MINERR

      DATA NDAYS /31,30,31,30,31,31,28,31,30,31,30,31/

      OPEN(UNIT=10, FILE='surplus.txt', STATUS='old')
      OPEN(UNIT=22, FILE='input.txt', STATUS='unknown')

! -----
! THIS SECTION READS THE INPUT DATA AND THEN WRITES
! IT TO A SINGLE FILE CALLED INPUT.TXT AS A CHECK
! INPUT FILES: SURPLUS.TXT, PPT.TXT, TMAX.TXT,
!             TMIN.TXT, STMAX.TXT, AREA.TXT
! OUTPUT FILES: OUTBEST.TXT, OUTCAL.TXT
! -----

      WRITE (22,*) '--OBSERVED SURPLUS--'
      WRITE (22,*) "
DO TANK=1,8
WRITE(22,*) "
WRITE(22,*) TANK:',TANK
DO YR=1,8
READ(10,*) (SURP_OBS(TANK,YR,MNTH), MNTH=1,12)
WRITE(22,500) TANK,YR,(SURP_OBS(TANK,YR,I), I=1,12)
ENDDO
ENDDO
```

```

500      FORMAT(I2,I2,12(F8.2))

      WRITE (22,*) "
      WRITE (22,*) '--PRECIPITATION--'

      OPEN(UNIT=20, FILE='ppt.txt', STATUS='old')
      DO TANK=1,8
      WRITE(22,*) "
      WRITE(22,*) 'TANK:',TANK
      DO YR=1,8
      READ(20,*) (P(TANK,YR,MNTH), MNTH=1,12)
      WRITE(22,500) TANK,YR,(P(TANK,YR,I), I=1,12)
      ENDDO
      ENDDO

      WRITE (22,*) "
      WRITE (22,*) '--MAXIMUM TEMP--'

      OPEN(UNIT=30, FILE='tmax.txt', STATUS='old')
      DO TANK=1,8
      WRITE(22,*) "
      WRITE(22,*) 'TANK:',TANK
      DO YR=1,8
      READ(30,*) (TMAX(TANK,YR,MNTH), MNTH=1,12)
      WRITE(22,500) TANK,YR,(TMAX(TANK,YR,I), I=1,12)
      ENDDO
      ENDDO

      WRITE(22,*) "
      WRITE(22,*) '--MINIMUM TEMP--'

      OPEN(UNIT=40, FILE='tmin.txt', STATUS='old')
      DO TANK=1,8
      WRITE(22,*) "
      WRITE(22,*) 'TANK:',TANK
      DO YR=1,8
      READ(40,*) (TMIN(TANK,YR,MNTH), MNTH=1,12)
      WRITE(22,500) TANK,YR,(TMIN(TANK,YR,I), I=1,12)
      ENDDO
      ENDDO

      OPEN(UNIT=50, FILE='stmax.txt', STATUS='old')
      DO TANK=1,8
      READ(50,*) STMAX(TANK)
      ENDDO

      OPEN(UNIT=60, FILE='area.txt', STATUS='old')
      DO TANK=1,8
      READ(60,*) AREA(TANK)

```

```

ENDDO

CLOSE(10)
CLOSE(20)
CLOSE(30)
CLOSE(40)
CLOSE(50)
CLOSE(60)
CLOSE(22)

OPEN(UNIT=51, FILE='outbest.txt', STATUS='unknown')
OPEN(UNIT=61, FILE='outcal.txt', STATUS='unknown')
WRITE(61, *) '      C      A      RSQ
&      E      BIGDIF'

PI=3.1415927
PHI=(29.+58./60.)*PI/180.
A=0.0
C=0.0
MINERR = 1000.
MAXRSQ = 0.0

PRINT *, "
PRINT *, '*****'
PRINT *, 'ENTER CALIBRATION PARAMETERS'
PRINT *, 'MINIMUM,MAXIMUM,STEP INTERVAL'
PRINT *, '*****'
PRINT *, "

PRINT *, 'KMIN: '
READ *, SMIN
PRINT *, 'KMAX: '
READ *, SMAX
PRINT *, 'KINT: '
READ *, SINT

PRINT *, 'AMIN: '
READ *, AMIN
PRINT *, 'AMAX: '
READ *, AMAX
PRINT *, 'AINT: '
READ *, AINT

PRINT *, 'STATS FOR TANK: '
READ *, TK

DO S = SMIN,SMAX,SINT
C = S
PRINT *, "

```

```

PRINT *, 'K =', C

DO T = AMIN,AMAX,AINT
  A = T
  PRINT *, "
PRINT *, 'K =', C
PRINT *, 'A =', A

DO TANK=1,8
DO YR=1,8
DO MNTH=1,12
SURP_PRD(TANK,YR,MNTH)=0
EVAP_BDG(TANK,YR,MNTH)=0
EVAP_PRD(TANK,YR,MNTH)=0
ST(TANK,YR,1)=0.01
ENDDO
ENDDO
ENDDO

DO TANK=1,8
DO YR=1,8
CONVERGE=.FALSE.
K=0
JDAY=212

! BEGIN BUDGET LOOP FOR GIVEN TANK

DO WHILE (K.LE.30.AND.(.NOT.CONVERGE))
  K=K+1

! INITIALIZE VARIABLES

DO MNTH=1,12
ST_TEMP=ST(TANK,YR,MNTH)
SURPTOT=0
EVAPTOT=0

! BEGIN PSEUDO-DAILY BUDGETING

DO D=1,NDAYS(MNTH)
SATUR=ST_TEMP/STMAX(TANK)
JDAY=JDAY+1
IF (JDAY>365) THEN
JDAY=1
ENDIF

! CALCULATE EVAPORATION

DIST=1+0.033*COS(2*PI*JDAY/365)

```



```

SIGMA=0.4093*SIN(2*PI*JDAY/365-1.405)
OMEGA=ACOS(-TAN(PHI)*TAN(SIGMA))
SORAD=15.392*DIST*(OMEGA*SIN(PHI)*SIN(SIGMA)+
&      COS(PHI)*COS(SIGMA)*SIN(OMEGA))
T_AVE=(TMAX(TANK,YR,MNTH)+TMIN(TANK,YR,MNTH))/2
E_POT=0.0023*SORAD*(TMAX(TANK,YR,MNTH)-
&      TMIN(TANK,YR,MNTH))*(T_AVE+17.8)
EVVAL=SATUR*C*E_POT
EVAPTOT=EVAPTOT+EVVAL

! CALCULATE RUNOFF

RC=SATUR*A**((STMAX(TANK)-ST_TEMP)/STMAX(TANK))
RUNOFF=RC*P(TANK,YR,MNTH)/NDAYS(MNTH)

! CALCULATE NEW SOIL MOISTURE

ST_TEMP=ST_TEMP+P(TANK,YR,MNTH)/NDAYS(MNTH)-
&      EVVAL-RUNOFF

IF (ST_TEMP.LT.0) THEN
ST_TEMP=0.01
ENDIF

IF (ST_TEMP.GT.STMAX(TANK)) THEN
DSURP=ST_TEMP-STMAX(TANK)
SURPTOT=SURPTOT+DSURP
ST_TEMP=STMAX(TANK)
ENDIF

SURPTOT=SURPTOT+RUNOFF

! FINISH DAILY LOOP
ENDDO

ST(TANK,YR,MNTH+1)=ST_TEMP
SURP_PRD(TANK,YR,MNTH)=SURPTOT
EVAP_PRD(TANK,YR,MNTH)=EVAPTOT

IF (MNTH.GT.1) THEN
DST(TANK,YR,MNTH)=ST(TANK,YR,MNTH+1)-
&      ST(TANK,YR,MNTH)
EVAP_BDG(TANK,YR,MNTH)=P(TANK,YR,MNTH)-
&      SURP_PRD(TANK,YR,MNTH)-DST(TANK,YR,MNTH)
ENDIF

! FINISH MONTHLY LOOP
SURP_PRD(TANK,YR,MNTH)=SURP_PRD(TANK,YR,MNTH)/10/30.48
&      *AREA(TANK)*5280**2/43560/1000

```

```

ENDDO

! TEST FOR CONVERGENCE
DIFF=ST(TANK,YR,1)-ST(TANK,YR,13)
IF (ABS(DIFF).LT.0.1) THEN
CONVERGE=.TRUE.
ENDIF

! ALTER INITIAL SOIL MOISTURE GUESS
ST(TANK,YR,1)=ST(TANK,YR,13)

! FINISH CONVERGENCE LOOP
ENDDO

IF (K.GT.30) THEN
WRITE(*,*) '--CONVERGENCE NOT ACHIEVED AFTER 30 ITERATIONS--'
STOP
ENDIF

! FINISH YEAR LOOP
ST(TANK,YR+1,1)=ST(TANK,YR,13)
ENDDO

! FINISH TANK LOOP
ENDDO

ERROR = 0.0
SUMOBS = 0.0
BIGDIF = 0.0
N=0.0
SUMX = 0.0
SUMY = 0.0
SUMXY = 0.0
SUMXSQ = 0.0
SUMYSQ = 0.0

DO I=TK,TK
TANK = I
IF (TANK.NE.5) THEN

DO YR=1,8
DO MNTH=1,12
N = N + 1.
SUMX = SUMX + SURP_OBS(TANK,YR,MNTH)
SUMY = SUMY + SURP_PRD(TANK,YR,MNTH)
SUMXY = SUMXY + SURP_OBS(TANK,YR,MNTH)*
&      SURP_PRD(TANK,YR,MNTH)
SUMXSQ = SUMXSQ + (SURP_OBS(TANK,YR,MNTH))**2.
SUMYSQ = SUMYSQ + (SURP_PRD(TANK,YR,MNTH))**2.

```

```

ERROR=ERROR + ABS((SURP_OBS(TANK,YR,MNTH)-
&      SURP_PRD(TANK,YR,MNTH)))
BIGDIF=BIGDIF + SURP_PRD(TANK,YR,MNTH)-
&      SURP_OBS(TANK,YR,MNTH)
SUMOBS = SUMOBS + SURP_OBS(TANK,YR,MNTH)
ENDDO
ENDDO

ENDIF
ENDDO

IF (BIGDIF.GT.0.0) THEN ! CONSTRAINT ADDED TO AVOID
UNDERPREDICTION

NUM = (N*SUMXY-SUMX*SUMY)**2.

DEN = ((N*SUMXSQ-SUMX**2.)*(N*SUMYSQ-SUMY**2.))

RSQ = NUM/DEN

PRINT *, 'RSQ = ', RSQ

IF (RSQ.GT.MAXRSQ) THEN
MAXRSQ = RSQ
ABESTR = A
CBESTR = C
BIGDIFR = BIGDIF
ENDIF

E = ERROR/SUMOBS

PRINT *, 'E = ', E
PRINT *, 'BIGDIF = ', BIGDIF

IF (E.LT.MINERR) THEN
MINERR = E
ABESTE = A
CBESTE = C
BIGDIFE= BIGDIF
ENDIF

ENDIF

WRITE(61,6000) C, A, RSQ,E,BIGDIF
6000  FORMAT(F15.4, F15.4, F15.4, F15.2, F15.0)

ENDDO
ENDDO

```

```

WRITE(51,*) "
WRITE(51,*) 'MAXRSQ =', MAXRSQ
WRITE(51,*) 'AT A =', ABESTR
WRITE(51,*) ' K =', CBESTR
WRITE(51,*) 'WHERE BIGDIF =',BIGDIFR

WRITE(51,*) "
WRITE(51,*) 'MINERR =', MINERR
WRITE(51,*) 'AT A =', ABESTE
WRITE(51,*) ' K =', CBESTE
WRITE(51,*) 'WHERE BIGDIF =',BIGDIFE
WRITE(51,*) "

PRINT *, "
PRINT *, 'MAXRSQ =', MAXRSQ
PRINT *, 'AT A =', ABESTR
PRINT *, ' K =', CBESTR
PRINT *, "
PRINT *, 'MINERR =', MINERR
PRINT *, 'AT A =', ABESTE
PRINT *, ' K =', CBESTE

CLOSE(51)
CLOSE(61)

STOP

10010 WRITE(*,*) '--COULD NOT OPEN OUTPUT FILE--'
STOP

END

```

Output.inc

```

CC  WRITE RESULTS

OPEN (UNIT=17,FILE='sim.out',STATUS='UNKNOWN')

WRITE(17,390) #Time ',(I,I=1,NBASIN),'Comal ', 'San M'
DO 305 J=1,NTSTEP
WRITE(17,380) J,(H(I,J),I=1,NBASIN),SFC(J),SFS(J)
305  CONTINUE
380  FORMAT(I3,9(1X,F6.1),2(1X,F5.1))
390  FORMAT(A,9(1X,I3,3X),2A)
395  FORMAT(A,9(1X,I3,3X))
CLOSE (17)

```

Read.inc

```

OPEN (UNIT=15,FILE='tank.dat',STATUS='OLD')
OPEN (UNIT=16,FILE='rech.dat',STATUS='OLD')
OPEN (UNIT=18,FILE='pump.dat',STATUS='OLD')
OPEN (UNIT=77,FILE='check.txt',STATUS='UNKNOWN')

CC READ PROBLEM DATA

5 READ(16,*)
  READ(16,*)
  DO 5 J=1,NTSTEP
    READ(16,*) NUM,(INFLOW(I,J),I=1,NBASIN)
    WRITE(77,*) NUM,(INFLOW(I,J),I=1,NBASIN)
  CONTINUE
  CLOSE (16)
  CLOSE (77)

  READ(15,*)
  READ(15,*)
  DO 7 I=1,NBASIN
    READ(15,*) NUM, TOP(I), BOT(I), SF(I), GF(I),
      & LF(I), HINIT(I), COND(I)
  CONTINUE
  CLOSE (15)

CC READ PUMPING RATES

9 READ(18,*)
  READ(18,*)
  DO 9 J=1,NTSTEP
    READ(18,*) NUM,(RATE(I,J),I=1,NBASIN)
  CONTINUE
  CLOSE (18)

```

Sim.f

PROGRAM TANK ! Original Program by Watkins (1997)

```
CC-----
C   Lumped parameter model of Edwards Aquifer based
C   on model by Wanakule and Anaya, 1993
C
C   Finite difference equations for nonlinear model
C   solved using Gauss-Siedel (overrelaxation) with
C   with Picard iteration (outer loop)
C
C   Monthly time step
C
C   Schematic: 4-->3
C               |
C   1-->2-->9-->5-->6-->7-->8
C               | |
C               C S   (C: Comal, S: San Marcos)
C
C   Includes San Pedro springs and Hueco flux
C
C   Compile using: f77 -o tanksim sim.f
CC-----
```

```
IMPLICIT REAL*8 (A-H,O-Z)
IMPLICIT INTEGER (I-N)
PARAMETER (MAXBASIN = 9)
PARAMETER (MAXTSTEP = 189)
PARAMETER (MAXFUN = (MAXBASIN+2)*MAXTSTEP+1)
PARAMETER (MAXVAR = MAXBASIN*MAXTSTEP+0)
REAL*8 LF,LR,LRP
REAL*8 INFLOW,INFLOWP
DATA ALPHA,BETA,GAMMA /0.5,0.5,1.1/
C
C   0<=Alpha<=1; = 0 for fully explicit
C   0<=Beta<=1; = 0 for parameters based on time j-1
C   1<=Gamma<=2; = 1.0 for Gauss Siedel
C
COMMON/PARAMETER/ NBASIN,NTSTEP,NNVARS,NFUN
COMMON /INTANK/ INFLOW, TOP,BOT,GF,SF,LF,HINIT,COND
COMMON /TOPRINT/ PUMP,TRAN,STOR,LR,H,SFS,SFC,SUMOBJ

DIMENSION H(MAXBASIN,0:MAXTSTEP),HINIT(MAXBASIN)
DIMENSION RATE(MAXBASIN,MAXTSTEP)
DIMENSION TOP(MAXBASIN),BOT(MAXBASIN),GF(MAXBASIN),
SF(MAXBASIN)
DIMENSION LF(MAXBASIN),COND(MAXBASIN),
TRAN(MAXBASIN,MAXTSTEP)
DIMENSION INFLOW(MAXBASIN,MAXTSTEP),LR(MAXBASIN,MAXTSTEP)
DIMENSION STOR(MAXBASIN,MAXTSTEP)
DIMENSION A(MAXBASIN),B(MAXBASIN),C(MAXBASIN)
```

```

DIMENSION SFS(MAXTSTEP),SFC(MAXTSTEP)
DIMENSION HT1(MAXBASIN),HT2(MAXBASIN)
DIMENSION HOLD(MAXBASIN),HNEW(MAXBASIN)
DIMENSION STORP(MAXBASIN),TRANP(MAXBASIN),LRP(MAXBASIN)
DIMENSION INFLOWP(MAXBASIN),RECHP(MAXBASIN)
DIMENSION RECH(MAXBASIN,MAXTSTEP),PUMP(MAXBASIN,MAXTSTEP)

OPEN (UNIT=20,FILE='test1.out')

NBASIN = 9
NTSTEP = 189
NNVARS = NBASIN*NTSTEP
NFUN = (NBASIN+2)*NTSTEP+1

INCLUDE 'read.inc' ! to read data if subroutine used for simulation

MAXIT1 = 10 ! inner loop for calculating heads
MAXIT2 = 10 ! outer loop for updating parameter values
EPS1 = 0.1 ! inner loop tolerance
EPS2 = 0.1 ! outer loop tolerance

DO 10 I=1,NBASIN
DO 15 J=1,NTSTEP
C      PUMP(I,J) = 0.0 ! try no pumping scenario
PUMP(I,J) = RATE(I,J) ! use pumping from pumpX.dat
15  CONTINUE
10  CONTINUE

DO 20 I = 1,NBASIN
H(I,0) = HINIT(I)
20  CONTINUE
KOUNT = 0

CC-----
DO 150 J=1,NTSTEP ! Start time-step loop

CC
CC Calculate parameters and recharge based on time-average of heads

DO 25 I=1,NBASIN
HT1(I) = H(I,J-1)
HT2(I) = H(I,J-1)
HOLD(I) = H(I,J-1)
HNEW(I) = H(I,J-1)
H(I,J) = H(I,J-1)
INFLOWP(I) = INFLOW(I,J)
25  CONTINUE

DO 100 N=1,MAXIT2 ! Start outer (Picard) iteration loop

```

```

DO 27 I=1,NBASIN
HT2(I) = H(I,J)
27 CONTINUE

CALL PCALC(HT1,HT2,INFLOWP,BETA,STORP,TRANP,LRP,RECHP,
&      SFCP,SFSP)

SFC(J) = SFCP
SFS(J) = SFSP
DO 30 I=1,NBASIN
TRAN(I,J) = TRANP(I)
LR(I,J) = LRP(I)
STOR(I,J) = STORP(I)
RECH(I,J) = RECHP(I)
30 CONTINUE

CC-----
CC Flow equations
C
C(1) = 1/TRAN(1,J)
C(4) = 1/TRAN(4,J)

B(1) = STOR(1,J)/TRAN(1,J)
B(4) = STOR(4,J)/TRAN(4,J)

A(1) = 1/(B(1) + ALPHA)
A(2) = 1/(STOR(2,J) + ALPHA*(TRAN(1,J)+TRAN(2,J)))
A(3) = 1/(STOR(3,J) + ALPHA*(TRAN(3,J)+TRAN(4,J)))
A(4) = 1/(B(4) + ALPHA)
A(5) = 1/(STOR(5,J) + ALPHA*(TRAN(5,J)+TRAN(9,J)))
A(6) = 1/(STOR(6,J) + ALPHA*(TRAN(5,J)+TRAN(6,J)))
B(6) = 1/(STOR(6,J) + ALPHA*(TRAN(5,J)+TRAN(6,J)+LF(6)))
A(7) = 1/(STOR(7,J) + ALPHA*(TRAN(6,J)+TRAN(7,J)))
B(7) = 1/(STOR(7,J) + ALPHA*(TRAN(6,J)+TRAN(7,J)+LF(7)))
A(8) = 1/(STOR(8,J) + ALPHA*(TRAN(7,J)))
B(8) = 1/(STOR(8,J) + ALPHA*(TRAN(7,J) + LF(8)))
A(9) = 1/(STOR(9,J) + ALPHA*(TRAN(3,J)+TRAN(2,J)
&      +TRAN(9,J)))

DO 50 K=1,MAXIT1  ! Start inner (SOR) iteration loop
KOUNT = KOUNT + 1
DIFMAX = 0.0

HNEW(1) = A(1)*(ALPHA*HOLD(2) + B(1)*H(1,J-1)
&      + (1-ALPHA)*(H(2,J-1) - H(1,J-1))
&      + C(1)*(RECH(1,J) - PUMP(1,J)))
HNEW(1) = (1-GAMMA)*HOLD(1) + GAMMA*HNEW(1)

```

```

HNEW(2) = A(2)*(STOR(2,J)*H(2,J-1)
&      + ALPHA*(TRAN(1,J)*HNEW(1) + TRAN(2,J)*HOLD(9))
&      + (1-ALPHA)*(TRAN(1,J)*(H(1,J-1)
&      - H(2,J-1)) + TRAN(2,J)*(H(9,J-1) - H(2,J-1)))
&      + RECH(2,J) - PUMP(2,J))
HNEW(2) = (1-GAMMA)*HOLD(2) + GAMMA*HNEW(2)

```

```

HNEW(4) = A(4)*(ALPHA*HOLD(3) + B(4)*H(4,J-1)
&      + (1-ALPHA)*(H(3,J-1)-H(4,J-1))
&      + C(4)*(RECH(4,J) - PUMP(4,J)))
HNEW(4) = (1-GAMMA)*HOLD(4) + GAMMA*HNEW(4)

```

```

HNEW(3) = A(3)*(STOR(3,J)*H(3,J-1)
&      + ALPHA*(TRAN(4,J)*HNEW(4) + TRAN(3,J)*HOLD(9))
&      + (1-ALPHA)*(TRAN(3,J)*(H(9,J-1)
&      - H(3,J-1)) + TRAN(4,J)*(H(4,J-1) - H(3,J-1)))
&      + RECH(3,J) - PUMP(3,J))
HNEW(3) = (1-GAMMA)*HOLD(3) + GAMMA*HNEW(3)

```

```

HNEW(9) = A(9)*(STOR(9,J)*H(9,J-1)
&      + ALPHA*(TRAN(2,J)*HNEW(2)
&      + TRAN(3,J)*HNEW(3) + TRAN(9,J)*HOLD(5))
&      + (1-ALPHA)*(TRAN(2,J)*(H(2,J-1)-H(9,J-1))
&      + TRAN(3,J)*(H(3,J-1)-H(9,J-1))
&      + TRAN(9,J)*(H(5,J-1)-H(9,J-1)))
&      + RECH(9,J) - PUMP(9,J))
HNEW(9) = (1-GAMMA)*HOLD(9) + GAMMA*HNEW(9)

```

```

HNEW(5) = A(5)*(STOR(5,J)*H(5,J-1)
&      + ALPHA*(TRAN(9,J)*HNEW(9) + TRAN(5,J)*HOLD(6))
&      + (1-ALPHA)*(TRAN(9,J)*(H(9,J-1)
&      - H(5,J-1)) + TRAN(5,J)*(H(6,J-1) - H(5,J-1)))
&      + RECH(5,J) - PUMP(5,J))
HNEW(5) = (1-GAMMA)*HOLD(5) + GAMMA*HNEW(5)

```

C

C Use the following if springflows computed in G-S iteration loop

C

IF(HOLD(6) .GT. 672.67) THEN

```

HNEW(6) = B(6)*(STOR(6,J)*H(6,J-1)
&      + ALPHA*(TRAN(5,J)*HNEW(5) + TRAN(6,J)*HOLD(7)
&      + LF(6)*672.67) + (1-ALPHA)*(TRAN(5,J)*(H(5,J-1)
&      - H(6,J-1)) + TRAN(6,J)*(H(7,J-1) - H(6,J-1))
&      - AMAX1(0.0, LF(6)*(H(6,J-1) - 672.67)))
&      + RECH(6,J) - PUMP(6,J))

```

ELSE

```

HNEW(6) = A(6)*(STOR(6,J)*H(6,J-1)
&      + ALPHA*(TRAN(5,J)*HNEW(5)
&      + TRAN(6,J)*HOLD(7)) + (1-ALPHA)*(TRAN(5,J)*(H(5,J-1)

```

```

&      - H(6,J-1)) + TRAN(6,J)*(H(7,J-1) - H(6,J-1))
&      - AMAX1(0.0, LF(6)*(H(6,J-1) - 672.67)))
&      + RECH(6,J) - PUMP(6,J))
ENDIF
HNEW(6) = (1-GAMMA)*HOLD(6) + GAMMA*HNEW(6)

IF(HOLD(7) .GT. 619.05) THEN
HNEW(7) = B(7)*(STOR(7,J)*H(7,J-1)
&      + ALPHA*(TRAN(6,J)*HNEW(6) + TRAN(7,J)*HOLD(8)
&      + LF(7)*618.05) + (1-ALPHA)*(TRAN(6,J)*(H(6,J-1)
&      - H(7,J-1)) + TRAN(7,J)*(H(8,J-1) - H(7,J-1))
&      - AMAX1(0.0, LF(7)*(H(7,J-1) - 619.05))))
&      + RECH(7,J) - PUMP(7,J))
ELSE
HNEW(7) = A(7)*(STOR(7,J)*H(7,J-1)
&      + ALPHA*(TRAN(6,J)*HNEW(6) + TRAN(7,J)*HOLD(8))
&      + (1-ALPHA)*(TRAN(6,J)*(H(6,J-1)
&      - H(7,J-1)) + TRAN(7,J)*(H(8,J-1) - H(7,J-1))
&      - AMAX1(0.0, LF(7)*(H(7,J-1) - 619.05))))
&      + RECH(7,J) - PUMP(7,J))
ENDIF
HNEW(7) = (1-GAMMA)*HOLD(7) + GAMMA*HNEW(7)

IF(HOLD(8) .GT. 571.11) THEN
HNEW(8) = B(8)*(STOR(8,J)*H(8,J-1)
&      + ALPHA*(TRAN(7,J)*HNEW(7) + LF(8)*571.11)
&      + (1-ALPHA)*(TRAN(7,J)*(H(7,J-1)-H(8,J-1))
&      - AMAX1(0.0, LF(8)*(H(8,J-1) - 571.11))))
&      + RECH(8,J) - PUMP(8,J))
ELSE
HNEW(8) = A(8)*(STOR(8,J)*H(8,J-1)
&      + ALPHA*(TRAN(7,J)*HNEW(7))
&      + (1-ALPHA)*(TRAN(7,J)*(H(7,J-1)-H(8,J-1))
&      - AMAX1(0.0, LF(8)*(H(8,J-1) - 571.11))))
&      + RECH(8,J) - PUMP(8,J))
ENDIF
HNEW(8) = (1-GAMMA)*HOLD(8) + GAMMA*HNEW(8)

DO 40 L=1,NBASIN
DIFF = DABS(HNEW(L) - HOLD(L))
IF (DIFF .GT. DIFMAX) DIFMAX = DIFF
CONTINUE

WRITE(20,44) 'HNEW: ',(HNEW(L),L=1,NBASIN)

IF (DIFMAX .LE. EPS1) THEN
WRITE(20,*) 'Inner loop converged in ',K,
&      ' iterations.'
GOTO 52

```

```

ENDIF
IF (K .EQ. MAXIT1) THEN
WRITE(20,*) 'Inner loop did not converge in ',
&          K, ' iterations'
WRITE(20,44) 'HNEW: ',(HNEW(L),L=1,NBASIN)
44  FORMAT(A,9(1X,F6.1))
ENDIF

DO 45 L=1,NBASIN
HOLD(L) = HNEW(L)
45  CONTINUE

50  CONTINUE

52  DIFMAX = 0.0
DO 55 L=1,NBASIN
DIFF = DABS(HNEW(L) - H(L,J))
IF (DIFF .GT. DIFMAX) DIFMAX = DIFF
55  CONTINUE

IF (DIFMAX .LE. EPS2) THEN
WRITE(20,*) J, ' OUTER LOOP CONVERGED IN ',N,
&          ' ITERATIONS.'
GOTO 150
ELSEIF (N .EQ. MAXIT2) THEN
WRITE(20,*) J, ' OUTER LOOP DID NOT CONVERGE IN ',
&          N, ' ITERATIONS'
ENDIF

60  DO 65 L=1,NBASIN
H(L,J) = HNEW(L)
65  CONTINUE

100 CONTINUE

150 CONTINUE
WRITE(20,*) KOUNT, ' total iterations'
CLOSE(20)

CC-----
CC Calculate value of the objective function
C
C  SUMOBJ = 0.0
C  DO 170 I=1,NBASIN
C    DO 175 J=1,NTSTEP
C      SUMOBJ = SUMOBJ+RATE(I,J)
C 175  CONTINUE
C 170 CONTINUE

```

CC Assign function values for gcomp

```
C  DO 180 I=1,NBASIN
C    DO 185 J=1,NTSTEP
C      L=(I-1)*NTSTEP+J
C      GFUNC(L) = H(I,J)
C 185  CONTINUE
C 180 CONTINUE
C
C  DO 190 J=1,NTSTEP
C    GFUNC(NBASIN*NTSTEP+J) = SFC(J)
C    GFUNC((NBASIN+1)*NTSTEP+J) = SFS(J)
C 190 CONTINUE
```

```
C  GFUNC(NFUN) = SUMOBJ
```

INCLUDE 'output.inc' ! to write results from simulation model

```
C
C End of tank.f
C-----
STOP
C  RETURN
END
```

```
C-----
C2345678901234567890123456789012345673456789012
CC
SUBROUTINE PCALC(HT1,HT2,INFLOWP,BETA,STORP,TRANP,LRP,RECHP,
& SFCP,SFSP)
```

```
IMPLICIT REAL*8 (A-H,O-Z)
IMPLICIT INTEGER (I-N)
```

```
PARAMETER (MAXBASIN = 9)
PARAMETER (MAXTSTEP = 189)
PARAMETER (MAXFUN = (MAXBASIN+2)*MAXTSTEP+1)
PARAMETER (MAXVAR = MAXBASIN*MAXTSTEP+0)
```

```
COMMON/PARAMETER/ NBASIN,NTSTEP,NNVARS,NFUN
COMMON /INTANK/ INFLOW,TOP,BOT,GF,SF,LF,HINIT,COND
REAL*8 LF,LRP,INFLOWP,INFLOW
```

```
DIMENSION TOP(MAXBASIN),HINIT(MAXBASIN)
DIMENSION BOT(MAXBASIN),GF(MAXBASIN),SF(MAXBASIN)
DIMENSION LF(MAXBASIN),COND(MAXBASIN),INFLOWP(MAXBASIN)
DIMENSION TRANP(MAXBASIN),LRP(MAXBASIN)
DIMENSION STORP(MAXBASIN),RECHP(MAXBASIN)
DIMENSION HT1(MAXBASIN),HT2(MAXBASIN)
```


210

```
DIMENSION HAVG(MAXBASIN),HACT(MAXBASIN)
DIMENSION INFLOW(MAXBASIN,MAXTSTEP)
```

```
DO 210 I=1,NBASIN
HAVG(I) = (1-BETA)*HT1(I) + BETA*HT2(I)
HACT(I) = AMIN1(HAVG(I), TOP(I))
CONTINUE
```

CC Compute transmissivities of links

```
TRANP(1) = COND(1)*0.0005*(HACT(1)+HACT(2)-BOT(1)-BOT(2))
TRANP(2) = COND(2)*0.0005*(HACT(2)+HACT(9)-BOT(2)-BOT(9))
TRANP(3) = COND(3)*0.0005*(HACT(3)+HACT(9)-BOT(3)-BOT(9))
TRANP(4) = COND(4)*0.0005*(HACT(4)+HACT(3)-BOT(4)-BOT(3))
TRANP(5) = COND(5)*0.0005*(HACT(5)+HACT(6)-BOT(5)-BOT(6))
TRANP(6) = COND(6)*0.0005*(HACT(6)+HACT(7)-BOT(6)-BOT(7))
TRANP(7) = COND(7)*0.0005*(HACT(7)+HACT(8)-BOT(7)-BOT(8))
TRANP(8) = 0.0
TRANP(9) = COND(9)*0.0005*(HACT(9)+HACT(5)-BOT(9)-BOT(5))
```

CC Compute loss ratios and recharge values from surface inflows

```
LRP(1) = AMIN1(1.0, 1.-(37.59/(927.65 - HAVG(1))))*3.6814)
RECHP(1) = AMIN1(29.0, LRP(1)*INFLOWP(1))
```

```
LRP(2) = AMIN1(1.0, AMAX1(0.,(4.9575 - LOG(INFLOWP(2)+
& .001))/1.7258))
RECHP(2) = 1.13*LRP(2)*INFLOWP(2)
```

```
LRP(3) = AMIN1(1.0, AMAX1(0., (3.637 - LOG(INFLOWP(3)+.001))
& /2.064))
IF ((LRP(3) .GT. 0.9) .AND. (HAVG(3) .LT. 824.0)) THEN
LRP(3) = 1 - 4.6786/(870 - HACT(3))
ENDIF
RECHP(3) = 1.10*LRP(3)*INFLOWP(3)
```

```
LRP(4) = AMIN1(1., AMAX1(0., (5.3641 - LOG(INFLOWP(4)+.001))
& /2.7761))
RECHP(4) = 1.52*LRP(4)*INFLOWP(4)
```

```
TERM5 = (263.8/(INFLOWP(5)-1.533) - 1)**.295
RECHP(5) = 2.996/TERM5
IF (HT2(5) .GT. HT1(5)) THEN
RECHP(5) = RECHP(5) + 3.381
ELSE
RECHP(5) = RECHP(5) + 1.0
ENDIF
```

```
TERM6 = 4.591*INFLOWP(6) + 0.001
```

```

LRP(6) = AMIN1(1.0, AMAX1(0., (4.4498 - LOG(TERM6))/1.84))
C lrp(6) = lrp(7)
RECHP(6) = 4.591*LRP(6)*INFLOWP(6)

C Add Hueco flux/slight head dependency
QH = .0363*HAVG(6) - 23.49
TERM7 = 4.006*INFLOWP(6) + 0.001
TERMX = 20.
LRP(7) = AMIN1(1.0, AMAX1(0.0, (4.4498 - LOG(TERM7))/1.84))
IF(HAVG(7).GE.626.) THEN
  LRP(7) = 0.8*LRP(7)
  TERMX = 10.
ELSEIF(HAVG(7).LE.625.) THEN
  LRP(7) = AMAX1(1.0, 1.2*LRP(7))
ELSEIF(HAVG(7).LE.623.) THEN
  LRP(7) = AMAX1(1.0, 1.4*LRP(7))
ENDIF
RECHP(7) = LRP(7)*4.006*INFLOWP(6) + AMIN1(20.,1.585*INFLOWP(7))
&      - QH

RECHP(8) = AMIN1(1.331,INFLOWP(8)) + AMIN1(20.,1.122*INFLOWP(7))

LRP(5) = 0.0
LRP(8) = 0.0
LRP(9) = 0.0
RECHP(9) = 0.0

CC Compute storage coefficients

DO 235 I=1,NBASIN
STORP(I) = SF(I)*GF(I)*(HACT(I) - BOT(I))* (GF(I)-1)
CONTINUE

CC Compute spring flows

SFCP = AMAX1(0., LF(7)*(HAVG(7) - 618.05))
SFSP = AMAX1(0., LF(8)*(HAVG(8) - 571.11))

RETURN
END

```

ToGrnd.for

PROGRAM TOGROUND ! Original program by Reed, Maidment, and Patoux (1997)

```

      IMPLICIT NONE
      REAL P(8,16,13), TMAX(8,16,13), TMIN(8,16,13)
      REAL STMAX(8), AREA(8), C(8), A(8)
      REAL SURP_OBS(8,16,13), SURP_PRD(8,16,13)
      REAL EVAP_BDG(8,16,13), EVAP_PRD(8,16,13)
      REAL ST(8,16,13), DST(8,16,13)
      REAL ST_TEMP, SATUR, DIFF
      REAL DIST, SIGMA, PHI, OMEGA, PI
      REAL SORAD, T_AVE, E_POT, EVVAL, EVAPTOT
      REAL RC, DSURP, SURPTOT, RUNOFF, NINE, PSCALE, TSCALE
      INTEGER NDAYS(12), D, MNTH, YEAR, YR, JDAY, MONTH
      INTEGER I, K, Z, TANK, TK
      LOGICAL CONVERGE

! *****
! CALIBRATION VARIABLES
! *****

      REAL N, SUMX, SUMY, SUMXSQ, SUMYSQ, SUMXY, RSQ, NUM, DEN
      REAL E, ERROR, SUMOBS, BIGDIF
      REAL MAXRSQ, MINERR

      DATA NDAYS /31,28,31,30,31,30,31,31,30,31,30,31/

! -----
! INPUT FILES: SURPLUS.TXT, PPT.TXT, TMAX.TXT,
! TMIN.TXT, STMAX.TXT, AREA.TXT
! K.TXT, A.TXT
! OUTPUT FILES: OUTPUT.TXT, TOGROUND.TXT
! -----

      PRINT *, "
      PRINT *, '*****'
      PRINT *, 'GENERATE OUTPUT FILE TOGROUND.TXT'
      PRINT *, "
      PRINT *, 'PPT AND TEMP CAN BE SCALED FOR'
      PRINT *, 'CLIMATE CHANGE SCENARIOS'
      PRINT *, '*****'
      PRINT *, "

      PRINT *, 'PRECIPITATION SCALING FACTOR:'
      READ *, PSCALE
      PRINT *, "
      PRINT *, 'TEMPERATURE SCALING FACTOR : '
      READ *, TSCALE
      PRINT *, "
```

```

PRINT *, 'GENERATING OUTPUT FILES:'
PRINT *, ' TOGROUND.TXT'
PRINT *, ' OUTPUT.TXT'
PRINT *, ' OUTSRP_P.TXT'
PRINT *, ' OUTSRP_O.TXT'
PRINT *, ' OUT_P.TXT'
PRINT *, "

OPEN(UNIT=10, FILE='surplus.txt', STATUS='old')
TK=12
DO TANK=1,8
TK=12
DO YR=1,16
IF (YR.EQ.16) THEN
TK=9
ENDIF
READ(10,*) (SURP_OBS(TANK,YR,MNTH), MNTH=1,TK)
ENDDO
ENDDO

```

500 FORMAT(I2,I2,12(F8.2))

```

OPEN(UNIT=20, FILE='ppt.txt', STATUS='old')
DO TANK=1,8
TK=12
DO YR=1,16
IF (YR.EQ.16) THEN
TK=9
ENDIF
READ(20,*) (P(TANK,YR,MNTH), MNTH=1,TK)
ENDDO
ENDDO

```

```

OPEN(UNIT=30, FILE='tmax.txt', STATUS='old')
DO TANK=1,8
TK=12
DO YR=1,16
IF (YR.EQ.16) THEN
TK=9
ENDIF
READ(30,*) (TMAX(TANK,YR,MNTH), MNTH=1,TK)
ENDDO
ENDDO

```

```

OPEN(UNIT=40, FILE='tmin.txt', STATUS='old')
DO TANK=1,8
TK=12
DO YR=1,16
IF (YR.EQ.16) THEN

```

```

TK=9
ENDIF
READ(40,*) (TMIN(TANK,YR,MNTH), MNTH=1,TK)
ENDDO
ENDDO

DO TANK=1,8
TK=12
DO YR=1,16
IF (YR.EQ.16) THEN
TK=9
ENDIF
DO MNTH=1,TK
P(TANK,YR,MNTH) = P(TANK,YR,MNTH) * PSCALE
TMAX(TANK,YR,MNTH) = TMAX(TANK,YR,MNTH) * TSCALE
TMIN(TANK,YR,MNTH) = TMIN(TANK,YR,MNTH) * TSCALE
ENDDO
ENDDO
ENDDO

OPEN(UNIT=50, FILE='stmax.txt', STATUS='old')
DO TANK=1,8
READ(50,*) STMAX(TANK)
ENDDO

OPEN(UNIT=60, FILE='area.txt', STATUS='old')
DO TANK=1,8
READ(60,*) AREA(TANK)
ENDDO

OPEN(UNIT=70, FILE='k.txt', STATUS='old')
DO TANK=1,8
READ(70,*) C(TANK)
ENDDO

OPEN(UNIT=80, FILE='a.txt', STATUS='old')
DO TANK=1,8
READ(80,*) A(TANK)
ENDDO

CLOSE(10)
CLOSE(20)
CLOSE(30)
CLOSE(40)
CLOSE(50)
CLOSE(60)
CLOSE(70)
CLOSE(80)

```

```

OPEN(UNIT=21, FILE='output.txt', STATUS='unknown', ERR=10010)
OPEN(UNIT=23, FILE='toground.txt',STATUS='unknown', ERR=10010)

PI=3.1415927
PHI = (29.+58./60.)*PI/180.
MINERR = 1000.
MAXRSQ = 0.0

DO TANK=1,8
TK=12
DO YR=1,16

IF (YR.EQ.16) THEN
TK=9
ENDIF

DO MNTH=1,TK
SURP_PRD(TANK,YR,MNTH)=0
EVAP_BDG(TANK,YR,MNTH)=0
EVAP_PRD(TANK,YR,MNTH)=0
ST(TANK,YR,1)=0.01
ENDDO
ENDDO
ENDDO

DO TANK=1,8
TK=12
DO YR=1,16

IF (YR.EQ.16) THEN
TK=9
ENDIF

CONVERGE=.FALSE.
K=0
JDAY=0

! BEGIN BUDGET LOOP FOR GIVEN TANK

DO WHILE (K.LE.30.AND.(.NOT.CONVERGE))
K=K+1

! INITIALIZE VARIABLES

DO MNTH=1,TK
ST_TEMP=ST(TANK,YR,MNTH)
SURPTOT=0
EVAPTOT=0

```

```

! BEGIN PSEUDO-DAILY BUDGETING

DO D=1,NDAYS(MNTH)
SATUR=ST_TEMP/STMAX(TANK)
JDAY=JDAY+1
IF (JDAY>365) THEN
JDAY=1
ENDIF

! CALCULATE EVAPORATION

DIST=1+0.033*COS(2*PI*JDAY/365)
SIGMA=0.4093*SIN(2*PI*JDAY/365-1.405)
OMEGA=ACOS(-TAN(PHI)*TAN(SIGMA))
SORAD=15.392*DIST*(OMEGA*SIN(PHI)*SIN(SIGMA)+
&      COS(PHI)*COS(SIGMA)*SIN(OMEGA))
T_AVE=(TMAX(TANK,YR,MNTH)+TMIN(TANK,YR,MNTH))/2
E_POT=0.0023*SORAD*(TMAX(TANK,YR,MNTH)-
&      TMIN(TANK,YR,MNTH))*(T_AVE+17.8)
EVVAL=SATUR*C(TANK)*E_POT
EVAPTOT=EVAPTOT+EVVAL

! CALCULATE RUNOFF

RC=SATUR*A(TANK)**((STMAX(TANK)-ST_TEMP)/STMAX(TANK))
RUNOFF=RC*P(TANK,YR,MNTH)/NDAYS(MNTH)

! CALCULATE NEW SOIL MOISTURE

ST_TEMP=ST_TEMP+P(TANK,YR,MNTH)/NDAYS(MNTH)-
&      EVVAL-RUNOFF

IF (ST_TEMP.LT.0) THEN
ST_TEMP=0.01
ENDIF

IF (ST_TEMP.GT.STMAX(TANK)) THEN
DSURP=ST_TEMP-STMAX(TANK)
SURPTOT=SURPTOT+DSURP
ST_TEMP=STMAX(TANK)
ENDIF

SURPTOT=SURPTOT+RUNOFF

! FINISH DAILY LOOP
ENDDO

ST(TANK,YR,MNTH+1)=ST_TEMP
SURP_PRD(TANK,YR,MNTH)=SURPTOT

```



```

EVAP_PRD(TANK,YR,MNTH)=EVAPTOT

IF (MNTH.GT.1) THEN
DST(TANK,YR,MNTH)=ST(TANK,YR,MNTH+1)-
& ST(TANK,YR,MNTH)
EVAP_BDG(TANK,YR,MNTH)=P(TANK,YR,MNTH)-
& SURP_PRD(TANK,YR,MNTH)-DST(TANK,YR,MNTH)
ENDIF

! FINISH MONTHLY LOOP
SURP_PRD(TANK,YR,MNTH)=SURP_PRD(TANK,YR,MNTH)/10/30.48
& *AREA(TANK)*5280**2/43560/1000
ENDDO

! TEST FOR CONVERGENCE
DIFF=ST(TANK,YR,1)-ST(TANK,YR,13)
IF (ABS(DIFF).LT.0.1) THEN
CONVERGE=.TRUE.
ENDIF

! ALTER INITIAL SOIL MOISTURE GUESS
ST(TANK,YR,1)=ST(TANK,YR,13)

! FINISH CONVERGENCE LOOP
ENDDO

IF (K.GT.30) THEN
WRITE(*,*) '--CONVERGENCE NOT ACHIEVED AFTER 30 ITERATIONS--'
STOP
ENDIF

! FINISH YEAR LOOP
ST(TANK,YR+1,1)=ST(TANK,YR,13)
ENDDO

! FINISH TANK LOOP
ENDDO

OPEN(UNIT=25, FILE='outsrp_p.txt', STATUS='unknown', ERR=10010)
OPEN(UNIT=26, FILE='outsrp_o.txt', STATUS='unknown', ERR=10010)
OPEN(UNIT=27, FILE='out_p.txt', STATUS='unknown', ERR=10010)

ERROR = 0.0
SUMOBS = 0.0
BIGDIF = 0.0
N=0.0
SUMX = 0.0
SUMY = 0.0
SUMXY = 0.0

```

```

SUMXSQ = 0.0
SUMYSQ = 0.0

DO I=1,8
TANK = I
TK=12
IF (TANK.NE.5) THEN

DO YR=1,16

IF (YR.EQ.16) THEN
TK=9
ENDIF

DO MNTH=1,TK

N = N + 1.
SUMX = SUMX + SURP_OBS(TANK,YR,MNTH)
SUMY = SUMY + SURP_PRD(TANK,YR,MNTH)
SUMXY = SUMXY + SURP_OBS(TANK,YR,MNTH)*
&      SURP_PRD(TANK,YR,MNTH)
SUMXSQ = SUMXSQ + (SURP_OBS(TANK,YR,MNTH))**2.
SUMYSQ = SUMYSQ + (SURP_PRD(TANK,YR,MNTH))**2.

ERROR=ERROR + ABS(SURP_OBS(TANK,YR,MNTH)-
&      SURP_PRD(TANK,YR,MNTH))
BIGDIF=BIGDIF + SURP_OBS(TANK,YR,MNTH)-
&      SURP_PRD(TANK,YR,MNTH)
SUMOBS = SUMOBS + SURP_OBS(TANK,YR,MNTH)

ENDDO
ENDDO

ENDIF
ENDDO

NUM = (N*SUMXY-SUMX*SUMY)**2.

DEN = ((N*SUMXSQ-SUMX**2.)*(N*SUMYSQ-SUMY**2.))

RSQ = NUM/DEN

WRITE(21,*) "
WRITE(21,*) 'RSQ = ', RSQ

PRINT *, 'RSQ = ', RSQ

E = ERROR/SUMOBS

```

```

WRITE(21,*) 'E = ', E

PRINT *, 'E = ', E

WRITE(21,*) 'BIGDIF = ', BIGDIF
WRITE(21,*) "

PRINT *, 'BIGDIF = ', BIGDIF

DO TANK=1,8
TK=12
WRITE(21,*) '-----'
WRITE(21,*) 'TANK=', TANK
DO YR=1,16
IF (YR.EQ.16) THEN
TK=9
ENDIF

YEAR=1974+YR
WRITE(21,*) YEAR
WRITE(21,*) "
WRITE(21,*) '--PREDICTED SURPLUS--'
WRITE(21,9000) (SURP_PRD(TANK,YR,MNTH), MNTH=1,TK)
WRITE(21,*) "
WRITE(21,*) '--OBSERVED SURPLUS--'
WRITE(21,9000) (SURP_OBS(TANK,YR,MNTH), MNTH=1,TK)
WRITE(21,*) "
WRITE(21,*) '--PREDICTIVE EVAPORATION--'
WRITE(21,9000) (EVAP_PRD(TANK,YR,MNTH), MNTH=1,TK)
WRITE(21,*) "
WRITE(21,*) '--BUDGETED EVAPORATION--'
WRITE(21,9000) (EVAP_BDG(TANK,YR,MNTH), MNTH=1,TK)
WRITE(21,*) "
WRITE(21,*) '--SOIL MOISTURE--'
WRITE(21,9000) (ST(TANK,YR,MNTH), MNTH=1,TK)
WRITE(21,*) "
ENDDO
ENDDO

TK=12

! READ KNOWN VALUES FOR MEDINA RESERVOIR (TANK 5)

DO YR=1,16
IF (YR.EQ.16) THEN
TK=9
ENDIF
DO MNTH=1,TK
SURP_PRD(5,YR,MNTH)=SURP_OBS(5,YR,MNTH)

```

```

ENDDO
TK=12
ENDDO

TK=12
MONTH=0
NINE=0.0

DO YR=1,16
IF (YR.EQ.16) THEN
TK=9
ENDIF
DO MNTH=1,TK
MONTH=MONTH+1
WRITE(23,3000) MONTH,(SURP_PRD(Z,YR,MNTH), Z=1,8), NINE
ENDDO
TK=12
ENDDO

3000    FORMAT(I3, 8(F9.2), F9.1)

TK=12
DO YR=1,16

IF (YR.EQ.16) THEN
TK=9
ENDIF

DO MNTH=1,TK
DO TANK=1,8
WRITE(25,8500) SURP_PRD(TANK,YR,MNTH)
WRITE(25,*) "
WRITE(26,8500) SURP_OBS(TANK,YR,MNTH)
WRITE(26,*) "
WRITE(27,8500) P(TANK,YR,MNTH)
WRITE(27,*) "
ENDDO
ENDDO
TK=12
ENDDO

CLOSE(21)
CLOSE(23)
CLOSE(25)
CLOSE(26)
CLOSE(27)

WRITE(*,*) '--WATER BUDGET COMPLETE--'

```

```
STOP
8500  FORMAT(F8.2)
9000  FORMAT(12(F8.2))

10010 WRITE(*,*) '--COULD NOT OPEN OUTPUT FILE--'
STOP

END
```

Validate.for

PROGRAM VALIDATE ! Original program by Reed, Maidment, and Patoux (1997)

```

      IMPLICIT NONE
      REAL P(8,8,13), TMAX(8,8,13), TMIN(8,8,13)
      REAL STMAX(8), AREA(8)
      REAL SURP_OBS(8,8,13), SURP_PRD(8,8,13)
      REAL EVAP_BDG(8,8,13), EVAP_PRD(8,8,13)
      REAL ST(8,8,13), DST(8,8,13)
      REAL ST_TEMP, SATUR, DIFF
      REAL DIST, SIGMA, PHI, OMEGA, PI
      REAL SORAD, T_AVE, E_POT, EVVAL, EVAPTOT
      REAL A, C, RC, DSURP, SURPTOT, RUNOFF
      INTEGER NDAYS(12), D, MNTH, YR, JDAY
      INTEGER I, K, TANK, TK
      LOGICAL CONVERGE

! *****
! CALIBRATION VARIABLES
! *****

      REAL N, SUMX, SUMY, SUMXSQ, SUMYSQ, SUMXY, RSQ, NUM, DEN
      REAL E, ERROR, SUMOBS, BIGDIF
      REAL MAXRSQ, MINERR

      DATA NDAYS /31,30,31,30,31,31,28,31,30,31,30,31/

! -----
! INPUT FILES: SURPLUS.TXT, PPT.TXT, TMAX.TXT,
!              TMIN.TXT, STMAX.TXT, AREA.TXT
! OUTPUT FILES: OUTSRP_P.TXT, OUTSRP_O.TXT,
!              OUT_P.TXT, OUTPUT.TXT
! -----

      OPEN(UNIT=10, FILE='surplus.txt', STATUS='old')
      DO TANK=1,8
      DO YR=1,8
      READ(10,*) (SURP_OBS(TANK,YR,MNTH), MNTH=1,12)
      ENDDO
      ENDDO

      OPEN(UNIT=20, FILE='ppt.txt', STATUS='old')
      DO TANK=1,8
      DO YR=1,8
      READ(20,*) (P(TANK,YR,MNTH), MNTH=1,12)
      ENDDO
      ENDDO

      OPEN(UNIT=30, FILE='tmax.txt', STATUS='old')
      DO TANK=1,8
```

```

DO YR=1,8
READ(30,*) (TMAX(TANK,YR,MNTH), MNTH=1,12)
ENDDO
ENDDO

OPEN(UNIT=40, FILE='tmin.txt', STATUS='old')
DO TANK=1,8
DO YR=1,8
READ(40,*) (TMIN(TANK,YR,MNTH), MNTH=1,12)
ENDDO
ENDDO

OPEN(UNIT=50, FILE='stmax.txt', STATUS='old')
DO TANK=1,8
READ(50,*) STMAX(TANK)
ENDDO

OPEN(UNIT=60, FILE='area.txt', STATUS='old')
DO TANK=1,8
READ(60,*) AREA(TANK)
ENDDO

CLOSE(10)
CLOSE(20)
CLOSE(30)
CLOSE(40)
CLOSE(50)
CLOSE(60)

OPEN(UNIT=21, FILE='output.txt', STATUS='unknown', ERR=10010)

PI=3.1415927
PHI = (29.+58./60.)*PI/180.
A = 0.0
C = 0.0
MINERR = 1000.
MAXRSQ = 0.0

PRINT *, '*****'
PRINT *, 'SINGLE TANK RUN'
PRINT *, ''
PRINT *, 'OUTPUT FILES HAVE PPT, SURP, EVAP, SOIL MOISTURE'
PRINT *, '*****'
PRINT *, ''
PRINT *, 'ENTER KNOWN PARAMETERS:'
PRINT *, ''

PRINT *, 'INPUT VALUE FOR A:'
READ *, A

```



```

PRINT *,INPUT VALUE FOR C:'
READ *, C
PRINT *,STATS FOR TANK  :'
READ *, TK

DO TANK=1,8
DO YR=1,8
DO MNTH=1,12
SURP_PRD(TANK,YR,MNTH)=0
EVAP_BDG(TANK,YR,MNTH)=0
EVAP_PRD(TANK,YR,MNTH)=0
ST(TANK,YR,1)=0.01
ENDDO
ENDDO
ENDDO

DO TANK=1,8
DO YR=1,8
CONVERGE=.FALSE.
K=0
JDAY=212

! BEGIN BUDGET LOOP FOR GIVEN TANK

DO WHILE (K.LE.30.AND.(.NOT.CONVERGE))
K=K+1

! INITIALIZE VARIABLES

DO MNTH=1,12
ST_TEMP=ST(TANK,YR,MNTH)
SURPTOT=0
EVAPTOT=0

! BEGIN PSEUDO-DAILY BUDGETING

DO D=1,NDAYS(MNTH)
SATUR=ST_TEMP/STMAX(TANK)
JDAY=JDAY+1
IF (JDAY>365) THEN
JDAY=1
ENDIF

! CALCULATE EVAPORATION

DIST=1+0.033*COS(2*PI*JDAY/365)
SIGMA=0.4093*SIN(2*PI*JDAY/365-1.405)
OMEGA=ACOS(-TAN(PHI)*TAN(SIGMA))
SORAD=15.392*DIST*(OMEGA*SIN(PHI)*SIN(SIGMA))+

```

```

&      COS(PHI)*COS(SIGMA)*SIN(OMEGA))
T_AVE=(TMAX(TANK,YR,MNTH)+TMIN(TANK,YR,MNTH))/2
E_POT=0.0023*SORAD*(TMAX(TANK,YR,MNTH)-
&      TMIN(TANK,YR,MNTH))*(T_AVE+17.8)
EVVAL=SATUR*C*E_POT
EVAPTOT=EVAPTOT+EVVAL

! CALCULATE RUNOFF

RC=SATUR*A**((STMAX(TANK)-ST_TEMP)/STMAX(TANK))
RUNOFF=RC*P(TANK,YR,MNTH)/NDAYS(MNTH)

! CALCULATE NEW SOIL MOISTURE

ST_TEMP=ST_TEMP+P(TANK,YR,MNTH)/NDAYS(MNTH)-
&      EVVAL-RUNOFF

IF (ST_TEMP.LT.0) THEN
ST_TEMP=0.01
ENDIF

IF (ST_TEMP.GT.STMAX(TANK)) THEN
DSURP=ST_TEMP-STMAX(TANK)
SURPTOT=SURPTOT+DSURP
ST_TEMP=STMAX(TANK)
ENDIF

SURPTOT=SURPTOT+RUNOFF

! FINISH DAILY LOOP
ENDDO

ST(TANK,YR,MNTH+1)=ST_TEMP
SURP_PRD(TANK,YR,MNTH)=SURPTOT
EVAP_PRD(TANK,YR,MNTH)=EVAPTOT

IF (MNTH.GT.1) THEN
DST(TANK,YR,MNTH)=ST(TANK,YR,MNTH+1)-
&      ST(TANK,YR,MNTH)
EVAP_BDG(TANK,YR,MNTH)=P(TANK,YR,MNTH)-
&      SURP_PRD(TANK,YR,MNTH)-DST(TANK,YR,MNTH)
ENDIF

! FINISH MONTHLY LOOP
SURP_PRD(TANK,YR,MNTH)=SURP_PRD(TANK,YR,MNTH)/10/30.48
&      *AREA(TANK)*5280**2/43560/1000
ENDDO

! TEST FOR CONVERGENCE

```

```

DIFF=ST(TANK,YR,1)-ST(TANK,YR,13)
IF (ABS(DIFF).LT.0.1) THEN
CONVERGE=.TRUE.
ENDIF

! ALTER INITIAL SOIL MOISTURE GUESS
ST(TANK,YR,1)=ST(TANK,YR,13)

! FINISH CONVERGENCE LOOP
ENDDO

IF (K.GT.30) THEN
WRITE(*,*) '--CONVERGENCE NOT ACHIEVED AFTER 30 ITERATIONS--'
STOP
ENDIF

! FINISH YEAR LOOP
ST(TANK,YR+1,1)=ST(TANK,YR,13)
ENDDO

! FINISH TANK LOOP
ENDDO

OPEN(UNIT=25, FILE='outsrp_p.txt', STATUS='unknown', ERR=10010)
OPEN(UNIT=26, FILE='outsrp_o.txt', STATUS='unknown', ERR=10010)
OPEN(UNIT=27, FILE='out_p.txt', STATUS='unknown', ERR=10010)

WRITE(21,*) 'A =' ,A
WRITE(21,*) 'K =' ,K

ERROR = 0.0
SUMOBS = 0.0
BIGDIF = 0.0
N=0.0
SUMX = 0.0
SUMY = 0.0
SUMXY = 0.0
SUMXSQ = 0.0
SUMYSQ = 0.0

DO I=TK,TK
TANK = I
IF (TANK.NE.5) THEN

DO YR=1,8
DO MNTH=1,12
N = N + 1.
SUMX = SUMX + SURP_OBS(TANK,YR,MNTH)
SUMY = SUMY + SURP_PRD(TANK,YR,MNTH)

```

```

SUMXY = SUMXY + SURP_OBS(TANK,YR,MNTH)*
&      SURP_PRD(TANK,YR,MNTH)
SUMXSQ = SUMXSQ + (SURP_OBS(TANK,YR,MNTH))**2.
SUMYSQ = SUMYSQ + (SURP_PRD(TANK,YR,MNTH))**2.

ERROR=ERROR + ABS(SURP_OBS(TANK,YR,MNTH)-
&      SURP_PRD(TANK,YR,MNTH))
BIGDIF=BIGDIF + SURP_PRD(TANK,YR,MNTH)-
&      SURP_OBS(TANK,YR,MNTH)
SUMOBS = SUMOBS + SURP_OBS(TANK,YR,MNTH)
ENDDO
ENDDO

ENDIF
ENDDO

NUM = (N*SUMXY-SUMX*SUMY)**2.

DEN = ((N*SUMXSQ-SUMX**2.)*(N*SUMYSQ-SUMY**2.))

RSQ = NUM/DEN

WRITE(21,*) "
WRITE(21,*) 'RSQ = ', RSQ

PRINT *, 'RSQ = ', RSQ

E = ERROR/SUMOBS

WRITE(21,*) 'E = ', E

PRINT *, 'E = ', E

WRITE(21,*) 'BIGDIF = ', BIGDIF
WRITE(21,*) "

DO TANK=1,8
WRITE(21,*) '-----'
WRITE(21,*) 'TANK=', TANK
DO YR=1,8
WRITE(21,*) 'YEAR=', YR
WRITE(21,*) "
WRITE(21,*) '--PREDICTED SURPLUS--'
WRITE(21,9000) (SURP_PRD(TANK,YR,MNTH), MNTH=1,12)
WRITE(21,*) "
WRITE(21,*) '--OBSERVED SURPLUS--'
WRITE(21,9000) (SURP_OBS(TANK,YR,MNTH), MNTH=1,12)
WRITE(21,*) "
WRITE(21,*) '--PREDICTIVE EVAPORATION--'

```

```

WRITE(21,9000) (EVAP_PRD(TANK,YR,MNTH), MNTH=1,12)
WRITE(21,*) "
WRITE(21,*) '--BUDGETED EVAPORATION--'
WRITE(21,9000) (EVAP_BDG(TANK,YR,MNTH), MNTH=1,12)
WRITE(21,*) "
WRITE(21,*) '--SOIL MOISTURE--'
WRITE(21,9000) (ST(TANK,YR,MNTH), MNTH=1,12)
WRITE(21,*) "
ENDDO
ENDDO

DO YR=1,8
DO MNTH=1,12
WRITE(25,8500) SURP_PRD(TK,YR,MNTH)
WRITE(26,8500) SURP_OBS(TK,YR,MNTH)
WRITE(27,8500) P(TK,YR,MNTH)
ENDDO
ENDDO

CLOSE(21)
CLOSE(25)
CLOSE(26)
CLOSE(27)

WRITE(*,*) '--WATER BUDGET COMPLETE--'

STOP

8500    FORMAT(F8.2)
9000    FORMAT(12(F8.2))

10010   WRITE(*,*) '--COULD NOT OPEN OUTPUT FILE--'
STOP

END

```

WHCcalc.ave

```

=====
NAME: whccalc.ave
DATE: Last Modified on 2/2/98
,
PURPOSE: Calculate Water Holding Capacity for
each of the components in a map unit and then for
each map unit.
,
INPUTS: STATSGO theme, Layer Table, Component Table
,
OUTPUTS: Program writes the WHC for each Map Unit to
the STATSGO feature table
,
COMMENTS:
,
=====

```

INITIALIZE TABLES

```

-----

layerTable = av.GetProject.FindDoc("layer.dbf")
lyerVTab = layerTable.GetVTab
compTable = av.GetProject.FindDoc("comp.dbf")
compVTab = compTable.GetVTab
theView = av.GetProject.FindDoc("view1")
muFTab = theView.FindTheme("Statsgo").GetFTab

compVTab.SetEditable(true)
muFTab.SetEditable(true)

muField = lyerVTab.FindField("muid")
compField = lyerVTab.FindField("seqnum")
layerField = lyerVTab.FindField("layernum")
awclField = lyerVTab.FindField("awcl")
awchField = lyerVTab.FindField("awch")
ldeplField = lyerVTab.FindField("laydepl")
ldephField = lyerVTab.FindField("laydeph")

muField2 = compVTab.FindField("muid")
compField2 = compVTab.FindField("seqnum")
pctField = compVTab.FindField("comppct")
f1 = compVTab.FindField("cwhc")

muField3 = muFTab.FindField("muid")
f2 = muFTab.FindField("WHC")

```

INITIALIZE ARRAYS AND VARIABLES

```

-----

```

```

whc = 0
lyerold = 0

d = Dictionary.Make(6000)    'comppct dictionary
twhc = Dictionary.Make(6000) 'component WHC dictionary
muwhc = Dictionary.Make(1000) 'map unit WHC dictionary

for each i in compVTab

    mu2 = compVTab.ReturnValue(muField2, i)
    comp2 = compVTab.ReturnValue(compField2, i)
    pct2 = compVTab.ReturnValue(pctField, i)
    tot = 0

    unique = mu2+comp2.AsString

    d.Add(unique, pct2)
    twhc.Add(unique, tot)

end

PERFORM COMPONENT WHC CALCULATION
'-----

for each j in lyerVTab

    mu = lyerVTab.ReturnValue(muField,j)
    comp = lyerVTab.ReturnValue(compField, j)
    lyer = lyerVTab.ReturnValue(layerField, j)
    awcl = lyerVTab.ReturnValue(awclField, j)
    awch = lyerVTab.ReturnValue(awchField, j)
    ldepl = lyerVTab.ReturnValue(ldeplField, j)
    ldeph = lyerVTab.ReturnValue(ldephField, j)

    ball = mu+comp.asString

    pct = d.Get(ball) 'Get compcpt from component table

    if (lyer > lyerold) then
        whc = pct / 100 * (awcl + awch) / 2.0 *
            (ldeph - ldepl) + whc
        twhc.Set(ball, whc)
        lyerold = lyer
    else
        whc = pct / 100 * (awcl + awch) / 2.0 *
            (ldeph - ldepl)
        twhc.Set(ball,whc)
        lyerold = lyer
    end
end

```



```

end

WRITE COMPONENT WHC VALUES TO COMPONENT TABLE
'-----

for each k in compVTab

    mu2 = compVTab.ReturnValue(muField2, k)
    comp2 = compVTab.ReturnValue(compField2, k)

    stick = mu2+comp2.AsString

    whc = twhc.Get(stick)

    compVTab.SetValue(f1, k, whc)

end

compVTab.SetEditable(false)

compold = 0
whc = 0

PERFORM MAP UNIT WHC CALCULATION
'-----

for each m in compVTab

    mu2 = compVTab.ReturnValue(muField2, m)
    comp2 = compVTab.ReturnValue (compField2, m)
    cwhc2 = compVTab.ReturnValue (f1, m)

    if (comp2 > compold) then
        whc = cwhc2 + whc
        muwhc.Set(mu2, whc)
        compold = comp2
    else
        whc = cwhc2
        muwhc.Set(mu2, whc)
        compold = comp2
    end

end

WRITE MAP UNIT WHC TO MAP UNIT FEATURE TABLE
'-----

```

```
for each n in muFTab
    mu3 = muFTab.ReturnValue(muField3, n)
    whc = muwhc.Get(mu3)
    muFTab.SetValue(f2, n, whc)
end
muFTab.SetEditable(false)
```

ZoneMean.ave

```

=====
NAME: zonemean.ave
DATE: Last Modified on 3/10/98
,
PURPOSE: Calculates the mean for each feature in a
zone theme. A value theme is converted to a grid
and cells that intersect or are contained in a
feature of the zone theme will be used to calculate
the mean for that feature. Calculations are
performed over a time period specified by the user.
,
INPUTS: Zone theme, Value theme
,
OUTPUTS: Program writes the mean for each of the
features to an output table specified by the user.
A separate field is created for each time period.
,
COMMENTS: Zone theme and Value theme can be
coverages or shapefiles.
,
=====

theView = av.GetProject.FindDoc( "view1" )

labels = { "Zone Theme" , "Value Theme" }
defaults = { "Basins.shp" , "Raingrd" }

GET ZONE THEME AND VALUE THEME
-----

aThmList = MsgBox.Multiinput ( "User Input","ZonalMean",
labels, defaults )

if (aThmList.IsEmpty) then
    MsgBox.Info("No Themes Selected", "Error" )
    exit
end

zoneString = aThmList.Get(0).AsString
zoneTheme = theView.FindTheme ( zoneString )
zoneFTab = zoneTheme.GetFTab
zoneField = zoneFTab.FindField( "Grid_code" )

valueString = aThmList.Get(1).AsString
valueTheme = theView.FindTheme ( valueString )
valueFTab = valueTheme.GetFTab

DICTIONARY -d- WILL STORE CALCULATED MEANS FOR EACH
OF THE FEATURES. CHANGE NUMBER IN MAKE(*) TO BE

```

```
'GREATER THAN THE NUMBER OF ZONES(WATERSHEDS) YOU HAVE
'
```

```
d = Dictionary.Make(100)
```

```
'USER SPECIFIES A TABLE WHERE CALCULATED MEANS
WILL BE WRITTEN
'
```

```
aTable = MsgBox.Input ( "Join Data to which Table?" ,
    "Add to Climate Table" , "pqttbl.dbf" )
```

```
if ( aTable = nil ) then
    MsgBox.Info ( "No Table Selected", "Error" )
    exit
end
```

```
fldString = MsgBox.Input( "In zone theme, which field contains unique IDs?",
    "Key Field","Grid_code")
```

```
climTable = av.GetProject.FindDoc (aTable)
climVTab = climTable.GetVTab
keyField = climVTab.FindField("Grid_code")
```

```
if ( fldString = nil ) then
    MsgBox.Info ( "Cannot Find Key Field","Error" )
    exit
end
```

```
climVTab.SetEditable (true)
```

```
'SET GRID ENVIRONMENT-CELL SIZE AND EXTENT
'
```

```
theAE = theView.GetExtension(AnalysisEnvironment)
theExtent = Rect.Make(0@0,1@1)
theCellSize = 1
```

```
if ((theAE.GetExtent(theExtent) <> #ANALYSENV_VALUE) or
    (theAE.GetCellSize(theCellSize) <> #ANALYSENV_VALUE)) then
```

```
    theCE = AnalysisPropertiesDialog.Show
    (theView,TRUE,"Conversion Extent")
```

```
    if (theCE = NIL) then
        return NIL
    end
```

```

    theCE.GetCellSize(theCellSize)
    theCE.GetExtent(theExtent)

end

aPrj = theView.GetProjection

'BEGIN STEPPING THROUGH MONTHLY FIELDS
'-----

beginString = MsgBox.Input
    ("In value theme, which field contains data for first time step?",
    "Beginning Field", "Jan_75")

endString = MsgBox.Input
    ("In value theme, which field contains data for last time step?",
    "End Field", "Dec_93")

if ((beginString = nil) OR (endString = nil)) then
    MsgBox.Info("No Fields Selected", "Error")
    exit
end

fieldList = valueFTab.GetFields

flag = 0

for each i in fieldList

    valueString = i.AsString

    if (valueString = beginString) then
        flag = 1
    end

    if (flag = 0) then
        continue
    end

    aFld = valueFTab.FindField(valueString)

    aGrid = Grid.MakeFromFTab(valueFTab, aPrj, aFld,
    { theCellSize, theExtent })
    theGTheme = GTheme.Make(aGrid)
    if (aGrid.HasError) then
        return NIL
    end

    theGrid = theGTheme.GetGrid

```

```

aFN = "stat.dbf".AsFileName

theVTab = theGrid.ZonalStatsTable ( zoneFTab,aPrj,
zoneField,FALSE,aFN )

if (theVTab.HasError) then
    return NIL
    MsgBox.Info("VTab Error","Error" )
    exit
end

statList = theVTab.GetFields

P = "*mean".AsPattern

for each n in statList
    if (n.AsString = P) then
        name = n.AsString
        break
    end
end

av.ShowMsg("Processing Month: "++valueString)

for each p in 0..1000
end

MeanField = theVTab.FindField ( name )
GridField = theVTab.FindField ( "Grid_code" )

f1 = Field.Make(valueString, #FIELD_DOUBLE, 10, 4)

climVTab.AddFields({f1})

for each j in theVTab
    meanValue = theVTab.ReturnValue(MeanField, j)
    gridValue = theVTab.ReturnValue(GridField, j)
    d.Set(gridValue, meanValue)
end

for each k in climVTab
    gc = climVTab.ReturnValue(keyField, k)
    ppt = d.Get(gc)
    climVTab.SetValue(f1, k, ppt)
end

if (valueString = endString) then

```

```
        break
    end

end

MsgBox.Info("Done!", "")
climVTab.SetEditable(FALSE)
```


Glossary

A	Soil-Saturation Parameter
AF	Acre-Feet
AWC	Average Water Capacity
BFZ	Balcones Fault Zone
CCC	Canadian Climate Centre
CSIRO	Commonwealth Scientific Industrial Research Organisation
Cm	Centimeter
CO ₂	Carbon Dioxide
DD	Decimal Degrees
DMS	Degrees, Minutes, and Seconds
DEM	Digital Elevation Model
ENSO	El Niño-Southern Oscillation
EROS	Earth Resources Observation System
ESRI	Environmental Systems Research Institute
Ft	Feet
GCM	General Circulation Model
GFDL	Geophysical Fluid Dynamics Laboratory
GIS	Geographic Information Systems
GISS	Goddard Institute for Space Studies
ID	Unique Identification Number
IPCC	Intergovernmental Panel on Climate Change
K _c	Crop Coefficient
Km	Kilometer
K _s	Soil-Moisture Extraction Function
M	Meter
Mi	Mile
Mm	Millimeter
NCDC	National Climatic Data Center
NOAA	National Oceanic and Atmospheric Administration
OSU	Oregon State University
PAT	Polygon Attribute Table
PMEL	Pacific Marine Environmental Laboratory
PRISM	Parameter Regressions on Independent Slopes Model
R ²	Pearson product moment correlation coefficient
RF1	Reach File 1

RMSE	Root-Mean Square Error
RR	Recharge Ratio
SCS	Soil Conservation Service
SMD	Sum of Mass Discrepancies
SOR	Successive Over Relaxation
STATSGO	State Soil Geographic Data Base
TNRCC	Texas Natural Resource Conservation Commission
TSMS	Texas Statewide Mapping System
TWDB	Texas Water Development Board
UKMO	United Kingdom Meteorological Office
USDA	United States Department of Agriculture
USGS	United States Geological Survey
VEMAP	Vegetation/Ecosystem Modeling and Analysis Project

Bibliography

- Alley, W.M. (1984). "On the treatment of evapotranspiration, soil moisture accounting, and aquifer recharge in monthly water balance models." *Water Resources Research*, Vol. 20(8), pp. 1137-1149
- Boer, G.J., McFarlane, N.A., and Lazare, M. (1992). "Greenhouse gas-induced climate change simulated with the CCC second-generation general circulation model." *Journal of Climate*, Vol. 5, pp. 1045-1077.
- Chow, V.T., Maidment, D.R., and Mays, L. (1988). *Applied Hydrology*, New York: McGraw-Hill, Inc.
- Clark, W.C. and Jäger J. (1997). "Evaluating climate change 1995." *Environment*, Vol. 39(9), pp. 5-33.
- Coles, N.A., Sivapalan, M., Larsen, J.E., Linnet, P.E., and Fahrner, C.K., "Modeling runoff generation on small agricultural catchments: Can real world runoff responses be captured?" *Hydrologic Processes*, Vol. 11, p. 111-136.
- Commonwealth Scientific Industrial Research Organisation (1996)," [Internet, WWW], ADDRESS: <http://www.dar.csiro.au/pub/programs/climod/impacts/scenaus.htm>.
- Daly, C., Neilson, R.P. and Phillips, D.L. (1994). "A statistical-topographic model for mapping climatological precipitation over mountainous terrain." *Journal of Applied Meteorology*, Vol. 33, pp. 140-158.
- Eckhardt, G.A. (1995). "The Edwards Aquifer home page," [Internet, WWW], ADDRESS: <http://www.txdirect.net/~eckhardt>.
- Environmental Systems Research Institute, Inc. (1997). *Understanding GIS-The ARC/INFO Method*, New York: John Wiley & Sons, Inc.
- Hansen, J., Lacis, A., Rind, D., Russel, G., Stone, P., Fung, I., Ruedy, R., and Lerner, J. (1984). "Climate sensitivity: Analysis of feedback mechanisms." *Climate Processes and Climate Sensitivity*, Geophysical

- Monograph 29, American Geophysical Union, Washington, D.C., pp. 130-163.
- HDR Engineering, Inc., and Espey, Huston and Assoc., Inc. (1993). "Guadalupe-San Antonio River Basin recharge enhancement study." *Volume II-Technical Report*, Ch. 4, pp. 5-8.
- Houghton, J.T., et al. (1996). "Contribution of Working Group I to the second assessment report of the Intergovernmental Panel on Climate Change." *Climate Change 1995: The Science of Climate Change*, New York: Cambridge University Press.
- Jenne, R.L. (1992). "Climate model description and impact on terrestrial climate." *Global Climate Change: Implications, Challenges and Mitigation Measures*, ed. Majumdar, S.K., Kalkstein, L.S., Yarnal, B., Miller, E.W., Rosenfeld, L.M., Pennsylvania Academy of Science, pp. 145-164.
- Kittel, T.G.F., Royle, J.A., Daly, C., Rosenbloom, N.A., Gibson, W.P., Fisher, H.H., Schimel, D.S., Berliner, L.M. and VEMAP2 Participants (1997). "A gridded historical (1895-1993) bioclimate dataset for the conterminous United States." *Proceedings of the 10th Conference on Applied Climatology*, American Meteorological Society, Reno, Nevada.
- Kittel, T.G.F., Rosenblum, N.A., Painter, T.H., Schimel, D.S., Fisher, H.H., Grimsdell, A., and VEMAP Participants (1996). "The VEMAP Phase I database: An integrated input dataset for ecosystem and vegetation modeling for the conterminous United States," CDROM and [Internet, WWW], ADDRESS: <http://www.cgd.ucar.edu/vemap>.
- Klemt, W.B., Knowles, T.R., Elder, G.R., Sieh, T.W. (1979). "Ground-water resources and model applications for the Edwards (Balcones Fault Zone) Aquifer in the San Antonio region, Texas." *Texas Department of Water Resources Report No. 239*, Austin, Texas.
- Maclay, R. W. (1989). "Edwards Aquifer in the San Antonio region: its hydrogeology and management." *South Texas Geological Society Bulletin*.
- Maclay, R.W. and Land, L.F. (1988). "Simulation of flow in the Edwards Aquifer, San Antonio region, Texas, and refinement of storage and flow concepts." *United States Geological Survey Water-Supply Paper No. 2336-A*, Denver, Colorado.

- Manabe S. and Wetherald, R.T. (1987). "Large-scale changes in soil wetness induced by increase in carbon dioxide." *Journal of Atmospheric Science*, Vol. 44, pp. 1211-1235.
- Manabe, S. and Wetherald, R.T. (1990). "Equilibrium change and its implications for the future." *Climate Change: The IPCC Scientific Assessment*, Cambridge: Cambridge University Press, pp. 131-172.
- National Oceanic and Atmospheric Administration, National Climatic Data Center (1997). "Normal daily mean temperature, deg F," [Internet, WWW], ADDRESS: <http://www.ncdc.noaa.gov/ol/climate/online/ccd/meantemp.html>.
- National Oceanic and Atmospheric Administration, Pacific Marine Environmental Laboratory (1997). "El Niño Theme Page," [Internet, WWW], ADDRESS: <http://www.pmel.noaa.gov/toga-tao/el-nino/home.html>.
- Pilgrim, D.H., and Cordery, I. (1993). "Flood Runoff." *Handbook of Hydrology*, ed. Maidment, D.R., New York: McGraw-Hill, Inc., Ch. 9, pp. 1-9.
- Puente, C. (1978). "Method of estimating natural recharge to the Edwards Aquifer in the San Antonio area, Texas." *United States Geological Survey Water-Resources Investigations 78-10*, Austin, Texas.
- Reed, S.M., Maidment, D.R., and Patoux, J. (1997). "Spatial water balance of Texas." *Center for Research in Water Resources Online Report 97-1*, [Internet, WWW], ADDRESS: <http://www.ce.utexas.edu/prof/maidment/gishyd97/library/wbtexas/wbtexas.htm>.
- Smith, P.N., Maidment, D.R. (1995). "Hydrologic Data Development System." *Center for Research in Water Resources Online Report 95-1*, [Internet, WWW], ADDRESS: http://www.ce.utexas.edu/prof/maidment/gishyd97/library/smith/rep95_1.htm
- Schlesinger, M.E. and Zhao, Z.C. (1989). "Seasonal climate changes induced by doubled CO₂ as simulated by the OSU atmospheric GCM-mixed layer ocean model." *Journal of Climate*, Vol. 2, pp. 459-495.
- Shuttleworth, W.J. (1993). "Evaporation." *Handbook of Hydrology*, ed. Maidment, D.R., New York: McGraw-Hill, Inc., Ch. 4, pp. 18, 30-31.
- Thorkildsen, D. and McElhaney, P.D. (1992). "Model refinement and applications for the Edwards (Balcones Fault Zone) Aquifer in the San Antonio region, Texas." *Texas Water Development Board Report No. 340*, Austin, Texas.

- Thorntwaite, C.W. (1948). "An approach toward a rational classification of climate." *Geographic Review*, Vol. 38(1), pp.55-94.
- United States Geological Survey (1997). "Daily streamflow data," [Internet, WWW], ADDRESS: <http://txwww.cr.usgs.gov/databases.html>.
- United States Geological Survey (1996). "United States Geo Data," [Internet, WWW], ADDRESS: <http://edcwww.cr.usgs.gov/doc/edchome/ndcdb/ndcdb.html>
- United States Department of Agriculture (1991). "State Soil Geographic Data Base (STATSGO)-Data user's guide." *Miscellaneous Publication No. 1492*.
- Valdés, J.B. (1997). "Impacts of global climate change on water resources management of the Edwards Aquifer hydrologic region." *Texas A&M University Progress Report*, Texas A&M University, College Station, Texas.
- Wanakule, N. and Anaya, R. (1993). "A lumped parameter model for the Edwards Aquifer." *Technical Report No. 163*, Texas Water Resources Institute, Texas A&M University, College Station, Texas.
- Wang, H. and Anderson, P. (1982). *Introduction to Groundwater Modeling*, New York: W.H. Freeman and Company.
- Watkins, D.W. Jr. (1997). "Optimization techniques for the planning and management of robust water resources systems," PhD dissertation, University of Texas, Austin, Texas.
- Wetherald, R.T. and Manabe, S. (1990). "Processes and modeling." *Climate Change: The IPCC Scientific Assessment*, Cambridge: Cambridge University Press, pp. 69-91.
- Wilson, C.A. and Mitchell, J.F.B. (1987). "A doubled CO₂ climate sensitivity experiment with a global climate model including a simple ocean." *Journal of Geophysical Resources*, Vol. 92 (D11), pp. 13,315-13,343.
- Ye, Z. (1996). "Map-based surface and subsurface flow simulation models," PhD dissertation, University of Texas, Austin, Texas.

Vita

Kris Lawrence Martinez was born in Denver, Colorado on March 7, 1970, the son of Evelyn Marie Martinez and Lawrence Charles Martinez. He graduated from Green Mountain High School in Lakewood, Colorado in 1988 and entered the University of Colorado at Boulder. In December 1992, he received the degree of Bachelor of Science in Chemical Engineering. After working in consulting for several years, Mr. Martinez entered graduate school at the University of Texas at Austin in the fall of 1996.

Permanent address: 13858 West Cedar Avenue
Golden, Colorado 80401

This thesis was typed by the author.